

# The Calibration of Portable and Airborne Gamma-Ray Spectrometers - Theory, Problems, and Facilities

**Løvborg, Leif**

*Publication date:*
1984

*Document Version*
Publisher's PDF, also known as Version of record

**Risø National Laboratory** **Risø-M-** 2456

Risø-M- 2456

Title and author(s)

# THE CALIBRATION OF PORTABLE AND AIRBORNE GAMMA-RAY SPECTROMETERS - THEORY, PROBLEMS, AND FACILITIES

Leif Løvborg

Date October 1984

Department or group
Nuclear Geophysics

Group's own registration number(s)
152-36-34

130 pages + 27 tables + 50 illustrations

Abstract

A gamma-ray spectrometer for use in geological exploration possesses four stripping ratios and three window sensitivities which must be determined to make the instrumentation applicable for field assay or airborre measurement of potassium, uranium, and thorium contents in the ground. Survey organizations in many parts of the world perform the instrument calibration using large pads of concrete which simulate a plane ground of known radioelement concentration. Calibration and monitoring trials with twelve facilities in ten countries prove that moisture absorption, radon exhalation, and particle-size effects can offset a radiometric grade assigned to concrete whose aggregate contains an embedded radioactive mineral. These and other calibration problems are discussed from a combined theoretical and practical viewpoint.

Copies to

IAEA, Vienna
CNEA, Buenos Aires
CSIRO, Sydney
CNEN, Rio de Janeiro
GSC, Ottawa
GSF, Espoo
Soreq, Yavne
NUCOR, Pretoria
SGAB, Luleå
TMC, Grand Junction

Available on request from Risø Library, Risø National Laboratory (Risø Bibliotek), Forsøgsanlæg Risø, DK-4000 Roskilde, Denmark
Telephone: (02) 37 12 12, ext. 2262. Telex: 43116

This work was done under research contract 2504/RB between the International Atomic Energy Agency and Risø National Laboratory. The contract was signed in December 1979 and was renewed three times so as to cover the period from January 1980 to August 1984. This document is the final report on the research project for which the author has the full scientific responsibility.

ISBN 87-550-1043-1
ISSN 0418-6435

**Risø repro 1984**

RISØ-M-2456 October 1984

# THE CALIBRATION OF PORTABLE AND AIRBORNE GAMMA-RAY SPECTROMETERS - THEORY, PROBLEMS, AND FACILITIES

Leif Løvborg

Risø National Laboratory
Postbox 49
DK-4000 Roskilde
Denmark

## SUMMARY

Portable and airborne gamma-ray spectrometers are used for mapping the natural concentrations of potassium, uranium (radium), and thorium in the surface of geological formations. Although the surveyed ground may not be plane, it is often permissible to assume a $2\pi$ measuring geometry on rock outcrops and in aerial scanning heights of typically 50 to 125 m. Accordingly, to get the equipment calibrated as a radiometric assay tool, the survey operator must have access to large and plane slab sources of known radioelement concentrations. Over the past several years, survey organizations in more than ten countries have built calibration pads which are up to 100 $m^2$ large and consist of concrete with evenly dispersed aggregate particles of orthoclase (K feldspar), pitchblende, thorite, or other radioactive mineral. Twelve of these pads facilities were monitored with a portable spectrometer to estimate the calibration performance obtained with concrete slab sources and to identify the possible problems associated with the manufacture and use of such sources. The experimental data plus various calculations in combination with information in the literature made it possible to reach the following ten main conclusions: 1) An adequate calibration facility

is formed by three concrete pads spiked with a predominant content of either potassium, uranium, or thorium. An additional pad of low radioelement content must be included to eliminate the background contribution from the surroundings. 2) Uranium and thorium pads of the required radioactive purity and homogeneity is best manufactured by mixing powdered high-grade ore into quartz or silica sand of about 3 mm maximum particle size. It is very important to select a uranium ore of negligible radon emanation power, and it may be advisable to strain off particles which are less than 75 µm across to limit the specific surface of the admixture. 3) Calibration pads for portable spectrometers are conveniently constructed by placing the wet mixes in circular metal containers, approximately 2 m in diameter and 50 cm deep. The uranium pad grade should not exceed 400 ppm to avoid pulse pile-up effects; grades of 100 ppm eU and 200 ppm eTh are useful calibration levels for field assays in general. 4) Designers of airport pads should make use of the IAEA recommendation from 1976 (minimum calibration surfaces of 50 $m^2$ and grades of 20 ppm eU and 40 ppm eTh). 5) Concrete (mortar) based on fine aggregate must be expected to be 20% porous and absorp up to 10% moisture in an outdoor environment. It is the most relevant to include the average pad moisture in the calibration grades and incorporate the seasonal moisture variation of perhaps ±3% as a grade uncertainty. 6) In-situ pad grades can be estimated quite well by gamma-ray analysis of freshly cured concrete in sealed sample cans. 7) The thorium reference materials presently available for assigning grades to pads are not satisfactory because their radium contents are unspecified. 8) Spectrometer counts recorded on calibration pads are conveniently processed by means of weighted, three-dimensional regression analysis. 9) Simple working expressions make it possible to include calibration uncertainty and counting statistics on the assay spot in the standard deviations of radioelement concentrations measured with a portable spectrometer. 10) An airborne spectrometer can be calibrated reasonably well by combining a calibration trial on pads with a theoretical correction for atmospheric gamma-ray attenuation. The normal practice of determining the window sensitivities from a flight over a test range presupposes a ground of moderate moisture content and little radon exhalation.

CONTENTS

# 1. INTRODUCTION

## 1.1. Subject and background of the research

The work reported here is a contribution to the knowledge on techniques and problems in the calibration of gamma-ray spectrometers designed to measure the concentrations of potassium, uranium (radium), and thorium in the ground. The relevance of the subject stems from the fact that the three natural radioelements are extremely valuable indicators of many geological and geochemical processes, in particular the formation of uranium and thorium ore deposits. Generally speaking, surveys with an airborne gamma-ray spectrometer are adequate for producing regional maps of the radioelement contents in the earth's surface, while field traverses with a portable spectrometer provide the detailed picture of the radioelement distribution in an area of increased natural radioactivity.

The gamma radiation emitted by potassium and some of the uranium and thorium daughters is very penetrating and possesses a usable line spectrum in heights of up to about 200 m over the formation. Because the essential emissions are separated by several hundred keV on the energy scale, large sodium-iodide scintillators can be utilized for the construction of efficient and relatively simple window spectrometers for the selection of potassium, uranium, and thorium counts. Calibrating the equipment involves a determination of numerical constants which make it possible to remove interfering counts from the energy windows and convert the resulting net counts into radioelement concentrations in the ground.

International recommendations regarding the best way to calibrate a portable or an airborne window spectrometer are contained in the IAEA report "Radiometric Reporting Methods and Calibration in Uranium Exploration" (IAEA, 1976). The recommended basic calibration source is a large slab or pad of concrete loaded with a

predominant and known concentration of either potassium, uranium (radium), or thorium. A set of three sources plus an additional concrete pad manufactured from a non-radioactive aggregate material enable the geologist to perform a complete calibration of a portable spectrometer. Window counts recorded with an equivalent airborne instrumentation placed on calibration pads supply the calibration factors of the measuring system at ground level and are not an immediately valid base for assaying radioelement concentrations from an aerial survey altitude. However, the absorption of gamma rays in the air can be taken into consideration theoretically, or one may determine the true window sensitivities from a flight over a natural ground with known radioelement concentrations. The latter approach implies that the concrete pads only are used to measure the calibration constants required to strip away the unwanted interfering counts in the energy windows.

An indirect consequence of the many gamma-ray surveys carried out for uranium exploration in the 1970s was the building of a series of pads calibration facilities in North America and Europe. In 1979 large concrete pads in support of aerial prospecting and mapping operations had been installed at airports in Canada, Finland, Sweden, and the USA, while similar smaller pads for use with portable spectrometers had become available near exploration offices in Canada, Denmark, and Sweden. Because this considerable effort to improve the processing of spectrometric survey data was a distinctive manifestation of the recommendations and thoughts in the IAEA report, the IAEA had an obvious interest in reviewing the possible problems in relation to the construction and use of concrete calibration pads. As a first step in such a review the author was asked to make an experimental intercomparison of calibration results obtained with facilities existing in 1979, and this was how the present study was started.

During the time the author was comparing calibration constants determined for a portable spectrometer on pads in North America and Scandinavia, similar facilities came into existence in other parts of the world, namely in Argentina, Australia, Brazil,

Israel, and South Africa. (The latter country actually took steps to construct a series of small pads in the early 1970s; an airport calibration facility was added in 1981). This was an opportunity to collect additional monitoring data so as to make the IAEA intercomparison experiment more comprehensive and conclusive. Observed discrepancies between laboratory-analysed pad radioelement concentrations on the one hand and monitoring results on the other prompted a detailed study of the possible causes of such discrepancies. It was found that moisture absorption, radon exhalation, and grain-size effects may offset a pad calibration grade from the assigned reference value. Problems like these were not foreseen in the IAEA calibration report which was based on experience with the limited number of pads facilities constructed before 1976. In reporting the observations made during four years of calibration and monitoring trials plus various follow-up investigations, the author found it relevant to present the material in the form of an exhaustive paper which is meant as a supplement to "Radiometric Reporting Methods and Calibration in Uranium Exploration".

## 1.2. Outline of the report

It has not been an easy job trying to describe the properties of a number of actually established calibration facilities while at the same time presenting information which proves that several of the facilities would have given more accurate calibrations if greater care had been exerted in selecting the radioactive admixtures for the pads. Nevertheless, the author thinks he has an obligation to be critical in view of the fact that he himself is among those who added uranium ore to concrete without thoroughly checking the emanation power of the ore particles. Another difficulty in writing up the present report was the wish to combine specialist information with a discussion of the calibration problems in general, including their relation to field uncertainties such as counting statistics, geometry effect, and moisture in the ground.

Chapter 2 is an attempt to highlight the basic principles and technicalities for executing a spectrometric in-situ assay or a

series of similar measurements along a flight line. Most of these topics were dealt with in greater detail in the IAEA reports "Recommended Instrumentation for Uranium and Thorium Exploration" (IAEA, 1974) and "Gamma-Ray Surveys in Uranium Exploration" (IAEA, 1979). It should here be mentioned that the IAEA also published "Borehole Logging for Uranium Exploration - A Manual" (IAEA, 1982) in which the reader will find extensive information on the use of gamma-ray spectrometry in subsurface geophysics. Other comprehensive reviews of relevance to the matters discussed in chapter 2 and later were presented by Darnley (1973), Kogan et al. (1976), Wollenberg (1977), Darnley (1977), Grasty (1979), Killeen (1979), Vavilin et al., (1982), and Bristow (1983).

It might be asked why the present author did not make allowance for potassium counts in the uranium and thorium windows in setting up the "stripping equations" for a spectrometer. The answer is, as far as the author sees the problem, that if such counts occur (because of poor sodium-iodide detector energy resolution), one may just as well use the complete 3 × 3 matrix equation (introduced in chapter 5) for calculating the radioelement concentrations in the ground. The reader might also object that the author omits any processing of counts recorded in the total-count window. However, an attempt to discuss the conversion of total gamma-ray counts into equivalent "units of radioelement concentration" or "Ur" would not fit the objective of a report specifically devoted to gamma-ray spectrometry. In the author's opinion the "Ur" (IAEA, 1976; OECD, 1981) has its greatest justification in the reporting of measurements executed with scintillation counters held over exposed radioactive mineralization. A last omission that some readers might regret is the rôle of atmospheric radon in airborne gamma-ray surveys and the associated use of an upward-looking detector for removing the resulting additional background in the uranium window. Regarding the involved calibration problem, the reader must consult other sources of information, for example Aviv and Vulkan (1983). The important new result presented in chapter 2 is the working expressions for calculating signal precision and <u>a priori</u> detection limits in radioelement assaying with a portable spectrometer. In fact, a method to estimate the effect of counting statistics on measured

radioelement concentrations is just as important as the availability of a calibration facility.

Chapter 3 is to a large extent theoretical and has been included especially to assess the counting geometry on a circular or rectangular calibration pad and to study the expected effects of moisture and radon diffusion in porous source media in general. In chapter 4 the design of a calibration facility is discussed using existing facilities to exemplify the factors which govern the choice of pad dimensions, the spacing of pads, and the radiometric pad grades. It is furthermore discussed how the fineness and spatial dilution of radioactive ore particles in concrete affect the volume of mix required to analyse a reliable pad grade. The chapter also contains recommendations regarding the selection of suitable ore materials and the use of these for manufacturing concrete of a satisfactory radioactive homogeneity and tightness. Chapter 5 deals with the problem of assigning pad grades which include moisture absorbed in the concrete porespaces. The use of sealed-can gamma-ray analysis is explained and currently available uranium-radium and thorium reference materials are mentioned. Readers who are especially interested in knowing how assigned radioelement concentrations and their estimated uncertainties are used in calibration trials on pads will find the desired information in this chapter.

The pads intercomparison experiment carried out on behalf of the IAEA is described in chapter 6. Six airport facilities and six other calibration sites in ten countries were incorporated in the experiment which lasted from February 1980 to August 1984. It has been attempted to use pads visited during 1980-81 for calibrating the monitoring spectrometer, while data recorded later have been utilized to test pad radioelement concentrations estimated from laboratory assays. The Appendix included after the list of references gives the details of each facility, including the assigned or monitored pad grades. This compilation of data sheets enables the reader to obtain an overview of the majority of spectrometer calibration sites established up to the present. Existing facilities not reported on here comprise: 1) Eleven smaller pads at the Pelindaba research centre of the Nuclear Development Corporation

of South Africa (Corner et al., 1979). Several of these pads were actually monitored by the author in October 1982, but their radiometric grades were considered too high for being exploited in the intercomparison. 2) A Czechoslovak facility for portable spectrometers at Bratkovice near Pribram (Rojko, 1976). 3) Seven sites for calibrating portable spectrometers in the USA (George and Knight, 1982; George et al., 1984). 4) An airport facility in Teheran, Iran (Killeen, 1979). 5) A series of four 8 × 8 m pads constructed in 1984 at U-Tapao airfield, 120 km south of Bangkok, Thailand (R.L. Grasty, personal communication).

It might be added that concrete blocks designed for the calibration of hand-held scintillation counters are available in Denmark and Greece (Løvborg, 1983) plus several places in the USA (Mathews and Kosanke, 1978).

## 2. SPECTROMETER WINDOW COUNTING

### 2.1. Portable spectrometers

Exploration geologists are typically becoming acquainted with the recording of gamma-ray window counts through the purchase of a portable spectrometer. Figure 1 shows a Geometrics model GR-410 portable spectrometer placed for counting on a granite outcrop. The bottom of the vertically positioned detector unit houses a 76 × 76 mm sodium-iodide crystal (thallium activated) in optical contact with a photomultiplier. A flexible cable feeds the detector pulses into a recording unit placed in the leather carrying case for the equipment. Assay of the radioelement contents in the outcrop is performed by switching the recording unit into the counting mode for a preselected time. Gamma-ray counts are then registered in three energy windows which select characteristic emissions at 1.46 MeV (potassium), 1.73 to 1.85 MeV (uranium), and 2.61 MeV (thorium). Table 1 shows the decay events producing these emissions as well as

the energy intervals used for window counting with a GR-410. The selected isotopes $^{214}Bi$ and $^{208}Tl$ are, respectively, radioactive daughters of $^{238}U$ and $^{232}Th$, while $^{40}K$ is a natural potassium radioisotope emitting 3.31 ± 0.03 photons/s per gram of potassium (Endt and Van der Leun, 1973).

The window settings of the GR-410 recording unit are provided through a permanent adjustment of internal turn dials. The settings in Table 1 are recommended in the GR-410 manual and correspond to the use of a constant relative window width of 12%. A supplementary total-count window with a lower energy limit of 0.5 MeV is available to make the instrument applicable for rapid selection of representative assay spots on the rock surface. Assays are terminated by initiating a readout cycle that displays the total counts and the high-energy counts in slow succession on a four-digit LED panel. A GR-410 spectrometer was used for executing the measurements reported in chapter 6. Portable spectrometers supplied by most other manufacturers of geophysical instrumentation are based on similar design concepts and operated with more or less identical window settings.

One of the most recent instrument developments is the Czechoslovak GS-256 spectrometer which is a compact multichannel device permitting energy windows to be set up as regions of interest. This new unit, manufactured by Geofyzika in Brno, can be connected to a desk calculator such as the HP-85 for the processing of calibration spectra and storage of the resulting window calibration factors in the memory of the spectrometer. A microprocessor in the latter makes it possible to get the field readings displayed in final form, i.e. as radioelement concentrations in the ground. (J. Bartošek, personal communication).

## 2.2. The generation of window counts

Gamma-ray energy distributions produced at the surface of a plane and infinite rock medium are presented in Figs. 2 to 4. These spectra of the radiation input to an assay device like a portable spectrometer were calculated by means of photon transport

codes which simulate the scattering and absorption of gamma radiation in the ground and the air (Kirkegaard and Løvborg, 1979; Kirkegaard and Løvborg, 1980). Figures 3 and 4 include essentially all photon emissions associated with the decay series of uranium and thorium and are based on up-to-date emission data in the Evaluated Nuclear Structure Data File (ENSDF) (Ewbank, 1980; Kocher, 1981). It can be seen that each radioelement generates a discrete flux spectrum superimposing a continuum with energies up to the maximum energy of the photons emitted by the radioelement. The discrete flux components represent directly transmitted gamma rays, while the continuously distributed flux is due to single and multiple Compton scattering along the transmission paths through the rock medium.

Figures 3 and 4 demonstrate that the potassium window of a field spectrometer (window 1) is sensitive to uranium and thorium. Detected along with the primarily selected 1.46 MeV photons from $^{40}K$ are several emissions around 1.5 MeV from $^{214}Bi$ and $^{228}Ac$ (another thorium daughter) plus scattered radiation from uranium and thorium emitters with energies exceeding the upper limit of the potassium window. From Fig. 4 it can be seen that there is a similar influx of thorium radiation into the uranium window (window 2). This undesirable sensitivity of an energy window to more than one radioelement is enhanced by the response of a sodium-iodide scintillator to a flux of terrestrial gamma radiation.

Gamma rays of any energy detected with a sodium-iodide crystal produce a full-energy peak which is accompanied by a Compton continuum arising from a partial outscatter of the incident radiation. If the gamma-ray energy is greater than 1.022 MeV, positron-electron pairs are created in the crystal. The unstable positrons annihilate into two oppositely directed 0.511 MeV photons whose escape from the crystal is responsible for the occurrence of two satellite peaks in the resulting pulse spectrum. These annihilation escape peaks are positioned 0.511 and 1.022 MeV below the full-energy peak. Scintillation-detector energy resolution is commonly expressed in terms of the relative width at half maximum (rwhm) of the full-energy peak obtained with the 0.662 MeV photons from a $^{137}Cs$ source. Further details

on the response characteristics of inorganic scintillators are given in a recommendable textbook by Croutamel (1970).

Figures 5 to 7 are computer-simulated pulse spectra calculated by combining the flux energy distributions in Figs. 2 to 4 with a model for the response of a 76 × 76 mm sodium-iodide scintillator introduced by Berger and Seltzer (1972). The model involves the use of parametrized expressions for the shape of the Compton continuum as a function of the incident gamma-ray energy. Its ability to reproduce a terrestrial pulse spectrum was demonstrated by Løvborg and Kirkegaard (1974) and extended to other detector dimensions by Gyurcsak and Lenda (1979).

Figure 5 applies to a crystal-photomultiplier assembly with an assumed energy resolution of 7.6%. Increased peak widths corresponding to less satisfactory resolutions of 8.8 and 10.0% have been adopted in Figs. 6 and 7. The observation made from these pulse spectra is an interaction between the energy windows in excess of that stipulated by the spectral distributions of the incident gamma-rays. There is an increased amount of downscatter from uranium and thorium into the potassium window and from thorium into the uranium window. Some of the thorium counts in these two windows are caused by the annihilation escape peak at 1.59 MeV from the $^{208}Tl$ photons selected by the thorium window (window 3). A special effect of the limited energy resolution attainable with a sodium-iodide detector is the recording of 2.45 MeV uranium gamma-rays in the thorium window. The only interaction not observed theoretically even with a poor resolution of 10% is an upscatter of potassium counts into the uranium window.

## 2.3. Stripping ratios and window sensitivities

It follows from the preceding subsection that the window count rates obtained over a ground with mixed radioelement contents can be expressed as

$$n_1 = n_{1,K} + n_{1,U} + n_{1,Th}$$

$$n_2 = n_{2,U} + n_{2,Th} \qquad (1)$$

$$n_3 = n_{3,Th} + n_{3,U}$$

where the numerical indices are the window numbers. To solve these equations with respect to the terms included at first on the right-hand side, it is convenient to introduce the following series of ratios between window count rates generated by one and the same radioelement:

$\alpha = n_{2,Th}/n_{3,Th}$
(Thorium counts in the uranium window per thorium count in the thorium window)

$\beta = n_{1,Th}/n_{3,Th}$
(Thorium counts in the potassium window per thorium count in the thorium window)

$\gamma = n_{1,U}/n_{2,U}$
(Uranium counts in the potassium window per uranium count in the uranium window)

$a = n_{3,U}/n_{2,U}$
(Uranium counts in the thorium window per uranium count in the uranium window).

These so-called stripping ratios make it possible to get a solution of the form

$$n_{3,Th} = (n_3 - an_2)/(1 - a\alpha)$$

$$n_{2,U} = (n_2 - \alpha n_3)/(1 - a\alpha) \qquad (2)$$

$$n_{1,K} = n_1 \quad \beta n_{3,Th} - \gamma n_{2,U} .$$

Each of the gamma-ray signals calculated in this way is a net or "stripped" window count rate that can be attributed to decaying $^{208}Tl$, $^{214}Bi$, and $^{40}K$ respectively.

A geologically informative assay result is obtained by expressing the activities of these radioisotopes as equivalent concentrations of thorium, uranium, and potassium. The reporting of experimental $^{40}K$ activity as a weight percentage of potassium does not have any associated ambiguity, provided it can be assumed that the potassium in rocks and has a constant isotopic composition. Equivalent uranium and thorium concentrations, on the other hand, are imaginary reporting quantities which can only be interpreted as chemical concentrations for ground material in which $^{214}Bi$ and $^{208}Tl$ are in radioactive equilibrium with their respective parents, $^{238}U$ and $^{232}Th$. Disequilibrium in the $^{238}U$ decay chain is a very common phenomenon in geological environments (Ivanovich and Harmon, 1982) and is a frequent cause of discrepancies between equivalent and chemical uranium concentrations. Uranium and thorium concentration equivalents are denoted by the letter "e" and conveniently stated in units of ppm eU and ppm eTh (IAEA, 1976) (1 ppm = 1 µg/g).

The step of calculating a spectrometer assay result is accomplished by dividing the stripped window count rates by a set of window sensitivities, $s_{Th}$, $s_U$, $s_K$, chosen as follows:

$s_{Th}$ = count rate in window 3 per ppm eTh
$s_U$ = count rate in window 2 per ppm eU
$s_K$ = count rate in window 1 per % K.

The determination of these three calibration constants plus the four stripping ratios, $\alpha$, $\beta$, $\gamma$, and a, is the objective of the instrument calibration required to make a field spectrometer applicable as an assay tool. Without such a calibration, a spectrometer can provide no more than a crude discrimination between ground concentrations of thorium, uranium, and potassium.

An impression of the stripping ratios and window sensitivities of a portable spectrometer can be obtained by integrating the computer-simulated spectra for a 76 × 76 mm detector between the energy limits of the spectrometer windows. This has been done for the spectra in Figs. 5 to 7 with their added energy windows of a Geometrics GR-410. Tables 2 and 3 show the resulting theoretical

calibration constants and their variation with the energy resolution assumed for the detector unit. In chapter 6 the data are compared with a set of experimentally determined calibration constants. It is seen that the stripping ratios $\alpha$ and $\beta$ and the window sensitivities $s_K$ and $s_U$ are significantly influenced by the resolution performance of the crystal-photomultiplier assembly. This is because of the counts excluded from the flanks of the full-energy peaks selected by the potassium and the uranium window. Reduced energy resolution with time, as expressed by an increased percent resolution, is encountered in practice due to a gradual loss of optical contact between the crystal and the photomultiplier. The initial contact between the two detector components may be prolonged by storing an unused detector probe in an upright position (J. Volný, personal communication).

## 2.4. Field assays

A spectrometer set-up like that in Figure 1 offers the advantage of providing a large sampling volume in the ground material. The window counts are contributed by a bowl-shaped region with a surface extension of a few meters and a depth extension below the assay spot of about 35 cm (Løvborg et al., 1969). Since the gamma-ray emitters contained in a volume of rock are detected less efficiently with increasing distances between the volume element and the assay spot, the geostatistical significance of the counts are small outside a surface radius of half a meter and below a depth of 15 cm. An associated effective sample can be calculated from the assumption that the radioelements have a random spatial distribution in the ground. The effective sample is geostatistically equivalent to a similar mass of excavated material and amounts to 40-50 kg in assays of uranium and thorium (Løvborg et al., 1971).

Most of the published assay data recorded with field spectrometers are from the days when it became possible to build equipment of the required portability and low power consumption, but when adequate calibration facilities had not become available yet (Richardson, 1964; Doig, 1968, Løvborg et al., 1969;

Killeen and Carmichael, 1970; Løvborg et al., 1971). These older reportings illustrate the geological relevance of the in-situ method and might prompt a number of similar applications based on the many pads calibration facilities constructed after 1970 (Appendix).

One application of great current interest in connection with environmental monitoring and remedial actions is the conversion of recorded ground radioelement concentrations into corresponding gamma-ray exposure rates and resulting population doses. Experimental work with portable spectrometers in this scientific area has been executed over soil and bedrock (Løvborg et al., 1979) and over massive occurrences of exposed uranium-thorium mineralization (Løvborg et al., 1980). Table 4 shows two sets of conversion factors that have been estimated from photon transport calculations applied to an infinite and plane soil medium. The data set from the work of Løvborg et al. (1971), is based on an older compilation of the photon emissions in the decay chains of $^{238}U$ and $^{232}Th$ (Beck, 1972). The other data set was calculated from the line intensities, with associated uncertainties, in the 1981 version of the Evaluated Nuclear Structure Data File. From the last result it can be seen that the thorium exposure rate is less accurately known than the exposure rates from potassium and uranium. This is because the intensities of the photon emissions from $^{228}Ac$ have large experimental uncertainties (Kocher, 1981). The factors for converting natural radioelement concentrations into radiation exposure are nearly identical for rocks and soils and are only slightly affected by the small contents of iron and other gamma-ray absorbers in common geological materials (Kirkegaard and Løvborg, 1980).

A practical problem arising from the use of field equipment designed for counting in narrow energy windows is presented by the temperature sensitivity of the photomultiplier contained in the detector unit. Depending on various features such as the number of stages in the dynode chain, a photomultiplier may exihibit temperature coefficients of either positive or negative sign at normal ambient temperatures; numerically the

amplitudes of the output pulses may change by as much as 2.5% per $^{o}C$ (Rohde, 1965). The effect of off-setting the energy calibration of a GR-410 spectrometer by 2% positive or negative is illustrated in Figs. 8 and 9 which are identical to Fig. 5 except for the factor correlating energy and pulse amplitude. Since the spectral peaks selected by the energy windows have become displaced with respect to the window centre positions, the count rates recorded with the spectrometer are not the same as those produced with the photomultiplier gain correctly adjusted. Table 5 shows the resulting variations imposed on the spectrometer calibration constants. It can be seen that an undected gain drift of plus or minus 2% changes the stripping ratios and window sensitivities by several percent, so that systematic errors on the assayed radioelement concentrations are introduced. Especially the stripping ratio "a" is sensitive to gain drift because this calibration constant depends on counts in the thorium window from a $^{214}Bi$ peak located near the lower window limit. A bias on the "a" stripping ratio produces large errors on the thorium content measured in ores with a predominant content of uranium.

The manufacturers of portable spectrometers have taken steps to enable the users to recognize and counterbalance bad instrument performance in the field due to variations in the overall system gain from the cathode of the photomultiplier to the input of the pulse-height selectors. In the Geometrics GR-410 the gain can be monitored by displaying an error signal on a moving coil meter which also serves as a count-rate meter and a device for checking the battery. The error signal is produced by a $^{133}Ba$ disc source attached to the bottom of the detector unit, in front of the sodium-iodide crystal. $^{133}Ba$ emits 0.356 MeV photons which can be recorded and used for reference purposes without generating counts in the high-energy windows, and with only a small injection of pulses into a total-count window having a lower energy limit of 0.5 MeV. Gain drift observed between the field readings is neutralized by adjusting the system gain manually until the error signal has been restored to zero. Unrestored error signals corresponding to more than ±2% gain drift are blocking the start of a new counting period. In the

GAD-6 spectrometer, manufactured by Scintrex, it is possible to include the error signal in a feed-back loop that automatically keeps the energy calibration of the equipment on a constant value.

The achievement of reliable assay results is more or less impossible on rock whose content of uranium or thorium is large enough to distort the shape of the scintillation spectrum. Geologists involved in gamma-ray borehole logging are familiar with the use of dead-time corrections which compensate for the counting losses introduced at gross count rates of several thousand counts per second. A dead-time correction applied to spectrometer window counts is of doubtful relevance due to the onset of spectral pile-up effects long before the dead time of the counting registers has to be taken into consideration. For example, a 76 × 76 mm detector placed on mineralization containing 2000 ppm eU produces a count rate of about 700 counts/s in the uranium window, while the full range of pulse amplitudes represents a count rate of nearly 120,000 counts/s. This corresponds to an average time interval of 8 μs between the detector pulses. Since the arrival times of the pulses are governed by Poisson statistics, there is a big chance that a new pulse arrives before the preceding one has died away (a process that takes 9 μs with the linear amplifier used in a GR-410). Pulses destined for the uranium window may therefore get their effective amplitudes increased and thus become lost or registered in the thorium window. This pile-up effect gives rise to an increase in the "a" stripping ratio. It sets in at a gross count rate of about 20,000 counts/s and excludes accurate determinations of small thorium contents in uranium ore containing more than a few hundred ppm eU. There is a similar upper limit for the use of a 76 × 76 mm detector over thorium mineralization, and it can be estimated that 1000 ppm eTh produces the same amount of pulse pile-up as 400 ppm eU.

## 2.5. Background counts

Before the equations (2) are used for the calculation of assay results, an estimated set of background count rates must be sub-

tracted from the recorded window signals, $n_1$, $n_2$, and $n_3$. Spectrometer background counts are generated by cosmic rays and internal detector radioactivity, especially $^{40}K$ in the glass envelope of the photomultiplier. In the uranium window there may be an additional and variable contribution from airborne $^{214}Bi$ produced by atmospheric $^{222}Rn$, the gaseous decay product in the $^{238}U$ decay chain. Table 6 shows five background determinations performed over water with the GR-410 used in the present study (chapter 6). The background readings were taken by accumulating window counts during one hour or more. In the Helsinki Bay area and on the lakes in Sweden and Colorado the instrument was operated on board light boats carrying very little natural radioactivity. The background recorded on Roskilde Fjord is from a cruise with a tourist steamer whose wooden materials may account for the greater number of potassium counts observed in this particular trial. The highest uranium and thorium background readings are those from Highline Lake near Grand Junction in Colorado. The high thorium reading probably reflects the increased cosmic-ray intensity in an altitude of 1433 m. In the uranium window the background measured in Colorado is enhanced by a factor of two, a likely effect of the concentration of $^{222}Rn$ in continental air masses (Larson and Bressan, 1980).

A peculiar rise in the background in the uranium window may occur due to $^{214}Bi$ deposited on the ground by rainfall. Figure 10 shows uranium and thorium counts recorded on two consecutive days in a GR-410 monitoring trial on the low-radioactivity "B" pad of the calibration facility at Malå, Sweden (Appendix). On the second day it began to rain after a long period of dry weather. In the course of a few hours after the onset of the rainfail the count rate in the uranium window rised to over 250% of the value recorded on the preceding day. When the counting was resumed in the afternoon, after the rain had ceased, the uranium count rate had returned to the value recorded the day before. This is an example of the washout and subsequent decay of airborne radon daughters (Minato, 1980). The reason for the short duration of the phenomenon is the short half-lives of $^{214}Bi$ and its immediate precursor, $^{214}Pb$ (26.8 m and 19.8 m respectively). Since the temporary increase in the uranium background

may pass unnoticed, it is not advisable to begin field assays at the upcoming of new rain.

## 2.6. Precision of measurement

Spectrometer window counts accumulated on an assay spot have statistical uncertainties, so that a repeated counting period will furnish a more or less different set of count rates. Assuming that the overall system gain has been kept under careful control, the precision of measurement can be predicted from Poisson statistics according to which N counts have an estimated standard deviation of $\sqrt{N}$. Precision is a measure of statistical significance and should not be confused with accuracy which is a different concept used for expressing the effect of calibration errors. The errors on experimental stripping ratios and window sensitivities as well as their incorporation in calculations of field accuracy are discussed in chapter 5.

Currie (1968) has given a rational approach to treat the statistical significance of a net signal obtained as the difference between an instrument reading and the "background" contained in the latter. In the present context a reading is represented by a number of window counts divided by the counting time, while "background" is the contribution to this count rate from interacting decay events in the ground plus real background events. In Currie's approach it is first investigated whether the net signal has in fact been detected. Quite clearly, a net uranium signal is not detected if the thorium counts stripped away from the uranium counts should happen to produce a negative count rate. Not even a small positive count rate guarantees a reliable detection of a net uranium signal since a small signal might be a purely statistical outcome of the stripping calculation. To reduce the risk of false radioelement detections to a level of 5%, the net count rate "n" in each energy window must exceed a critical level $n_C$ given by

$$n_C = 1.645\ \sigma_o \qquad (3)$$

where $\sigma_o$ is the standard deviation of n when n is zero. One point in Currie's suggestion for the reporting of assay results is the use of an upper limit for the content of an undetected substance. Such an upper limit may be estimated from the observed net signal by increasing the signal with two times its calculated standard deviation.

The statistics of net signals recorded with a portable spectrometer is evaluated by first rewriting the stripping equations (2) on the complete form

$$n_{3,Th} = \frac{(n_3-b_3)-a(n_2-b_2)}{1-a\alpha}$$

$$n_{2,U} = \frac{(n_2-b_2)-\alpha(n_3-b_3)}{1-a\alpha} \qquad (4)$$

$$n_{1,K} = n_1 - \beta n_{3,Th} - \gamma n_{2,U} - b_1$$

where $(b_1,b_2,b_3)$ and their standard deviations $(\sigma_{b1},\sigma_{b2},\sigma_{b3})$ are supposed to have been estimated from background measurements over water or other non-radioactive material. The expressions for $n_{3,Th}$ and $n_{2,U}$ are direct functions of recorded counts, and it is quite easy to write down the associated standard deviations. In doing so, one uses the fact that a count rate n recorded by counting in t seconds has an estimated variance of

$$\sigma_n^2 = n/t \ . \qquad (5)$$

Furthermore, for a linear combination of statistically independent terms,

$$z = g \cdot x + h \cdot y \ , \qquad (6)$$

a resulting variance is calculated as

$$\sigma_z^2 = g^2 \cdot \sigma_x^2 + h^2 \cdot \sigma_y^2 \ . \qquad (7)$$

Since the squared stripping ratios for a spectrometer equipped with a 76 × 76 mm detector are smaller than unity (cf. Table 2), it is permissible to disregard the small statistical influence of the background in one energy window on the signal in another window. Also, upon the insertion of the net count rates $n_{3,Th}$ and $n_{2,U}$ into the expression for $n_{1,K}$, a term $(\beta - \alpha\gamma)n_3$ is generated which is numerically small and can be neglected for statistical purposes. Leaving out the insignificant product $a\alpha$, one arrives at the approximations

$$\begin{aligned} n_{3,Th} &\approx n_3 - (an_2 + b_3) \\ n_{2,U} &\approx n_2 - (\alpha n_3 + b_2) \\ n_{1,K} &\approx n_1 - (\gamma n_2 + b_1) \; . \end{aligned} \tag{6}$$

These are of the form

$$n = p - (k \cdot q + b) \tag{7}$$

which has a variance of

$$\begin{aligned} \sigma_n^2 &= \sigma_p^2 + k^2 \, \sigma_q^2 + \sigma_b^2 \\ &= p/t + k^2 \, q/t + \sigma_b^2 \; . \end{aligned} \tag{8}$$

The square root of this expression divided by the window sensitivity is the estimated absolute precision of the assayed radioelement concentration. The variance $\sigma_o^2$ required for deciding whether the radioelement in question was detected or not is calculated from (8) using the condition $n = o$, corresponding to $p = k \cdot q + b$:

$$\sigma_o^2 = (kq + b)/t + k^2 \, q/t + \sigma_b^2 \; . \tag{9}$$

The format shown in Table 7 makes it easy to set up a program on a portable calculator for performing the statistical processing of spectrometric field data.

Critical levels and precision calculated from recorded counts are a posteriori estimates going with an actual field assay. It has also interest to determine with what precision a radioelement can be assayed, given the counting time and the concentrations of the two other radioelements. For this a priori problem it is convenient first to introduce a detection limit, again based on a critical level which ensures that less than 5% of the insignificant signals are accepted. Since a fraction of the signals with a mean value equal to the detection limit may not exceed the critical level, it is relevant to build in the additional protection that less than 5% of the significant signals are rejected. Currie showed that with this double choice of a 5% risk level, a net count rate n with an associated standard deviation of $\sigma_o$ for n = 0 has an a priori detection limit of

$$n_D = 2.71/t + 3.29\ \sigma_o \qquad (10)$$

where t as before is the counting time. To get $\sigma_o$ and hence $n_D$ for a spectrometer window, one replaces the product k · q in (7) with the known count rate "r" produced by the two other radioelements. In analogy with formula (8) one obtains

$$\sigma_n^2 = p/t + r/t + \sigma_b^2 \qquad (11)$$

and consequently

$$\sigma_o^2 = (2r + b)/t + \sigma_b^2\ . \qquad (12)$$

Another a priori quantity useful in the planning of field measurements is the determination limit for a radioelement, i.e. the least concentration that can be determined with a prescribed precision. In terms of net signal, Currie derived the following formula for the determination limit $n_Q$ when a precision of 10% is wanted:

$$n_Q = 50\ \left\{\frac{1}{t} + \sqrt{\frac{1}{t^2} + \frac{\sigma_o^2}{25}}\ \right\}\ . \qquad (13)$$

In Table 8 $n_D$ and $n_Q$ are written explicitely as functions of the interfering contributions and background in spectrometer energy windows. To express a detection or determination limit in radioelement concentration units, one has to divide the calculated signal by the proper window sensitivity.

Determination limits for the GR-410 spectrometer used in the present study can be read from the curves in Figs. 11 to 13. These data are based on experimental calibration constants determined for the unit (chapter 6), and they incorporate the likely background count rates stated at the bottom of Table 6. The curves illustrate the advantages offered by increasing the counting time from 1 to 20 minutes, the probable maximum time one would be willing to spend on a single assay.

Consider for example Fig. 11, thorium. For accompanying uranium concentrations of less than about 10 ppm eU it is possible to make a 10% precise assay of 15 ppm eTh in 1 min, while a similar precision on 2.5 ppm eTh would require a counting time of 20 min. Most of the statistical uncertainty is here contributed by counts supplied by thorium and background in the thorium window. On ground containing tens or hundreds of ppm eU there is an additional statistical influence from uranium counts delivered into the thorium window through the "a" stripping ratio. It can be seen that a 10% precise assay of 5 ppm eTh in 150 ppm eU cannot be made in less than 20 minutes. Figure 12 shows that the determination of 5 ppm eU in 150 ppm eTh would also require 20 min of counting time.

The potassium determination limits in Fig. 13 are plotted against the sum contents of uranium and thorium in the ground assuming a typical abundance ratio of Th/U = 3. If one requires a 10% precision in the measurement of 0.5% K, the counting time cannot be smaller than 2 min in any case, and there must be less than 120 ppm (eU + eTh) in the ground even when the counting is extended to 20 min. It should be stressed that these statements apply to a particular instrument whose background readings are as suggested by the experimental data in Table 6. The conclusions obtained for other portable spectrometers might be slightly dif-

ferent, but would still dictate counting times of around 20 minutes for measuring a content of, say, 5 ppm eTh in 150 ppm eU with a precision of 10%.

## 2.7. Airborne gamma-ray surveys

The obvious step of mounting a window spectrometer on a flying survey platform was effectuated in the 1960s by several research groups and geophysical companies. Experiments done by a group at Rice University in Houston demonstrated that airborne measurement of the radioelement concentrations in the ground is possible with a moderately sized sodium-iodide detector (292 × 102 mm) flown at low speed close to the terrain surface (Schwarzer and Adams, 1973). The advantages offered by a compact survey system that can be installed in a light helicopter such as the Bell Jet Ranger have been confirmed from uranium reconnaissance carried out by Risø over the past several years in mountaineous areas in Greenland and Turkey. These operations are normally performed with 7,400 $cm^3$ of sodium-iodide scintillator using a nominal terrain clearance of 50 meters. A portable GAD-6 spectrometer interfaced to a microprocessor and a digital cartridge tape-unit makes up the system for getting a continuous recording of window counts along the survey tracks. Figures 14 and 15 show the equipment.

In 1968 the Geological Survey of Canada (GSC) introduced a high-sensitivity survey system based on the use of about 50,000 $cm^3$ of sodium iodide (Darnley et al., 1969). This is the approximate detector volume needed for efficient spectrometric mapping of large and relatively flat areas that favour the choice of a fixed-wing survey aircraft operated in a height of about 125 m with a speed of 50 to 60 m/s. The GSC survey system is flown in a Skyvan aircraft and has been used for the production of radiometric profiles and maps for more than a decade (see, for example, Darnley and Grasty (1971)). Like most other similar equipment developed over the years, the GSC spectrometer has been upgraded into a 256-channel recording system used in conjunction with an array of square-prismatic sodium-iodide detectors that

can be closely packed and require only one photomultiplier per detector (Bristow, 1983). The two adjacent containers in Fig. 16 provide thermal and electrical shielding for twelve prismatic detectors, each having a cross-section of 102 × 102 mm and a length of 406 mm. Figure 17 shows the associated data acquisition panel which incorporates a NOVA minicomputer for the recording and analysis of 256-channel spectra. The availability of detailed spectral information point by point along a flight line makes it possible to monitor the position of the $^{40}K$ full-energy peak at 1.46 MeV for keeping the spectrometer energy-calibrated at all times. Another aspect of accumulating counts with a multichannel spectrometer is the use of a coherent and wider spectral region than that selected by three separate energy windows. The improved measuring performance obtainable with fitting techniques and other spectrum processing methods with built-in redundancy were described by Lindén and Åkerblom (1977) and Grasty (1982).

Insight into the generation of normal spectrometer window counts at aerial survey altitudes can be gathered by first considering the atmospheric perturbation of the gamma-ray flux from the ground. Figures 18 to 20 are theoretical flux energy spectra calculated with the photon transport codes of Kirkegaard and Løvborg (1979) for a survey height of 125 m. Corresponding tabulated flux data based on energy steps of 0.05 MeV and covering the height interval from 0 to 200 m in steps of 25 m were presented by Løvborg and Kirkegaard (1975). A comparison of Figures 18 to 20 with the corresponding flux spectra at ground level (Figs. 2 to 4) shows that the discrete flux components detected in normally set energy windows (1, 2 and 3) are attenuated more than twice by 125 m of air. This attenuation reduces the window sensitivities by a similar factor. Another characteristic feature of the spectra at 125 m is an increased ratio between continuous (scattered) and discrete flux components. The relatively greater amount of scattered thorium radiation detected in the uranium window (window 2) corresponds to an increase in the stripping ratio $\alpha$ with increasing survey heights. Grasty (1975a) estimated the magnitude of this effect and showed that uranium determinations made by airborne gamma-ray spectrometry can be significantly in error if not the height dependence of $\alpha$ is taken

into consideration. Løvborg et al. (1976) derived the influence of the survey height on the two other primary stripping ratios, $\beta$ and $\gamma$. Linear working expressions for the stripping-ratio increments per meter of standard air were presented by IAEA (1979).

Predictions of window sensitivities for airborne spectrometers are hampered by the extensive Monte Carlo calculations required for setting up a response-function model as detailed as that used to describe the terrestrial spectra produced by a 76 × 76 mm detector in a portable spectrometer (subsection 2.2). Løvborg et al. (1976) suggested the use of simplified spectrum calculations in which only the full-energy peaks (and the annihilation escape peak from 2.61 MeV photons) are evaluated by means of Monte Carlo techniques. The Compton continuum associated with each peak is established by neglecting the modest amount of curvature in the continuum generated by a large scintillator. This method provided theoretical window sensitivities (and stripping ratios) for 102 mm thick, cylindrical sodium-iodide crystals at ground level and in survey altitudes of 50 and 125 m (Løvborg et al., 1978). The estimated K, U, and Th sensitivities are plotted in Figures 21 to 23 from which it may be concluded that a window sensitivity increases in a proportional manner with the detector volume. A subsequent plot of the window sensitivities against the reference heights of 0, 50, and 125 m furnishes an exponential height attenuation factor for each energy window. The approximate exponential height dependence of window count rates recorded over an infinite ground were observed experimentally by Darnley et al. (1969). It is therefore possible to predict a spectrometer window sensitivity from an expression of the form

$$S = s \cdot v \cdot \exp(-\mu h) \qquad (14)$$

where v is the detector volume and h the survey height, while s and $\mu$ are suggested numerical constants.

Table 9 shows the theoretical values of s and $\mu$ for 102 mm thick detector crystals. It should be noted that $\mu$ is specified for standard air of the density 0.001293 g/cm$^3$, and that another air

condition can be accommodated from the proportionality between density and attenuation coefficient. The $\mu$ values reported represent a best fit of the decreasing window sensitivities from 0 to 125 m; the coefficients required to remove the effect of minor departures from the nominal survey altitude are smaller (Grasty, 1976; Løvborg et al., 1978). Factors that influence the overall drop-off of the thorium count rate with increasing distances to the ground were discussed by Grasty (1975b).

The application of formula (14) to the 50,000 $cm^3$ of sodium-iodide volume contained in the GSC spectrometer system is illustrated in Table 10 which also shows the corresponding experimental window sensitivities recorded with the system over the Breckenridge test strip near Ottawa. For both the cylindrical and prismatic detectors, the calculated and experimental data are in agreement to within $\pm$ 20% or better. Formula (14), used in conjunction with the numerical values in Table 9, is accordingly usable for rough estimation of spectrometer sensitivities. A calculation based on the parameters for Risø's helicopter spectrometer ($v$ = 7,400 $cm^3$, $h$ = 50 m) shows that this system is three to four times less sensitive than the GSC survey system. However, while the Canadian Skyvan aircraft is flown at a speed of typically 60 m/s, the survey speed used by Risø is only about 30 m/s. In terms of counts per unit distance, a relatively modest helicopter spectrometer flown slowly in low altitude may produce survey data of a quality comparable to that obtainable with a fast high-sensitivity system.

## 3. BASIC CALIBRATION PROBLEMS

### 3.1. General considerations

The early applications of field gamma-ray spectrometry were based on calibration trials over ground whose radioelement concentrations were known from sampling or drilling with subsequent

laboratory determinations. Killeen and Carmichael (1970) were successful in getting the calibration constants of a portable spectrometer from a statistical analysis of field and laboratory data for more than one hundred experimental sites in the Blind River uranium region of Ontario. A similar attempt by Løvborg et al. (1969) to determine uranium and thorium calibration factors from a series of calibration measurements on the Kvanefjeld U-Th deposit, South Greenland, did not produce a reliable uranium calibration because the deposit has a predominant abundance of thorium (Nielsen, 1981). In general a system of natural calibration stations must possess a diversity of radioelement concentrations to permit a sound statistical evaluation of the four stripping ratios and three window sensitivities.

The first artifical spectrometer calibration facility was established by the Geological Survey of Canada in 1968 (Grasty and Darnley, 1971). It is situated at Uplands airport, Ottawa, and consists of five slabs or pads of concrete which are 7.6 × 7.6 m across and 46 cm thick. These sources have known and evenly distributed radioelement concentrations and make up a system of five calibration platforms which are replacing a much larger system of natural calibration sites. The dimensions and radiometric grades of the pads at Uplands airport accomodate calibration trials with high-sensitivity equipment such as that contained in the GSC Skyvan aircraft. Over the past decade similar facilities have become available at airports in five other western countries (Appendix). Figure 24 shows two survey aircraft in calibration positions on pads installed by Swedish Geological at Borlänge airport, central Sweden. Calibration pads for portable spectrometers do not require similar large dimensions since the desired counting geometry of nearly $2\pi$ can be obtained by placing the detector units in contact with the pads. Pads facilities for portable spectrometers have become available in eight countries on five continents. Figure 25 shows the GR-410 spectrometer of the present study on a removable pad which is 1 m in diameter and 50 cm thick and belongs to a facility established at Villa 25 de Mayo in the Mendoza province, Argentina.

Calibration sources prepared from radioactively loaded concrete mixes simulate a rock medium and imitates the gamma-ray transport in such a medium. The use of concrete as a source material is justified by the low cost of the mix ingredients and the large amount of expertise available on mix design and manufacturing processes. Concrete is a composite material that has many properties in common with sandstones. It consists of aggregate particles held together by hardened cement paste. In a calibration pad a smaller or larger fraction of the concrete aggregate is substituted by material of increased natural radioactivity, for example pitchblende (U), monazite or thorite (Th), and potassium feldspar (K). The greatest problems in establishing a calibration facility are associated with the procurement of suitable radioactive admixtures and with the assignment of reliable reference concentrations to the pads.

A calibration pad which is at least one meter in diameter generates spatially uniform radiation in a region around the surface centre, so that the exact positioning of the equipment is rather unimportant. Wormald and Clayton (1976) argued that the fixed planar and semi-infinite calibration geometry may be a poor representation of the geological reality and suggested a calibration system based on a granular fluid bed. Such a system might consist of a large sand box in which a point source can be placed in various positions for determining the effect of distance and depth on window counts recorded above the sand surface. By applying the resultant data to models of the field geometry, it is possible to derive the optimum calibration factors for use on narrow veins and other small exploration targets. Attenuation introduced by thin overburden (up to 20 cm) or curved terrain may also be taken into consideration. This "variable pad" concept deserves attention as a means of simulating non-uniform field geometries, but it would hardly be useful for routine calibrations which generally require a minimum of effort. Field measurements on heterogeneous ground material may be executed with a lead-collimated detector which improves the assay reliability and eliminates the need of specially adapted calibration sources (Adams and Fryer, 1964; Løvborg et al., 1971).

While a portable spectrometer placed on a concrete pad is an easily comprehensive imitation of counting with the instrument on the outcrop, it is not so obvious that experiments with aircraft parked on pads can provide the calibration constants needed in an airborne gamma-ray survey. Calibration trials like those in Fig. 25 furnish the stripping ratios and window sensitivities at ground level for the survey systems; these calibration data include the slight gamma-ray attenuation exerted by the aircraft materials. In chapter 2 it was mentioned that linear expressions are available for estimating the increments shown by the stripping ratios with increasing survey heights. Since these increments are quite small (about 1% per 10 m), it is not a problem to get the stripping ratios at an aerial survey altitude from surface measurements on pads. A window sensitivity, on the other hand, decreases more or less exponentially with increasing distances to the ground, and even a small error on the estimated height attenuation coefficient ($\mu$ in formula (14)) might jeopardize the reliability of an exponential correction applied to a window sensitivity measured on pads. In spite of the considerable number of airport calibration facilities installed over the years, the majority of survey organizations actually abstain from using their pads for the estimation of in-flight sensitivity factors. Instead it has become the practice to get these calibration constants from the stripped window count rates recorded in flights over selected test ranges.

A test range may be represented by a strip of ground, between 2 and 10 km long, whose radioelement concentrations have been determined by intense sampling or from grid-assays with portable spectrometers. Test ranges are available in Canada (Grasty and Charbonneau, 1974), Finland (Multala, 1981), Israel (Aviv and Vulkan, 1983), and the USA (Poote, 1978). Recent experiments over the Canadian Breckenridge strip near Ottawa show that an area covered by soil may produce seasonally varying window count rates (Grasty, 1984). The Breckenridge strip is formed by clay soil. In the spring, when the soil is still frozen, the uranium count rate is high, because there is very little leakage of $^{222}Rn$ from the ground. Later in the season the radon seal represented by soil moisture is weakened due to evaporation, so

that insufficient radon becomes available for sustaining the equilibrium content of $^{214}Bi$ in the ground. As a result the uranium count rate over the area shows an overall decrease of about 30% between March and July. In the two other energy windows, thorium and potassium, the reduced soil moisture has the adverse effect of increasing the count rates by 50 to 60% because there are fewer water molecules to attenuate the gamma-ray flux. Calibration conditions like these are far from ideal and serve as a warning against an uncritical use of test ranges.

A likely method to determine the airborne window sensitivities from calibration measurements with pads may evoke from a study of Dickson et al. (1981) who placed a package of four prismatic sodium-iodide detectors on plywood sheets and recorded the spectra from the airport pads in Grand Junction, Colorado (Appendix). By varying the number of sheets and converting the total plywood thicknesses into equivalent columns of air, it was possible to simulate aerial survey heights of up to 112 m. The purpose of this experiment was to perform a mathematical analysis of the spectral shape as a function of the detector-source distance in air. Similar measurements with standard geophysical detector packages might be effectuated routinely for calibration purposes. Such a technique would involve a summation of the window sensitivities recorded for the individual detector packages of a high-sensitivity spectrometer system. It would also be necessary to measure the attenuation from installing the equipment behind an aircraft structure.

Risø's helicopter spectrometer (Figs. 14 and 15) is calibrated at intervals by placing the detector units successively on calibration pads that are only 3 m in diameter. Figure 26 shows such a calibration trial, executed directly on the pad surface without inserted sheets of plywood to simulate the gamma-ray absorption in the air. The window sensitivities determined in this way are adapted to a nominal survey height of 50 m by means of exponential correction factors similar to those calculated with formula (14) and stated in Table 23 of the IAEA report "Gamma-Ray Surveys in Uranium Exploration" (IAEA, 1979). This simplified calibration technique was tested from a flight along a 1.5 km long survey

line traversing exposed mineralization on the plateau formed by the Kvanefjeld U-Th deposit, South Greenland. The area had previously been surveyed in detail with portable spectrometers (Løvborg et al., 1980), and the resulting uranium contour map was used for estimating the U surface concentrations along the airborne track. Five fiducial markers from the test flight made it possible to obtain ground and airborne estimates of the average U concentrations in four sectors of the flight line. These estimates are plotted against each other in Fig. 27. The regression line for the data suggests that the uranium calibration of the helicopter spectrometer (as expressed by the stripping ratio $\alpha$ and the window sensitivity $s_U$) is giving reasonable field results. Airborne uranium measurements based on direct pad calibrations and a subsequent theoretical height correction may apparently be less than about 15% in error.

## 3.2. Counting and calibration geometries

The tens of meters of detector elevation in an airborne gamma-ray survey make the window count rates insensitive to a surface relief of several meters and justify instrument calibrations in planar geometry. In field work with a portable spectrometer the detector unit is placed on the terrain surface, and there is no other elevation than that represented by the distance from the assay spot to the centre of the sodium-iodide crystal. For the 76 × 76 mm detector used with GR-410 spectrometers this distance amounts to 70 mm. An elevation this small is of the same magnitude as the relief of even a rather smooth and plane natural rock face. Many of the outcrops assayed in a typical grid survey would probably have reliefs of several hundred millimeters.

To justify the calibration of portable spectrometers on smooth and plane concrete pads, consider Fig. 28 in which P is a detector point above a homogeneous and uniformly radioactive rock medium that crops out between $P_1$ and $P_2$. An arbitrarily oriented spherical co-ordinate system $(r,\theta,\phi)$ is used to describe the envelope of the medium and the transport of gamma rays from an emitter point to P. Useful information which can be expressed in

simple mathematical form is obtained from the introduction of three additional model assumptions: 1) The envelope of the rock medium is of the functional form $r = r(\theta,\phi)$, i.e. no line drawn from P can intersect the rock surface more than once; 2) the overburden is a 100% effective gamma-ray absorber; and 3) there is no absorption of gamma rays in the air between P and the outcrop.

It is relevant to start the mathematical treatment by introducing the small solid angle $d\Omega = \sin\theta\, d\theta\, d\phi$ defined by small displacements $d\theta$ and $d\phi$ from a fixed spatial direction $(\theta,\phi)$. To get the flux of photons at P from a small rock volume $dV = R^2\, d\Omega dR$ with co-ordinates $(R,\theta,\phi)$, one has to place a unit area normally to $(\theta,\phi)$ in P. Since the photons from dV are evenly distributed on all directions, the fraction directed against such a unit area equals $1/4\pi R^2$. Some of the photons in the beam from dV to P are scattered or absorbed along the travelling length R-r in the rock medium. The corresponding attenuation factor is given by $\exp[-\mu(R-r)]$ where $\mu$ is the total linear attenuation coefficient of the medium for gamma-rays of the energy considered. This quantity should not be confused with the $\mu$ in formula (14) which is an empirical height attenuation coefficient for use in airborne gamma-ray surveys. Assuming that each $cm^3$ of the rock medium emits just one gamma photon per second, the desired flux contribution becomes

$$d\phi = \frac{1}{4\pi R^2} \int_{R=r}^{\infty} \exp[-\mu(R-r)]dV$$

$$= \frac{d\Omega}{4\pi} \int_{r}^{\infty} \exp[-\mu(R-r)]dR \qquad (15)$$

$$= \frac{d\Omega}{4\pi\mu} .$$

This result shows that $d\phi/d\Omega$ is constant and independent of r, i.e. the angular flux density is the same in all directions from P towards the exposed rock surface, regardless of the relief

shown by the latter. The total photon flux in P is consequently given by

$$\phi = \frac{\Omega}{4\pi\mu} \tag{16}$$

where $\Omega$ is the solid angle in which the outcrop is viewed from P. A window sensitivity for this geometry would be identical to the sensitivity recorded over a plane calibration source in a solid angle of $\Omega$.

As indicated in the preceding subsection, the reference geometry adopted in the use of calibration pads is not only planar, but also semi-infinite. When the envelope of the rock medium in Fig. 28 degenerates into an infinite surface without overburden, the calculation of $\Omega$ takes the simple form

$$\Omega = \int_{\phi=o}^{2\pi} \int_{\theta=o}^{\pi/2} \sin\theta \, d\theta = 2\pi \, , \tag{17}$$

i.e.

$$\phi_{\infty} = \frac{2\pi}{4\pi\mu} = \frac{1}{2\mu} \, . \tag{18}$$

The associated geometry factor,

$$F_g = \frac{\phi}{\phi_{\infty}} = \frac{\Omega}{2\pi} \tag{19}$$

is not particularly relevant in the field where it is difficult to make a reliable estimate of $\Omega$. $F_g$ is however the figure needed for expressing how closely a $2\pi$ measuring geometry is reproduced in recording calibration counts on a pad. Many of the calibration facilities established up to the present are based on pads which are either circular or approximate circular sources. Løvborg et al. (1972) presented an expression for calculating the geometry factor centrally above a cylindrical source cylinder of arbitrary

dimensions. The expression contains first and second order exponential integrals and does not provide an immediate idea of the manner in which the counting geometry is influenced by the detector elevation and the source radius. As outlined in Fig. 29, it is worthwhile trying to regard the surface of a calibration pad as a plane outcrop of an infinite medium whose envelope is a cone drawn from the detector point. The solid angle for this simplied geometry is obtained by replacing the upper $\theta$ integration limit in (17) by the half cone angle $\theta_{max}$, i.e.

$$\Omega = 2\pi(1 - \cos\theta_{max}) \ . \qquad (20)$$

Assuming now that the detector elevation h is much smaller than the pad radius R, it is permissible to calculate $\cos\theta_{max}$ as h/R. One then arrives at the very simple result

$$F_g \approx 1 - h/R \ . \qquad (21)$$

To estimate the application range of (21), the corresponding exact formula of Løvborg et al. (1972) was used to simulate the detection of 2.61 MeV gamma rays over pads supposed to be 0.5 cm thick (a typical dimension; Appendix). The pads were ascribed a density of 2.2 g/cm$^3$, corresponding to a linear attenuation coefficient of 0.087 cm$^{-1}$ derivable from Table 12 in the next subsection. The formula was evaluated numerically for source radii of between 40 cm and 4 m using detector elevations selected from a series of constant h/R ratios. From the plot, Fig. 30, it can be seen that the approximation provided by (21) is the better, the smaller the detector elevation. For $R > 1$ m and $h/R < 0.20$ the approximated geometry factors are less than 3% overestimated. An error of this size is acceptable since it may be hard to estimate h very accurately. The steep slope of the curves in Fig. 30 for source radii smaller than 0.5 m shows the difficulty of estimating reliable geometry factors for small pads.

Four of the airport facilities included in the Appendix consist of rectangular or square pads. Geometry factors for these may be derived by replacing them mathematically with a series of equi-

valent circular pads. The equivalent surface radius $R_e$ of a rectangular source with side lengths "a" and "b" is calculated as indicated in Fig. 31 which is a top view of a source with added inscribed and equivalent circles. As suggested by the arrow, the procedure consists in replacing the four corner areas by four ring segments attached to the incribed circle. This is done so that the solid angle of detection from a point on the source axis remains the same. For reasonably small detector elevations h, a small surface element dA in a radial distance of $r > \frac{1}{2} a$ is viewed in a solid angle of

$$d\Omega = \frac{dA \cdot \cos\theta}{h^2 + r^2} \approx dA \cdot \frac{h}{r^3} \qquad (22)$$

where $\theta$ is an azimuth angle similar to that in Fig. 28. The integration of $d\Omega$ over the respective target areas (the shaded areas in Fig. 31) is easily performed in a polar co-ordinate system. The two resulting $\Omega$ contributions are identical for

$$R_e \approx \frac{\pi}{4} \frac{ab}{\sqrt{a^2 + b^2}} . \qquad (23)$$

$R_e$ might also be estimated simply by calculating the circle that has the same area as the real calibration pad. The resulting expression

$$R_e = \sqrt{ab/\pi} \qquad (24)$$

is actually less than 2% different from that in (23) when a=b.

## 3.3. Gamma-ray mass attenuation

As they were introduced in subsection 2.3, spectrometer window sensitivities are postulated proportionality factors which relate the window count rates to the radioelement concentrations by weight in the ground. To establish the connection from these calibration factors to source parameters such as chemical composition, density, and moisture content it is relevant to let "x" denote an in-situ concentration relating the mass of radioelement in a unit volume to the mass of all atoms present in

With this definition of x, the gamma-ray emission from a unit volume becomes proportional to $x \cdot \rho$ where $\rho$ is the bulk density of the source medium. It then follows from (18) and (19) that the flux input to a spectrometer window can be represented by the expression

$$\phi = \frac{C}{\mu/\rho} \cdot x \qquad (25)$$

where C contains the geometry factor and the photon yield of the radioelement. The physical and chemical properties of the source is contained in the term $\mu/\rho$ which is the mass attenuation coefficient of the source material and is measured in units of $cm^2/g$. Gamma-ray attenuation is principally an overall effect of Compton scattering, photoelectric effect, and pair production (the last process starting at a photon energy of 1.022 MeV). Table 11 shows the contributions to $\mu/\rho$ from these processes in $SiO_2$ (quartz) at photon energies of 1.46, 1.76, and 2.61 MeV. These data are from a library of evaluated photon interaction cross-sections based on a compilation by the Lawrence Livermore Laboratory and available from the NEA Data Bank at Gif sur Yvette, France. A similar up-to-date tabulation of total mass attenuation coefficients for 40 elements was published by Hubbell (1982). Table 11 shows that Compton scattering (incoherent scattering) is the only really important interaction process between 1.5 and 3 MeV in a chemical constituent like $SiO_2$ which is more than 40% abundant in most earth materials. The same applies to the other standard oxides used for expressing the concentrations of major elements in analysed sample material.

In a Compton scattering event the incident gamma-ray photon interacts with an orbital electron to which a fraction of the photon energy is imparted. The fundamental relations giving the energy loss and change of direction for the photon are presented and explained in, for example, a classical textbook of Evans (1955). Assuming that the electrons of the scattering medium can be regarded as unbound, and neglecting the small probabilities of photoelectric effect and pair production, the linear attenuation coefficient $\mu$ becomes proportional to $\Sigma n_e$, the total number of electrons per unit volume of the medium. An element with

atomic number Z, atomic weight A, and mass abundance w contributes

$$n_e = \frac{\rho w}{A} N_o \cdot Z \qquad (26)$$

electrons per $cm^3$ where $N_o = 6.025 \times 10^{23}$ atoms per mole is Avogadro's number. Consequently, by introducing an energy-dependent proportionality factor k one may write

$$\mu/\rho = k \cdot \sum_i w_i \frac{Z_i}{A_i} = k \cdot \overline{Z/A} \qquad (27)$$

in which the summation is extended over all elements present in the substance. If the latter is thought of as a rock medium or the concrete of a calibration pad, it can be seen that the chemical effect associated with field gamma-ray spectrometry depends on the average ratio $\overline{Z/A}$ for the elements contained in the sources. Over the range of atomic numbers from Z = 2 to Z = 30 the number of protons and neutrons in the nuclei is approximately the same, corresponding to Z/A = 0.5 (Evans, 1955). This observation suggests that the elements from helium to zink have comparable mass attenuation coefficients at the energies for which scattering is the predominant interaction mode. Hydrogen is the only element whose nuclei do not contain neutrons, so that Z/A = 1. The hydrogen supplied to a source material in the form of absorbed moisture generates surplus gamma-ray attenuation which is specially dealt with in the following subsection.

Formula (27) has the advantage that it makes it possible to calculate the thickness of one material that will produce the same gamma-ray attenuation as a known thickness of another material. For example, 1 cm of aluminium metal ($\rho$ = 2.7 $g/cm^3$, Z/A = 0.482) is equivalent to 20.17 m of standard air ($\rho$ = 0.001293 $g/cm^3$, $\overline{Z/A}$ = 0.499). Such a conversion can be used in airborne gamma-ray surveys to incorporate the aircraft floor and detector container as an equivalent additional survey height (Grasty, 1975b; Løvborg and Kirkegaard, 1975).

Table 12 contains a set of mass attenuation coefficients derived for standard chemical rock constituents by means of the Lawrence

Livermore compilation of elemental photon cross sections. The listed data can be used to estimate the attenuation of spectrometer signals in a ground material of specified composition. An overall attenuation coefficient is calculated as

$$\mu/\rho = \sum_j w_j \, (\mu/\rho)_j \qquad (28)$$

where $w_j$ is the weight abundance of the j'th standard oxide in the chemical code for the substance. Table 12 shows that the contributions to $\mu/\rho$ from the single chemical constituents vary by as little as 2% when $H_2O$ is left out. It is therefore unimportant whether the detected gamma rays are coming from an outcrop of solid granite, a soil formation, or a concrete calibration pad. As long as the source material is dry and has a negligible content of elements with $Z \gtrsim 30$, the flux of high-energy photons per mass concentration unit of radioelement remains the same.

The concrete included in Table 12 is of a composition like that used by Løvborg (1983) for the manufacture of total-count calibration blocks with approximately 80 ppm eU and 160 ppm eTh ("M" concrete). The total content of $H_2O$ in this source material amounts to 11% of which roughly 4% is pore moisture and the rest consumed mix water. Mass attenuation coefficients for air are presented in the table to demonstrate the uniformity of $\mu/\rho$ independently of the physical state of the attenuating medium.

## 3.4. Moisture effect

For any porous source material it is possible to distuinguish between pore moisture on the one hand and chemically bound $H_2O$ on the other. The distinction is based on the fact that pore moisture can be evaporated by heating to 105°C which is below the temperatures required to release $H_2O$ molecules from the chemical bondings. Drying at 105°C until constant weight is a routinely used precaution in connection with laboratory analysis of granular sample material and justifies the introduction of an "$x_d$", the radioelement concentration per dry weight of material. The link between $x_d$ and the in-situ concentration "x" from the

preceding subsection is provided by the evaporable moisture content of the field target or calibration pad in question.

It is the most appropriate to describe an evaporable moisture content "w" by dividing the weight of solid material contained in a source volume into the weight of the pore moisture absorbed in that volume. This definition of w corresponds to the relation

$$x = x_d/(1 + w) \ . \tag{29}$$

To get the largest possible deviation between x and $x_d$, one has to estimate the maximum moisture absorption in the source. For a coherent material like rock or concrete, $w_{max}$ is given by

$$w_{max} = \frac{1}{\rho_d} \cdot \frac{p}{1-p} \tag{30}$$

where p is the porosity and $\rho_d$ the average density of the "dry" source constituents in $g/cm^3$.

In a "wet" source the pore moisture has an abundance of w/(1+w). While the ratio $\overline{Z/A}$ equals 0.555 for water, the solid source material can be ascribed a $\overline{Z/A}$ of 0.50 (assuming a negligible effect of the chemically bound $H_2O$). Formula (27) accordingly suggests a resulting value of

$$\overline{Z/A} = \frac{0.50 + 0.555\ w}{1 + w}$$

$$= 0.5 \cdot \frac{1 + 1.11\ w}{1 + w} \ . \tag{31}$$

By combining (29) and (31) with (25) and (27) it can be seen that the gamma-ray emission (flux) from a source containing pore moisture is governed by an expression of the form

$$\phi = \phi_{1,d} \frac{x_d}{1 + 1.11\ w} \tag{32}$$

where $\phi_{1,d}$ represents the emission from a dry source containing one unit of radioelement concentration.

Formula (32) supplies the information for answering the question whether the calibration of a field spectrometer should be based on "wet" or "dry" reference concentrations. A calibration pad whose radioelement concentration has been estimated from assays of crushed and dried concrete (as described in chapter 5) might simply be assigned a reference concentration of $x_d$ followed by an attempt to measure the concentration by dry weight, $y_d$, in a field target. The error $\Delta y_d$ associated with such a procedure depends on the moisture contents $w_x$ and $w_y$ of calibration pad and target material respectively. It is easily shown that the relative magnitude of this error is

$$\frac{\Delta y_d}{y_d} = \frac{1 + 1.11\ w_x}{1 + 1.11\ w_y} - 1 \ . \qquad (33)$$

Alternatively, the in-situ concentration "x" of the calibration pad might be evaluated and used as a reference value for measuring the similar concentration "y" in the field target. This "wet-to-wet" experimental approach has an associated relative error of

$$\frac{\Delta y}{y} = \frac{(1 + 1.11\ w_x)(1 + w_y)}{(1 + 1.11\ w_y)(1 + w_x)} - 1. \qquad (34)$$

In Fig. 32 the two error expressions are plotted for source moisture contents of up to 30%. The calibration pad is assumed to contain 5% pore moisture, so that a ground of this moisture content is assayed without error for both "dry" and "wet" calibration conditions. From the curve labelled "dry calibration" it is seen that the direct use of radioelement concentration per dry weight of material is inappropriate when there is an unknown difference of several percent between the moisture contents of field target and calibration pad. In other words, a field gamma-ray spectrometer cannot provide a set of normal analytical K-eU-eTh concentrations for characterizing the radioactivity of an earth material. Conversely, the use of in-situ, or "wet", radioelement

concentrations reduces the assay error to 2% even for a moisture difference of 30% between the target material and the pad.

Experimental in-situ radioelement concentrations are of immediate relevance in calculations of exposure rates from spectrometric survey data (cf. the conversion factors in Table 4). Grasty et al. (1984) were recently involved in estimating the ground-level exposures in 33 areas of Canada that have been surveyed from the air with the GSC high-sensitivity spectrometer system. This study demonstrated the large seasonal soil moisture variations which occur in a climate like that in Canada. For example, the soil forming the Breckenridge test strip of the GSC has an average moisture content of typically 27% in the summer, while about 40% moisture is representative for samples collected in the autumn. These and other observations of soil moisture suggest that it may be advisable to combine the use of a portable spectrometer in soil-covered areas with the collection of material for moisture assay. Once the moisture has been estimated, the recorded in-situ concentrations may be converted into normal concentrations by dry weight of soil for use in geochemical interpretations.

## 3.5. Radioelement depth variations

For field targets in general one must expect at least some variation of the radioelement content down through the upper ~ 35 cm of the ground material. The extreme case is presented by a layer of overburden whose natural radioactivity is negligible compared to the radioactivity of the underlying mineralization. Such a layer attenuates the window count rates in the same way as do the air masses involved in airborne gamma-ray surveys. For example, 10 cm of soil with a bulk density of 1.6 g/cm$^3$ can be represented by ~ 125 m of standard air which in turn reduces the count rate in the thorium window by approximately a factor of 3. A cover of water or snow produces a similar effect. Given the water or snow thickness, the equivalent air column in g/cm$^2$ is 11% greater than the $H_2O$ surface density in g/cm$^2$. In subsection 2.7 it was mentioned that increasing aerial survey altitudes cause a spectral shift in which the continuous part of the flux energy spectrum is increased relative to the discrete flux components. Con-

sequently, it is theoretically possible to estimate an overburden effect by forming the ratio between two data regions selecting different proportions of scattered and direct radiation. Dickson et al. (1979) showed experimentally that good contrast of measurement can be obtained by combining a total-count threshold of 0.18 MeV with an energy window from 0.66 to 1.01 MeV. Field use of a 76 × 76 mm detector should make it possible to assess up to 60 $g/cm^2$ of overburden on uranium mineralization with a grade of 0.25% $U_3O_8$. Thus, a five-channel portable spectrometer, or even better: a multichannel spectrum-recording device like the Czechoslovak GS-256, seem to have potential for extending the application of in-situ radioelement assays. Calibration pads used in conjunction with a plywood cover would provide the factors required to overcome the effect of shallow overburden.

A more difficult problem occurs when a natural gamma-ray emitter becomes progressively depleted with decreasing distances in the source material to the air-ground interface. Negative concentration gradients in the direction of the interface are exhibited by $^{214}Bi$ deposited by diffusing $^{222}Rn$ (radon) in dry soil. The resulting diminuation of the photon flux at 1.76 MeV can be estimated computationally from the emanation power P and the effective diffusion coefficient D* describing, respectively, the amount and mobility of the radon in the voids between the soil particles. It can be shown that the sum content of bound and mobile radon has an exponential depth distribution given by

$$q(z) = q_\infty \left[1 - P \cdot \exp(- z \sqrt{\lambda/D^*})\right] \qquad (35)$$

where z is the vertical depth, $q_\infty$ the radon concentration at infinite depth, and $\lambda = 2.10 \times 10^{-6}\ s^{-1}$ the decay constant of $^{222}Rn$. Since formula (35) also governs the vertical distribution of the $^{214}Bi$ emitters in the ground, the resulting gamma-ray flux at the surface can be obtained by placing a usual spherical coordinate system in a detector point above a plane soil medium of exponentially increasing radioactivity. By normalizing the result to the result for a source with uniformly distributed $^{214}Bi$ (formula (18)), it is possible to derive the relative flux diminuation over soil containing diffusing radon. The expression for the radiation loss turns out to be

$$-\frac{\Delta\phi}{\phi} = P \cdot \mu\sqrt{D^*/\lambda} \cdot \ln(1 + \frac{1}{\mu}\sqrt{\lambda/D^*}). \qquad (36)$$

Since the $^{214}Bi$ radiation is detected by window counting at 1.76 MeV, the $\mu$ in (36) would be taken as the product of the soil density and an estimated mass attenuation coefficient of 0.048 $cm^2/g$ (Table 12).

The first observation made from (36) is a proportional relation between the radiation loss and the emanation power P which is the ratio between escape and production of radon for the soil particles. According to Barretto et al. (1972), calcareous soils and alluvium are particularly strong emanators yielding P values of 20 to almost 60%. Clay soil emanates between 20 and 35%, while sandy soil comes at the bottom with P in the range from 10 to 20%. These differences in emanation power are related to the residence mode of the $^{226}Ra$ which is the immediate source of $^{222}Rn$ production. The stronger emanation of clay soil relative to sandy soil can be explained by the large emanating surface formed by clay particles with a radium coating orginating from adsorbed uranium.

To illustrate the significance of the effective diffusion coefficient D*, consider Fig. 33 in which the curve for $\rho$ = 1.4 $g/cm^3$ is supposed to represent dry soil of 100% emanation power. Schroeder et al. (1965) measured D* = 0.036 $cm^2/s$ in dry and sandy alluvium; a value amounting to as much as 0.10 $cm^2/s$ was recorded for very dry and powdery soil without any appreciable cover. Diffusion coefficients greater than about 0.01 $cm^2/s$ are typical of granular materials with little or no moisture in the porespaces (Tanner, 1964). Figure 33 shows that the associated loss of gamma radiation at the surface exceeds 0.9 P and consequently may run as high as ~ 55% over certain soil formations. Concrete, on the other hand, is a compact material offering a considerable resistance to the migration of radon in the pore spaces. Culot et al. (1976) found a relaxation distance of around 10 cm for radon diffusing across a concrete wall, corresponding to a diffusion coefficient of about $2 \times 10^{-5}$ $cm^2/s$. This value used in conjunction with the curve for $\rho$ = 2.2 $g/cm^3$ in Fig. 33

suggests a radiation loss of 0.45 P on the surface of a calibration pad loaded with uranium ore of P% emanation power. Since the similar figure for uranium ore intermixed with unconsolidated sand would be approximately 0.9 P, there is a net advantage of embedding the particles in a cement paste for reducing the radon diffusion speed.

Absorbed moisture has a retarding influence on the migration of radon in a porous source medium. Water in itself has a radon diffusion coefficient of $1.13 \times 10^{-5}$ cm$^2$/s, but in a saturated medium there is virtually no radon migration since the diffusion is confined to porespaces rather than to a uniform volume of water (Tanner, 1964). Uranium counts recorded over initially saturated soil are negatively affected by the radon exhalation caused by moisture evaporation, while there is an adverse influence of the reduced gamma-ray attenuation in unsaturated material. One can get a quantitative impression of the resulting overall effect in the uranium window by considering a typical clay soil with a saturation moisture content of 40% and an emanation power of 30%. Assuming that the soil particles contain 1 ppm eU ($x_d$ = 1 ppm), the spectrometer would record 0.69 ppm eU with the soil in the saturated state and no occurrence of radon migration (use of formula (32) for a "dry" spectrometer calibration). In the completely dry state of the soil one would have a radon diffusion coefficient of around $10^{-2}$ cm$^2$/s, which corresponds to a radiation loss of 27% and a recorded concentration of 1-0.27 = 0.73 ppm eU. These numerical data for uranium assays under saturated and dry soil moisture conditions suggest a resulting increase of 6% in the uranium count rate during a hypothetical phase of complete moisture evaporation. The similar increase shown by the thorium count rate would only be governed by the reduced gamma-ray attenuation which amounts to 44%.

The above example does not fit the <u>decrease</u> of 30% shown by the airborne uranium data collected between spring and summer over the clay soil of the Canadian Breckenridge test strip (subsection 3.1). In fact, several mechanisms are active in causing a depleted radon content in soil surfaces subject to drying or in a dry state. Tanner (1980) discussed the enhanced emanation power

of mineral grains surrounded by a water film in which recoiling $^{222}Rn$ atoms from the alpha decay of $^{226}Ra$ are entrapped. This radon becomes mobile when evaporation begins and is an additional source of gamma radiation losses as long as there is any moisture left in the porespaces. Another factor to be considered is the soaking action of atmospheric pressure drops on the soil gas in unsaturated pore systems. Not only soil, but also a number of common rock types and uranium ores have emanation powers exceeding 10% (Barretto, 1972; Austin, 1975). The use of an ore of low emanation power is obviously an urgent necessity in the construction of a uranium-loaded calibration pad.

## 4. CALIBRATION FACILITIES BASED ON CONCRETE PADS

### 4.1. Calibration equations

The first question that arises in the planning of a spectrometer calibration facility is the number of sources required and the radioelement concentrations to be contained in the sources. A theoretical approach to the problem can be made by setting up a linear expression for the count rate n recorded over a calibration pad in an arbitrarily selected spectral region. Such an expression is of the form

$$n = g_K \cdot x_K + g_U \cdot x_U + g_{Th} \cdot x_{Th} + b \qquad (37)$$

where $x_K$, $x_U$, and $x_{Th}$ are the pad concentrations in %K, ppm eU, and ppm eTh. The "g" factors represent radioelement sensitivity in the considered energy interval ($g_K = 0$ if the interval is placed above the potassium window). "b" is an extended background term which may include a terrestrial contribution from the area chosen as a calibration site. To facilitate the formulation of (37) for a series of P pads, the radioelements are conveniently numbered from 1 to 3, so that "1" denotes potassium, "2" uranium, and "3" thorium. In assigning numbers to the pads,

it is adequate to progress from 0 to P-1 with pad 0 taken as the source that produces the smallest count rate. Using these numbering conventions, the system of P linear equations can be represented by the single matrix equation

$$\bar{\bar{N}} = \bar{\bar{X}} \cdot \{g_K, g_U, g_{Th}\} + \bar{\bar{B}} \tag{38}$$

with

$$\bar{\bar{X}} = \begin{bmatrix} x_{01} & x_{02} & x_{03} \\ x_{11} & x_{12} & x_{13} \\ \cdot & \cdot & \cdot \\ \cdot & \cdot & \cdot \\ \cdot & \cdot & \cdot \\ x_{p-1,1} & x_{p-1,2} & x_{p-1,3} \end{bmatrix}$$

and

$$\bar{\bar{B}} = \begin{bmatrix} b_0 \\ b_1 \\ \cdot \\ \cdot \\ \cdot \\ b_{p-1} \end{bmatrix}.$$

If the pads are going to serve as reliable calibration sources, they must be placed in an area of low and uniform natural radioactivity. Assuming thus that the "background" is the same on all the pads, i.e. $b_0 = b_1 = \cdots = b_{p-1}$, we can eliminate the $\bar{\bar{B}}$ term in (38) by subtracting the equation for pad 0 from all the other equations contained in (38). The new equations generated by this subtraction can be written in the compact matrix form

$$\bar{\bar{\Delta}}_n = \bar{\bar{\Delta}}_x \cdot \{g_K, g_U, g_{Th}\} \tag{39}$$

with

$$\underline{\underline{\Delta}}_n = \begin{bmatrix} n_1 - n_0 \\ n_2 - n_0 \\ \cdot \\ \cdot \\ \cdot \\ n_{p-1} - n_0 \end{bmatrix}$$

and

$$\underline{\underline{\Delta}}_x = \begin{bmatrix} x_{11}-x_{01} & x_{12}-x_{02} & x_{13}-x_{03} \\ x_{21}-x_{01} & x_{22}-x_{02} & x_{23}-x_{03} \\ \cdot & \cdot & \\ \cdot & \cdot & \\ \cdot & \cdot & \\ x_{p-1,1}-x_{01} & x_{p-1,2}-x_{02} & x_{p-1,3}-x_{03} \end{bmatrix} .$$

Equation (39) is seen to provide a connection between count rate differences and differences between calibration grades, calculated by using pad 0 as a zero reference. To solve (39) with respect to $\{g_K, g_U, g_{Th}\}$, the facility must obviously contain a minimum of four pads, including the zero reference. If a calibration system based on P = 4 is accepted, the determination of the calibration factors involves a solution of three simultaneous equations. To make a solution possible, the pad concentrations must be chosen so that the determinant associated with $\underline{\underline{\Delta}}_x$ becomes different from zero. This implies that it is necessary to spike pads 1, 2, and 3 with varying proportions of K, U, and Th.

The concrete pads of an ideal minimum calibration system would provide grade differences of the matrix

$$\underline{\underline{\Delta}}_x = \begin{bmatrix} \delta_K & 0 & 0 \\ 0 & \delta_U & 0 \\ 0 & 0 & \delta_{Th} \end{bmatrix}$$

which makes it possible to measure an instrumental response to a particular radioelement on a particular pad. According to IAEA (1976), the primary sources for the calibration of portable spectrometers should be spiked with concentrations of $\delta_K$ = 5% K, $\delta_U$ = 20 ppm eU, and $\delta_{Th}$ = 40 ppm eTh. Identical uranium and thorium calibration grades are specified in the IAEA recommendation for the pads required to determine the stripping ratios of an airborne spectrometer at the surface. In practice it is not possible to manufacture a source which is exclusively enriched in a single radioelement. Potassium presents the greatest problem since the K feldspar typically needed to obtain a pad concentration of 5% K may contain several ppm more uranium and thorium than the low-radioactivity material selected for the zero reference. It may also be necessary to accept an unwanted concentration of U or Th in the raw materials available for the preparation of uranium and thorium concrete mixes.

There are two reasons why it may be desirable to expand a basic system of three calibration sources plus a zero reference. Firstly, the inclusion of extra sources offers some security against calibration inaccuracy due to an error on the calibration grade assigned to a single source. Such an error might occur because a pad is less homogeneous than believed, or it could result from radon exhaled from the pad surface. Secondly, a series of pads that have been spiked with a whole range of uranium and thorium contents makes it possible to select the combination of sources that best accomodates the radioactivity levels to be dealt with in the field. This latter consideration is relevant in the design of facilities for portable instruments whose main application is ore grade estimation. When more than four pads are involved in a calibration trial, it is the most expedient to estimate the wanted calibration factors from the application of least-square techniques to the Eq. (38) (chapter 5).

## 4.2. Existing calibration systems

The tabulations in the Appendix contain information on the source configurations and calibration grades for pads facilities visited in the present study. The data show that there are different preferences behind the calibration systems implemented in different parts of the world. A key for describing such a system in condensed form has been introduced by assigning letters to pads of various radioactive compositions. Pads with a preferential enrichment in potassium, uranium, or thorium are identified by the letters K, U, and T respectively. If a pad loaded with uranium ore contains thorium in a proportion corresponding to Th/U > 0.3, the letter M is used for classifying the pad as "mixed". A pad serving as a zero reference is characterized by the letter B which stands for "background" or "blank". The further use of a numerical index to describe the occurrence of more than one pad of a particular type makes it possible to describe a calibration system by a simple compound code.

The existing airport calibration facilities are based on a configuration of four or five large pads. The older installation at Uplands airport, Ottawa, represents a $T_2M_2B$ calibration system whose potassium concentrations differ by less than 0.7% K. Such a system does not permit an accurate determination of K window sensitivities. The facilities at Helsinki, Soreq (Israel), Lanseria (South Africa), Borlänge (Sweden), and U-Tapao (Thailand) are of a more recent design and exemplify the basic KUTB configuration. At Walker Field airport in Grand Junction, Colorado, a KUTMB system has been chosen. The uranium and thorium grades associated with five of these facilities do not exceed 30 ppm eU and 50 ppm eTh, in fair agreement with the IAEA recommendation of 20 and 40 ppm respectively. Two facilities (the ones at Helsinki and Lanseria) possess grades of 50 to 60 ppm eU and over 100 ppm eTh. A high-sensitivity airborne spectrometer system exposed to radioactive concentrations of this magnitude may easily be overloaded with a high rate of detector pulses. Aviv and Vulkan (1983) found that the concentration of 30 ppm eTh in the T pad at Soreq was sufficient to produce a pulse pile-up effect of 4% in the thorium window of

a spectrometer in which ten prismatic detectors were coupled together to provide a total sodium-iodide volume of 42,000 $cm^3$. Therefore, even when the radioelement spikings of airport pads are modest, it may be necessary to calibrate the detectors in the aircraft individually or in pairs.

Calibration systems for portable spectrometers offer the possibility of using multiple source configurations by virtue of the relatively low cost associated with the manufacture of small concrete pads. The facilities included in the Appendix contain from five to as much as ten sources. The ten pads at Bell Corners near Ottawa form a $K_3U_3T_3B$ configuration designed for calibration trials at levels of (1, 10, 10), (1.5, 40, 80), and (3, 500, 400) where the numbers represent approximate calibration grades in %K, ppm eU, and ppm eTh. Sources spiked with several thousand ppm uranium or thorium are available at Pelindaba (South Africa) and Villa 25 de Mayo (Argentina). These sources are too hot for being incorporated in the calibration of an instrument like the Geometrics GR-410, whereas they may serve as useful reference targets for total-count scintillometers or GM counters.

From the Appendix it is obvious that the laboratories in general have loaded their pads for portable spectrometers more heavily than specified in the IAEA recommendation. This is mainly because of the long time needed for counting on a source with 20 ppm eU or 40 ppm eTh. With a GR-410 unit it would take half an hour to get a precision of 1% on the window counts recorded on such a source. The Australian facility at the CSIRO Institute of Energy and Earth Resources are based on U and Th calibration grades of 90 and 160 ppm respectively and permits a reliable measurement of U and and Th calibration constants in about two times 10 minutes. Spiking levels of 100 ppm eU and 200 ppm eTh should perhaps be the accepted standard in the future.

## 4.3. Physical dimensions involved

Numerical calculations similar to those used for getting the unapproximated geometry factors plotted in Fig. 30 suggest that the effect of increasing the thickness of a gamma-ray source is very

limited beyond a mass per unit area of 70 g/cm$^2$. About 35 cm of normally dense concrete are sufficient to produce 99% of the radiation that would have been obtained with a much thicker source. Pads listed in the Appendix are between 25 and 60 cm thick, a thickness of about 50 cm being the most common. Half a meter of concrete mix is sufficient to furnish the strength required for supporting a fully loaded geophysical aircraft and is also suited for being deposited in a sheet metal compartment or other frame.

According to IAEA (1976), calibration sources for airborne spectrometers should be at least 8 m in diameter, while a minimum source diameter of 2 m is recommended for calibrating a portable spectrometer. When a survey aircraft is parked on a large pad for the recording of calibration counts, there are tens of centimeters between the detector system and the pad surface. Assuming that the calibration trial is characterized by an effective detector elevation of 80 cm, a pad diameter of 8 m would produce a geometry factor of 0.80 (formula (21)). The pads required to get an improved geometry factor of 0.90 would have to be 16 m in diameter, corresponding to a very large concrete consumption of 100 m$^3$ per pad. Manufacturing cost is also a relevant consideration in the design of small pads. With a pad diameter of 2 m, the geometry factors that can be obtained in heights of up to 10 cm above the pad surface are greater than 0.90. By increasing the pad diameter to 3 m it is possible to calibrate a detector probe in a geometry that amounts to at least 93% of $2\pi$, but this improvement would raise the concrete consumption from 1.5 to 3.5 m$^3$.

An experiment like that in Fig. 26, in which a rather voluminous detector unit belonging to an airborne spectrometer is placed for calibration on a small pad, cannot be justified if there is a significant drop-off in the radiation intensity with increasing distances to the central calibration point. The decreasing counting geometry along source radials of constant elevation "h" can be estimated by integrating the flux contributed by a unit source volume in points displaced a distance of "d" with respect to the source axis. Figure 34 shows two curves that can be used to de-

termine the source radius R needed to get an almost constant geometry factor $F_g$ within a given distance from the source centre. The curves are based on a spatial numerical integration of the 2.61 MeV flux produced by cylindrical sources of R = 1 m and R = 4 m. These two computational cases gave almost the same results when the elevation and displacement were normalized against R. For h/R = 0.20, $F_g$ has decreased to 95% of its central value in a distance of d = 0.45 R. A source with a diameter of 3 m therefore makes it possible to obtain a 135 cm wide and 30 cm high calibration space in which the radiation intensity varies by less than 5%. Close to the source surface (h/R = 0.05) the radiation diminuation is smaller than 5% for radial displacements of up to d = 0.65 R.

There is no particular advantage connected with the use of circular calibration sources apart from the fact that they make it easier to perform a flux calculation such as that mentioned above. Concrete pads of large horizontal dimensions are most conveniently manufactured by depositing the mixes in a rectangular or square form. Figure 35 is an outline of the facility at Walker Field airport in Grand Junction. The five pads are 9.1 × 12.2 m large with an associated effective diameter of 11.5 m (formula (23)). An asphalt track in flush with the pad surfaces allows planes to taxi through the area and return to the airfield. In Finland and Israel the airport calibration facilities are based on pad dimensions of 8 × 8 m which corresponds to an effective source diameter of roughly 9 m. The pads at Lanseria airport are circular with a diameter of 8 m and consist of coherent concrete, while the almost circular sources at Borlänge airport (Fig. 24) are composed of stacked layers of interlocking concrete bricks which are loaded with radioactive admixtures. Most of the smaller pads constructed for use with portable instruments are concrete cylinders with or without a metallic cladding; their diameters range from 1 to 3 m. A sketch of the $K_2TM_4B$ configuration at the Instituto de Radioproteção e Dosimetrica (I.R.D.), Rio de Janeiro, is shown in Fig. 36. The eight sources are 3 m in diameter and spaced along the circumference of a circular area on which quartz sand has been deposited up to the level formed by the calibration surfaces. The facility

includes a central pool for the recording of "true" background counts over water.

The radiation from the surface of a pad of appreciable radioelement content can be detected several meters away and may interfer with the radiation on a nearby pad of small radioelement content. To minimize this effect, the IAEA recommendation specifies the use of a distance of a least 15 m between the pad centres. Such a spacing is quite feasible in an airport area where there is plenty of unoccupied ground along the taxiways. For example, the area made available for establishing a calibration facility at Walker Field airport permitted the five pads to be emplaced at intervals of 20 m (Fig. 35). A series of pads for calibrating portable instruments is conveniently installed at the compound of a scientific laboratory or geological field office where buildings and roads may prevent the sources to be placed 15 m apart. In the source arrangement chosen at the I.R.D. (Fig. 36) there are about 6.5 m between the calibration points.

Formula (22) provides the small solid angle $\delta\Omega$ in which a radiant surface $\delta A = \pi R^2$ is viewed from an elevation of "h" in a distance of "r" and can be used to estimate the interfering radiation over pads which are recessed in the ground or embedded in shielding material such as quartz sand. In Fig. 37, the two sources I and II are supposed to have identical concentrations of a considered radioelement. A detector of uniform angular sensitivity placed over source II would respond to source I as if the grade of source II had been increased by a certain fraction, $F_i$. Neglecting the gamma-ray attenuation in the air along the transmission path from source I to source II, formula (22) results in the following estimate of $F_i$:

$$F_i \approx \frac{\delta\Omega}{2\pi} \approx \frac{hR^2}{2r^3} \quad . \tag{40}$$

Consequently, the spacing of calibration pads should accomodate the square of the pad radius, so that for example pads with a diameter of 3 m would require 30% more separation than pads which are only 2 m in diameter. Since the amount of interfering radiation on a source is governed by an inverse cubic function

of the distance to the neighbouring sources, it may not be a problem to place the sources less than 15 m apart. With the spacing of ~ 6.5 m used in the facility at the I.R.D., an effective detector elevation of 70 mm would produce an interference factor of $3 \times 10^{-4}$. On the B pad a contribution of 0.05 ppm eTh should therefore be expected from the content of about 170 ppm eTh in an adjoining T pad. Since the B pad contains 1.5 ppm eTh, the resulting offset of the thorium zero level is negligible.

## 4.4. Homogeneity characteristics of radioactive concrete

Concrete mixes manufactured for construction purposes consist of water, cement, fine aggregate, and coarse aggregate in a weight proportion of typically 0.5:1:2:3. Coarse aggregate is formed by particles which are from 5 to about 20-40 mm large and is included to reduce the cost of a required quantum of mix and to supply strength and density to the finished concrete structure. Fine aggregate or "sand" consists of particles of size from less than 0.3 mm to about 4 mm. In mixing concrete the cement paste and the fine aggregate combine into a mortar which fills in the space between the coarse particles and provides the mix with the necessary plasticity. Cement paste cures into a binder material for the aggregate particles and is the weakest constituent of hardened concrete due to its content of pores and air voids (Troxell et al., 1968; Neville, 1981).

In proportioning mixes for the manufacture of calibration pads, one has to decide in which form the radioactive materials should be added, coarse or fine. The use of large particles is in principle undersirable since the goal is to produce sources of the greatest possible radioactive homogeneity. On the other hand, mixes entirely based on fine aggregate require more cement paste per $m^3$, are not very workable, and do not solidify into material of the strength and compactness obtained with usual concrete mixes. If the raw material selected for a pad is uniformly radioactive and possesses a radioelement concentration that suits the calibration trials, the material may be crushed to furnish

a usable combination of fine and coarse aggregate. Løvborg (1983) described the construction of total-count calibration blocks using ore which had been crushed to supply a maximum particle size of 6 mm. The associated range of particle dimensions made it possible to vibrate the mixes into compact and homogeneous source materials.

There are two considerations which speak against the use of aggregate exclusively formed by crushed ore material. Firstly, the angular and more or less fissured particles delivered by a rock crusher are a source of unwanted additional concrete porosity (Løvborg, 1983). Secondly, uranium ores of the low grade typically required in the determination of eU calibration factors are potential carriers of thorium which is an unwanted radioelement in the manufacture of U pads. Consequently, it may be the best choice to let the bulk of the aggregate consist of natural granular material of low radioactivity while adding to the mix a small amount of high-grade ore of the desired radioactive purity. This manufacturing technique also makes it possible to utilize monazite or thorite of high thorium content and low uranium content for the construction of T pads.

A radioelement concentration provided by ore particles dispersed in concrete cannot be reliably estimated unless sufficiently many particles are included in the laboratory assay required for assigning a calibration grade to the pad. Quite obviously, the amount of mix that has to be sampled is the greater, the fewer particles there are per unit volume of mix. A simplified theoretical approach to the sampling problem can be made by considering a concrete batch prepared by mixing $N_1$ radioactive particles together with $N_2$ neutral aggregate particles. If the cement paste holding the particles together is disregarded, the ratio

$$p = \frac{N_1}{N_1+N_2} \tag{41}$$

represents the dilution of an ore grade into a pad radioelement concentration. Assuming a constant probability of p that a particle selected at random from the mix is radioactive, the probability of finding $n_1$ radioactive particles in a sample consist-

ing of n particles is given by a binomial distribution of mean value $\mu = np$ and variance $\sigma^2 = np(1-p)$. This corresponds to a relative standard deviation of

$$\sigma_r = \frac{\sigma}{\mu} = \sqrt{(1-p)/np} \qquad (42)$$

on the radioelement concentration analysed in the sample. One can make a very rough estimate of the sample volume "v" required to provide a sample of n particles by setting $v = nd^3$ where "d" is a dimension representative of the particle size. In a real mix the particles are not closely packed since they are surrounded by cement paste, and because the particle density is overestimated, there is no justification for the term (1-p) in (42). The sampling error is therefore estimated as

$$\sigma_r \approx \sqrt{d^3/pv} \ . \qquad (43)$$

Thus, to assay a pad radioelement concentration with a given precision, the amount of mix collected for analysis should be increased in proportion to the dilution of ore grade into calibration grade. The decrease of the sampling error with the square root of the sampling volume is characteristic of randomly dispersed elemental abundance and represents a limiting case in the theory of regionalized variables (Matheron, 1963).

The T pad at Risø National Laboratory contains 150 ppm eTh and was manufactured by mixing 17.4 kg of monazite sand of 6% thorium content into 6900 kg of cement mortar whose aggregate consisted of beach sand of 0.3 mm average particle size. While the batches were deposited in the framework for the pad, 305 mix samples were collected in 170 ml cans for thorium analysis by gamma-ray counting. A relative standard deviation of 2% was recorded for the thorium contents measured in this trial (Løvborg et al., 1972), while the standard deviation suggested by formula (43) only amounts to 0.8% ($d = 0.03$ cm, $p = 0.0025$, $v = 170$ cm$^3$). This example shows that the use of an average particle size may underestimate the sampling error. Ninety-five percent of the aggregate used in the example was finer than 0.6 mm which happens to be the particle size providing the observed standard deviation of 2%.

Perhaps, therefore, the "d" in formula (43) should be the maximum size rather than the average size of the aggregate particles.

Results obtained with the formula for mixes which are based on coarse aggregate are illustrated by considering the U pad of the facility at Lanseria airport. The pad was manufactured from a mix of uranium ore and neutral aggregate, both materials in a nominal particle size of 20 mm (Corner and Smit, 1983). The ore contained approximately 170 ppm eU, while 57 ppm eU is the reference concentration adopted for the pad. With p = 57/170 = 0.34 and a wanted $\sigma_r$ of less than 2%, the calculated quantity of mix that should be analysed for such a calibration source amounts to 59 liters, or about 130 kg. In good agreement with this suggested sample size, the South African personnel took 59 grab samples of 2 kg each during placement of the mix.

Calibration pads which are loaded with a small fraction of ore particles ($p << 1$) can be regarded as systems of randomly distributed point sources in a radiation absorbing matrix. The capability of such a pad to simulate a uniformly radioactive source medium is the better, the less the ore particles are spaced and the higher the calibration point is positioned. In principle there is no uncertainty associated with the radiation intensity in any calibration point since the sources are fixed. However, if another pad of the same ore content were manufactured, the radioactive particles would assume a new configuration, while their average spacing would remain the same. It is therefore possible to assign a standard deviation to radiation intensities produced by discrete and random source distributions. The calibration error represented by this standard deviation can be estimated from a source model in which a calibration pad is formed by adjoining cubic cells of the side length "a" (Fig. 38). By letting the radioelement contents of the cells fluctuate independently of each other, one can generate a resulting frequence distribution for the photon flux $\phi$ in a central detector point P of elevation h. Assuming a particle size of "d" and an overall fraction of "p" radioactive particles in the real pad, the relative standard deviation $\sigma'_r$ on $\phi$ is conveniently stated in terms of a dimensionless factor F chosen as

$$\sigma_r' = F \cdot \sigma_r$$

with (44)

$$\sigma_r = \sqrt{(d/a)^3/p} \ .$$

The suggested Monte Carlo technique was applied to a 50 cm thick source of the surface dimensions 8 × 8 m. A unit cell size of a = 2 cm was adopted, and the computer program was written so as provide F directly, independently of d and p. Ascribing a linear attenuation coefficient of 0.9 $cm^{-1}$ to the source, the results obtained became representative of the uncertainties on uranium and thorium count rates produced by discrete source radioactivity. In a large elevation of h = 1 m, a value of F = 0.0017 was recorded, while setting h equal to 70 mm increased F to 0.015. Consequently, a large pad of the homogeneity sufficient for calibrating elevated detector systems may not be homogeneous enough for the recording of calibration counts on the surface.

Calibration error due to source inhomogeneity was estimated for the U pad of the facility at Walker Field airport. In this pad the ore particles are up to 2 mm large and embedded in an aggregate of masonry sand, likewise of the maximum particle size d = 2 mm (Ward, 1978). The pad is characterized by an ore-to-mix ratio of p = 0.001. One can make a coarse estimate of the associated spacing "s" of the ore particles by assuming that there are $n_1 = p/d^3$ ore particles per unit volume of the pad. This corresponds to a spacing of

$$s = d/\sqrt[3]{p} \ , \qquad (45)$$

or 2 cm. If the fluctuations shown by "s" are distributed on cells of the size a = 2 cm, the relative standard deviation on the radioelement content in a single cell is estimated to be $\sigma_r = 1$, or 100%. Since the F factors presented above were evaluated for a source that was somewhat smaller than the Walker Field pads, calibration error based on these factors is slightly overestimated. The value of F = 0.015 for h = 70 mm suggests an r.m.s. error of less than 1.5% on U window sensitivities deter-

mined for portable spectrometers placed on the pad. Stromswold (1978) scanned the surface of the U pad using a large sodium-iodide detector (292 × 102 mm) mounted within a thermally insulated container. His map of uranium window counts recorded more than 3 m from the edges of the pad corresponds to an experimental standard deviation of 1.0% on the radiation flux approximately 18 cm above the pad surface.

## 4.5. Criteria for the selection of mix ingredients

In making preparations for the construction of a calibration facility, it is natural to search for qualified concrete aggregate materials and admixtures among available domestic supplies. Since the sand and stony material utilized by the concrete industry often derive from granitic or volcanic rocks, an effort may be required to find a neutral aggregate of the desired low radioactivity. Table 13 shows the approximate radiometric grades of B pads manufactured from various geologic materials. The beaches south of Tel Aviv and Rio de Janeiro are examples of places where natural aggregates containing less than 0.3% K, 1 ppm eU, and 2 ppm eTh are available. Sand and gravel not predominantly formed by quartz carry over 1% potassium and several ppm uranium and thorium in the typical case and are conveniently replaced by crushed low-radioactivity rock, such as done in South Africa and Sweden. It should be noted that ordinary Portland cement can be a radioactive contaminant in the manufacture of calibration pads. Wollenberg and Smith (1966a) investigated the radioactivities of cements from 147 producers in the US and Canada and estimated average contents of about 0.4% K, 3 ppm eU, and 4 ppm eTh. Alumina and silica used for the production of cement clinkers were shown to be the main contributors of uranium and thorium; depending on the geological source of these raw materials, the cement manufactured by some plants may contain as much as 10 ppm of uranium or thorium. Therefore, neither the aggregate or the cement for a B pad should be purchased without checking the radioelement contents of these materials (using sealed-can gamma-ray analysis, as described in the next chapter).

K pads do not present a difficult raw materials problem since potassium feldspar of ~10% K is quarried or available as a commercial product in most countries with a ceramics industry. Nepheline syenite without uranium and thorium bearing accessory minerals is another source of potassium which came into application for loading the K pads at Bells Corners, Canada. The radiometric grades for K pads constructed up to the present demonstrate that such pads must be expected to contain several ppm eU and eTh supplied by the potassium aggregate which normally is used unblended with sand to obtain a K calibration grade of 4 to 7%.

Uranium admixtures for U and M pads can be obtained from many sources and are easily procured in countries in which there are operating uranium mines. Table 14 gives an impression of the mines and deposits that have delivered the uranium for a broad selection of existing calibration facilities. If an U pad contained no thorium, it would permit a direct measurement of uranium window sensitivities and uranium stripping ratios, $\gamma$ and "a". It is therefore relevant to search for a uranium admixture whose thorium content is small. The data shown in Table 15 suggest that a pad loaded with ore of low uranium grade (< 0.1% U) cannot be expected to possess a Th/U ratio below 0.10. High-grade ore diluted by a suitable amount of neutral aggregate seems to be the best choice, provided the neutral aggregate is of sufficiently low thorium content.

By far the most important property determining whether or not a uranium ore is a usable source material is the emanation power, P, of the ore. Since the gamma radiation detected on a pad is diminished by roughly 0.5% when the amount of radon available for diffusion in the concrete is increased by 1% (subsection 3.5), it seems reasonable to select the uranium admixture among ores that emanate less than about 2% radon. If a laboratory gamma-ray spectrometer is available, it is an easy matter to test the emanation power of an ore sample by sealing the sample in a metal can and recording the build-up of $^{214}Bi$ activity from an initial count and a final count performed one or more radon half-lives later ($T_{1/2}$ = 3.82 days for $^{222}Rn$). Using this tech-

nique, Austin (1975) found that the emanation associated with the uranium deposits in the western United States can vary from about 1% to as much as 90%. Ores carrying uranium in the form of millimeter or centimeter large particles of massive uraninite (pitchblende) were identified as the weakest emanators (P = 1 to 12%), while ore samples in which the uranium was supplied by sand grains with a coating of uraninite or coffinite typically emanated about 70% radon. Pereira (1980) studied emanation shown by the uranium-bearing alkaline rocks of the Poços de Caldas massif, Brazil, and was able to relate strong emanation (P ~ 50%) to surplus $^{226}Ra$ originating from a suggested isotopic remobilization mechanism in the deposit.

It is probably the safest to spike U and M calibration pads with an admixture prepared by crushing large and unaltered crystals of a primary uranium mineral which does not retain the internal radiation damage caused by the alpha particles in the uranium decay series. Minerals having reached the metamict state are unqualified because they are strong emanators (Barretto, 1975). Crushing an ore into very fine powder increases the specific surface with a resulting increase of the emanation power due to recoil effect in the alpha decay of $^{226}Ra$ (Tanner, 1980). There is consequently a conflict in choosing the particle size into which the ore should be crushed. The U pad of the spectrometer calibration facility at Risø is spiked with Saskatchewan pitchblende ore of 0.5 mm maximum particle size; about 30% of the ore particles are smaller than 40 µm. An emanation test performed with hardened and powdered samples of the concrete mix suggested that roughly one fifth of the radon produced by the uranium admixture collects in the concrete porespaces through which it may migrate and escape from the pad surface (Løvborg, 1983). The radiation loss on the pad is greatest in dry and warm weather and may correspond to a decrease in the radiometric pad grade from 230 to 150 ppm eU, or 35% (Løvborg et al., 1978; Løvborg, 1983). The example emphasizes the necessity to check the radon emanation of a powered ore sample before using the material as an admixture. It may be an advantage to strain off particles which are less than ~ 75 µm across by the use of a 200 mesh sieve; this was done in manufacturing the U pad of the recently established airport

calibration facility in Thailand (R.L. Grasty, personal communication).

The most important criterion in selecting the thorium admixture for a T pad is the amount of uranium that can be accepted in such a pad. A low ratio between the eU and eTh calibration grades is in particular desirable for facilities which are based on the combined use of T and M pads for getting a set of thorium and uranium calibration factors. In principle this is effectuated by recording the thorium window sensitivity $s_{Th}$ and the stripping ratio $a$ on a T pad, after which the uranium sensitivity $s_U$ is obtained on an M pad by stripping away the thorium contribution to the uranium window counts. (The "a" stripping ratio cannot be reliably measured with a facility in which there is no U pad). It is easy to show that an error $\epsilon$ on the U/Th ratio estimated for the T pad results in the following error, $\epsilon_a$, on the stripping ratio $a$:

$$\epsilon_a = - \frac{s_U}{s_T} \cdot \epsilon \ . \qquad (46)$$

For a portable spectrometer with $s_U/s_{Th} \approx 2.5$ and $a = 0.6$, $a$ would be overestimated by 20% on a T pad supposed to contain no uranium, but actually having a U/Th ratio of 0.05. This example shows that a minor pad radioelement concentration can have a significant influence on the outcome of a calibration trial and therefore either should be avoided or determined rather accurately.

From Table 16 it can be seen that thorium admixtures based on monazite or thorite typically produce U/Th calibration grade ratios of 0.03 to 0.07. Monazite sand is a commercial product derived from placer deposits in, for example, Australia and Malaysia. The diorite used in Sweden for spiking the bricks of the T pad at Borlänge gave the bricks a U/Th ratio of 0.07, while a ratio of 0.11 resulted from loading the T pad at Helsinki-Vantaa airport with thorium-rich granitic rock. Thorium oxide, a chemical compound applied in the construction of the Canadian facility at Bells Corners, must be regarded a less suitable admixture unless the material is sufficiently old to

have come into radioactive equilibrium. The ingrowth of $^{208}Tl$ in a pure thorium compound is governed by the 6.7 yr and 1.9 yr half-lives of the two intermediate decay products, $^{228}Ra$ and $^{228}Th$. Equilibrium is not obtained until about 45 years after the compound was manufactured (Adams and Gasparini, 1970).

## 4.6. The manufacture of calibration pads

It is impossible within the scope of the present report to enumerate more than a few of the precautions and steps involved in the blending and placement of concrete mixes for a series of calibration pads demanded to be radioactively homogeneous, non-hygroscopic, and durable. The construction of an airport calibration facility is in fact a rather big concreting job which should not be executed without consulting an engineering specialist. Blending operations and procedures used for constructing the Walker Field facility were described by Ward (1978). Readers who might wish a comprehensive overview of professional concrete making will find the desired information in the previously quoted textbooks of Troxell et al. (1968) and Neville (1981). The various chemical admixtures available for improving the workability and final properties of concrete were thoroughly discussed by Rixom (1978). The following considerations and suggestions are based on the assumption that it has been decided to build calibration pads prepared from sand-cement mortars whose U and Th concentrations are provided by small amounts of specially selected pitchblende ore and monazite (or thorite). In the preceding subsection it was suggested that this is the best way of manufacturing pads of a high preferential enrichment in either uranium or thorium.

The first step in proportioning the mixes is to fix the maximum particle size for the neutral sand aggregate. This is done by demanding that the added radioactive particles should not be unduly spaced by larger sand grains. For use in a numerical example it may be mentioned that the commercial monazite sand used for the T pad at Risø was delivered in a grading so that 95% of the particles were between 0.1 and 0.3 mm large. Assuming

that radioactive material of this fineness is blended with 1000 times as much sand of the same fineness, one would expect to find an ore particle at 1 to 3 mm intervals throughout the mixture (formula (45)). This example suggests an upper limit of about 3 mm for the particle size of the neutral aggregate. Figure 39 shows the particle gradings for the beach sand and the masonry sand used, respectively, for constructing the calibration facilities at Risø and Walker Field. It can be seen that beach sand may be a finer aggregate than necessary due to a very small fraction of particles with sizes above 0.5 mm. The grading curve for the potassium feldspar in the K pad at Risø is also shown in Fig. 39. This material was supplied as a flotation product and makes up the total aggregate for the pad. The very similar grading curves for the beach sand and the feldspar make the pads of the Risø facility almost identical in regard to density and porosity.

The blending of kilogram amounts of ore with tons of sand into uniformly radioactive aggregate material can be done batchwise using a concrete mixer that fits the job. It may be advisable to execute the operation in two stages involving, respectively, an initial blending of ore and sand in a ratio of about 1:100 and a final blending of the resulting mixture with sand for diluting the ore by a further factor of 10. Such a procedure was followed in the construction of the new airport pads in Thailand (R.L. Grasty, personal communication). In rotating a dry mixture of sand and ore particles there is a risk of gravity separation because the densities of monazite and pitchblende are 2 to 3 times greater than the density of quartz. An extremely long blending time per lot of granular material may therefore not be desirable. The spiked aggregates for the pads at Walker Field were prepared in the form of ten lots per pad, each lot comprising 5.4 $m^3$ of material blended for 10 minutes. Dry-blending operations performed a time before the concreting job can be assisted by sampling and radiometric analysis to judge whether the material should be rotated more or is sufficiently homogeneous for becoming transferred to storage barrels.

In the actual pad manufacturing operation, aggregate material, cement, and water are rotated to produce a coherent concrete

(mortar) that can be placed with as high a degree of compaction as possible in the framework or container used to give the pad its required shape and dimensions. Each batch of concrete is distributed over the surface formed by the mass of already deposited concrete and is united with this mass using hand ramming or, probably better, the force excerted by an immersion vibrator.

The purpose of ramming or vibration is to remove the air bubbles entrapped in the added portion of mix. Very strong and lasting mechanical action cannot be used due to the risk of getting the ore particles seggregated. It is therefore important that the mix has a consistency that makes it amenable to compaction by a small amount of external force. Consistency, or workability, is traditionally measured in a so-called slump test in which a metal mold is used for producing a 30 cm high truncated cone of freshly manufactured mix. The slump of the mix is the vertical settling shown by the test cone. A mix exhibiting a slump of less than 50 mm is rigid to work with, and one should aim at a slump of about 75 mm for producing a sufficiently workable mix. Workability is primarily controlled by the grading of the aggregate particles and the amount of cement paste available as a lubricant for these particles. When no coarse aggregate is incorporated, it can be anticipated that the mix should be based on a sand-cement ratio of 3:1. This ratio was used in manufacturing the airport pads at Walker Field and in Thailand.

A cement paste is a suspension of cement particles in water. Cement paste cures and hardens into cement gel by hydration and requires approximately 0.25 weight parts of water per weight part of cement to hydrate completely. To become workable, a mix must have a water-cement ratio of at least 0.4. It is not advisable to increase this ratio above 0.5 since surplus mix water produces a hardened paste of high porosity and low strength. With an expected mix density of about 2000 kg/m$^3$, a suggested mix composition might be:

| | | |
|---|---|---|
| Fine aggregate | 1350 kg/m$^3$ | |
| Cement | 450 " | |
| Tap water | 200 " | (approximately). |

It may be an advantage to produce the paste from a mixture of Portland cement and a pozzolanic material in the form of finely divided silica. In the wet mix a pozzolan provides a lubricating action; during the curing period it reacts with the lime constituents of the cement so that the hardened paste becomes more dense. The mixes for the total-count calibration blocks described by Løvborg (1983) were supplied with 8 kg of silicate dust per 100 kg of cement. The use of fly-ash as a pozzalan is not recommended since fly-ash may contain radium.

A water-reducing agent in the form of a superplasticizer is very effective for manufacturing mixes of extremely good coherency and plasticity at low water-cement ratios. Superplasticizers are commercial products which are based on lignosulphonates or sulphonated formaldehyde condensates and act by dispersing the cement particles in a mix through ionic repulsion. They are typically added in amounts of about 2 kg per 100 kg of cement.

Figure 40 shows superplasticized concrete (mortar) mixed and poured for one of the calibration pads of the CSIRO facility in Sydney. It can be seen that such a mix is very little rigid and therefore easy to place. Another useful admixture is an air-entraining agent whose action is to introduce a large number of tiny air bubbles in the mix. It may seem a paradox to increase the porosity of concrete by adding air to it, typically around 10% by volume for mixes prepared from fine aggregate. However, air entrainment produces concrete of a non-coherent pore structure and is the proper means of making a calibration pad resistant to freezing and thawing. The total-count calibration blocks at Risø are air-entrained; the resulting pore structure is shown on microscope-pictures in the documentation report (Løvborg, 1983).

# 5. ASSAY AND USE OF PAD RADIOELEMENT CONCENTRATIONS

## 5.1. Pad moisture - an intricate problem

In subsection 3.4 it was shown that spectrometer calibrations should be based on the in-situ or "wet" radioelement concentrations of the pads in the facility. The problem is that pad moisture is a variable quantity, so that the use of "wet" pad concentrations as calibration grades has an associated uncertainty which adds to the other uncertainties involved in a calibration trial. It is also a problem to plan the sampling and assay procedure for fixing the calibration grades in such a manner that the most likely value of the pad moisture can be incorporated in the assay results, either directly or through a separate moisture determination performed on drill core.

The quantity of sample material needed for a statistically reliable estimate of pad radioelement concentrations is conveniently collected in the form of mix lumps from the batches deposited in the framework or container for the pad. Figure 40 shows how the sampling may be done. Assuming a mix manufactured from 1 mm particles of which one out of thousand is radioactive, it is necessary to collect about 10 liters of mix for reducing the sampling error to 1% (formula (43)). One can either let the mix lumps cure in plastic bags, or it may be decided to clamp the material into metal cans for gamma-ray analysis without any any further sample preparation. In both cases one ends up with cured concrete in the course of a few hours. To describe the curing process, it is useful to write down the following equation for the involved masses of aggregate (A), cement (C), and mix water (W):

$$M = A + C + W_h + W_r \ . \qquad (47)$$

$W_h$ is the water that has reacted with the cement at a given time and therefore is chemically bound in cement gel. The remaining

part of the mix water, $W_r$, is housed in capillary pores and in extremely small gel pores which are the centres of gel formation. It is customary to assume that fully hydrated cement binds 25% of water per dry weight of cement, so that $W_h$ can be estimated as

$$W_h = 0.25\ \lambda \cdot C \tag{48}$$

where $\lambda$ is the actual degree of hydration. By furthermore introducing the A/C ratio of 3 typically chosen for the manufacture of cement mortars, the hydrated (dry) mass of concrete is calculated to be

$$\begin{aligned} M_d &= A + C + W_h \\ &= (4 + 0.25\ \lambda) \cdot C \end{aligned} \tag{49}$$

It should here be noted that it lasts many months until a concrete mass is fully hydrated. Cured mix lumps will normally not be stored very long before they are crushed, and it is obvious that some uncombined mix water will be lost in the grinding process. In the typical case a composite sample is manufactured by carefully mixing sample powders together, and the radioelement assay is performed with splits that have been dried at 105°C until constant weight. The "dry" assay value obtained in this way is given by

$$x_d = \frac{A \cdot x_o}{M_d} = \frac{3}{4+0.25\lambda}\, x_o \tag{50}$$

where $x_o$ is the radioelement concentration of the particle mixture used as an aggregate.

The "wet" radioelement concentration of the calibration pad may also be stated in terms of $x_o$. This is done by introducing the previously defined moisture fraction

$$w = \frac{W_p}{M_d} \tag{51}$$

where $W_p$ is the pore moisture in $M_d$ grams of cured pad concrete. Assuming that the pad is sufficiently old to have become fully hydrated ($\lambda$=1), formula (29) used in conjunction with formula (50) leads to the estimate

$$x = \frac{0.71}{1+w} x_o \quad . \tag{52}$$

The moisture in an old pad is controlled by an exchange of pore water between the pad and the surroundings. By having the pad contained in a metal cylinder or lined with asphalt or plastic, the moisture transport is limited to take place through the calibration surface. By furthermore keeping the surface protected from rain and snow between the calibration trials, one only has to consider the absorption and desorption of water vapour in the concrete pores. Herholdt et al. (1979) presented the amount of hygroscopic water in old cement paste as a function of the air humidity. According to these data, concrete manufactured from a mix of A/C = 3 can be expected to contain 2 to 3% moisture when stored in air of 20% relative humidity. For a humidity of 100% the moisture absorption is almost as large as the absorption in concrete immersed in water. The relation between the saturation absorption and the total porosity of the concrete was presented in formula (30). Concrete containing no coarse aggregate is indeed a porous and therefore hygroscopic source material even when great care has been exercized to reduce the W/C ratio for the mix to about 0.4. The average porosity determined for the five pads of the CSIRO facility in Sydney amounts to 21.2% (B.L. Dickson, personal communication). Assuming a solid density of 2.65 g/cm$^3$ for the aggregate material and hardened cement paste, formula (30) suggests that these pads may absorp up to 10.2% moisture. This predicted absorption is in excellent agreement with a saturation experiment (performed with drill core) which gave an estimated absorption of 10.0% when differences between the concretes were averaged out. For comparison it may be mentioned that the "H" total-count calibration blocks at Risø were found to be 19-23% porous with a corresponding saturation absorption of 9-11% (Løvborg, 1983).

Consequently, it seems reasonable to assume that the moisture in a calibration pad adjusts itself on values of between 2 and 10%. A pad moisture as small as 2% can only be expected with facilities situated in extremely hot and dry climates, and the other extreme of 10% moisture would probably rarely occur even in a moist climate. Løvborg et al. (1981) measured the water content in drill-core from several of the spectrometer calibration pads at Risø and arrived at an estimated pad moisture of 6 ± 1 percent. The following theoretical comparison of radiometric in-situ grades and laboratory-assayed pad radioelement concentrations is based on pad moistures of 2, 6, and 10% to cover one "normal" and two extreme moisture situations. The first column of Table 17 shows the corresponding ratios $x_d/x$ calculated by means of (50) and (52). It has been assumed that the cured mix lumps were 33% hydrated when they were crushed and dried ($\lambda$ = 0.33). This is a typical degree of hydration in concrete that has been manufactured from a rapid Portland cement and cures for 2 days at 15°C (Herholdt et al., 1979). The second column of Table 17 pertains to a laboratory assay of wet mix that has been sealed in the sample cans since the beginning of the curing period. In this case the mass of sample material includes the mix water, $W = W_h + W_r$. It has been assumed that the mix is of W/C = 0.45, corresponding to an assayed "wet" radioelement concentration of

$$x' = \frac{3Cx_o}{3C+C+0.45C} = 0.67\ x_o \quad . \tag{53}$$

One can see that a pad calibration grade based on "dry" assays invariably is overestimated and should be reduced by about 10% to accomodate a typical pad moisture of 6%. By instead performing the assays with the mix water retained one gets a much more realistic estimate of the pad grade. Grade assignment based on natural mix samples is tedious because it involves many single assays to reduce the overall sampling error to an acceptable level. Grades were assigned to the pads of the Walker Field facility using 70 wet mix samples per pad. However, the sample cans were not sealed until after their contents had cured, so that some of the initial mix water were allowed to evaporate. The resulting grades as well as the radioelement concentrations determined in dried concrete powders were presented by Stromswold and Kosanke

(1978). For the major radioelements in the pads the "dry-to-wet" concentration ratio amounts to 1.13 ± 0.03, in fair agreement with the ratio of 1.10 estimated from Table 17. The experimental moisture determinations for the Walker Field pads range from 4.0 to 7.5% (Ward, 1978).

## 5.2. Sealed-can gamma-ray counting

If large composite samples of finely divided concrete powders have been prepared, it is lays near at hand to analyse the materials for potassium, uranium, and thorium using standard wet-chemical or instrumental analytical procedures. For example, X-ray fluorescence analysis may come into question as the primary means of ascribing potassium grades to calibration pads, while neutron activation analysis might be considered a good choice for determining a wide range of uranium and thorium pad concentrations. For pads containing no chemically processed thorium it is safe to set 1 ppm Th = 1 ppm eTh. A similar translation of U concentrations into eU calibration grades may not be valid, as explained in a moment. It is a severe problem that usual elemental assays are performed with typically a few hundred milligrams of sample material. Large composite samples of pad mixes loaded with small amounts of high-grade ore must therefore be extremely well homogeneized before splits are taken for analysis. Random and systematic assay errors can be kept under control by distributing sub-samples among various analytical laboratories, but it may be quite difficult to combine the data into pad grades of the desired small standard deviations. This is demonstrated by the interlaboratory determinations executed in South Africa for providing the grades of the pads at Pelindaba and Lanseria (Corner et al., 1979; Corner and Smit, 1982).

At this point it must be stated that the concentrations of elemental uranium in spectrometer calibration pads in principle are irrelevant quantities. Since all gamma radiation associated with uranium, in the MeV region, originates from $^{214}Bi$, one has to assay the element which can sustain $^{214}Bi$ radioactivity over a time span of years without support from uranium. This element is

radium ($^{226}Ra$) which has a half-life of 1600 yr and therefore can maintain a gamma-ray flux which decreases by less than 1% in 20 years. The relation between a concentration of radium and the resulting equivalent uranium grade is calculated by considering a system in which $^{226}Ra$ is in radioactive equilibrium with its parent $^{238}U$, i.e. the decay rates of the two isotopes are supposed to be the same. By including the current uncertainties on the $^{226}Ra$ and $^{238}U$ half-lives, 1600 ± 7 yr and (4.468 ± 0.005) × $10^9$ yr respectively, one arrives at the correspondance:

$$1 \text{ ppm eU} = (3.376 \pm 0.015) \times 10^{-7} \text{ g Ra/g} . \qquad (54)$$

(For the derivation of the main term, see Dickson et al. (1982)). Although the radium and uranium in calibration pads do not need to be in radioactive equilibrium, it is always advisable to check the equilibrium state by combining the necessary radium assay with a uranium assay. Surplus radium is indicative of enhanced radon emanation since this radium may occur as particle coatings rather than as atoms in the interior of crystals (subsection 4.5). Equilibrium is desirable whenever it might come into question to use a uranium loaded pad for the calibration of total-count scintillometers in units of counts/s per Ur (1 Ur = 1 ppm U in equilibrium). The reason is that nearly 4% of a gross uranium count rate are contributed by low-energy gamma rays emitted by $^{235}U$ (Løvborg, 1983).

The determination of the radium in a pad mix, in terms of an eU calibration grade, is conveniently done by three-channel window counting, so that the pad concentrations of K and eTh are measured along with the eU concentration. The procedure is based on the use of metal cans which contain several hundred grams of dry or wet mix sample and remain sealed from 3 to 4 weeks before the counting is started. A gas-tight seal is necessary to warrant the equilibrium in the system $^{226}Ra$ - $^{222}Rn$ - $^{214}Bi$ when the counting is performed. Since the requested pad grades are measured simultaneously in samples consisting of hundreds of times as much material as the splits used for a chemical assay, a laboratory gamma-ray spectrometer is far the best tool to use for grade assignment. A suitable counting system may comprise a large

sodium-iodide detector mounted inside a background shield of steel or lead and operated in conjunction with a multichannel analyser. The performance requirements in regard to photomultiplier gain stability, pulse pile-up effect, and counting statistics is the same for such a laboratory instrumentation as described for portable spectrometers in chapter 2. It is in general easier to perform a gamma-ray assay in the laboratory than in the field since the background shield provides thermal insulation for the detector. Also, the counting geometry does not vary, and it is possible to accumulate sample and background counts over very long periods of time.

Figure 41 shows a spectrometer counting facility at the CSIRO Institute of Energy and Earth Resources in Sydney. The sample cans are here exchanged manually by hoisting a plug which forms the upper part of the lead shield. The spectrometer shown in Fig. 42 is sited at Risø National Laboratory and has an attached sample changer, so that night and weeekend hours may be utilized for counting a series of samples. In both these counting systems the multichannel analyser is used to define three more or less wide energy windows in the spectral interval from 1.3 to 3 MeV. A background correction and a subsequent calculation of "stripped" window count rates are carried out precisely as in a field assay with a portable spectrometer. In a laboratory assay a stripped window signal is assumed to be proportional to the total mass of radioelement contained in the sample. The use of normal window sensitivities, i.e. count rates per radioelement concentration unit, must therefore be preceded by a normalization of all recorded count rates to a common reference sample weight. The sample cans used with the Risø spectrometer are 75 mm in diameter and 39 mm deep and can be packed with between 200 and 300 g of material, depending on the density and size of the particles. A reference weight of 250 g has accordingly been adopted in this assay system.

Radiometric pad grades provided by means of a laboratory spectrometer are linked up with the quoted or calculated radioelement concentrations in reference materials used to calibrate the instrumentation. A potassium salt which contains no chemically

bound $H_2O$ is an obvious K calibration standard since the weight percentage of potassium directly follows from the chemical formula. Figure 43 shows the result of calibrating the Risø spectrometer with ten potassium salts which were dried for 2 days at 105°C before they were packed and sealed in sample cans. If the count rate in the potassium window had been strictly proportional to the amount of potassium contained in a sample, the normalized sensitivity

$$s_{K,norm} = s_K \cdot \frac{250}{W}$$

would be independent of the sample weight W. From Fig. 43 it is obvious that $s_{K,norm}$ decreases with W, and this effect must be ascribed to self-absorption in the 39 mm thick layer of sample material. Since all experimental points except the point for $K_2CO_3$ seem to fit a straight line, it is natural to use this line in calculating the values of $s_K$ obtained with different sample weights. The resulting expression is added in Fig. 43. The plot suggests that $K_2CO_3$ (potassium carbonate) may be an unreliabe reference material; this salt is actually very hygroscopic and therefore difficult to dry properly.

Nearly all users of laboratory gamma-ray analysis prepare their radium and thorium counting standards from analysed radioactive ores. The Geological Survey of Canada is an exceptional example of a laboratory where primary counting standards have been prepared using a certified radium solution and a thorium salt manufactured in 1906 (Grasty et al., 1982). Thorium of this age is in equilibrium with $^{224}Ra$ which is the analogous isotope in the $^{232}Th$ decay chain to $^{226}Ra$ in the $^{238}U$ decay chain. A number of other laboratories base the analysis of eU and eTh on reference ores prepared by the New Brunswick Laboratory (NBL) of the US Department of Energy. Various series of NBL reference ores have been emitted since the 1950s, and it has generally been assumed that the uranium standards are in radioactive equilibrium by virtue of a stated Ra/U ratio of $3.44 \times 10^{-7}$ for the pitchblende selected as a master material in the preparation of the standards. Since no information was available on the uncertainty of this ratio, many analysts felt uneasy about using the NBL refer-

ence materials as counting standards. A single of the older U standards (NBL-103) has been found to contain more uranium than quoted in the NBL certificate (Dickson et al., 1982; Grasty et al., 1982). The new so-called 100-A series of NBL reference materials has been subjected to a US interlaboratory measurement program described by Trahey et al. (1982). This series was manufactured by diluting pitchblende and monazite with silica (99.9% $SiO_2$) to provide reference grades of approximately 10,000, 1000, 500, 100, and 10 ppm U or Th. Grades of between 100 and 1000 ppm are suitable for calibrating a typical laboratory spectrometer. The radium content of the pitchblende ore was assayed by NBL plus the National Bureau of Standards and Argonne National Laboratory. From these 3 determinations the U standards (101-A to 105-A) are estimated to possess a Ra/U ratio of $(3.40 \pm 0.06) \times 10^{-7}$. This estimate suggests that the certified U concentrations can be replaced by identical eU concentrations, cf. formula (54). The greatest remaining problem in the use of NBL reference materials as counting standards is the missing information on the $^{226}Ra$ contents of the thorium series, 106-A to 110-A. The monazite used to produce this series has a U/Th ratio of 0.040, so that a set of a reliable eTh calibration factors cannot be obtained without executing a correction for the associated eU concentrations.

Another supply of uranium reference material is the Canada Centre for Mineral and Energy Technology (CANMET). The most versatile CANMET standard is the BL-5 which is an ore concentrate from Beaverlodge, Saskatchewan, certified to contain 7.09% U with a 95% confidence interval of ± 0.03% U (Faye et al., 1979). By diluting a quantity of BL-5 with silica powder the user can manufacture a counting standard of any desired reference grade. Interlaboratory measurements of $^{226}Ra$ have shown that BL-5 and other of the CANMET standards can be assumed to be in radioactive equilibrium (Smith and Steger, 1983). Uranium reference ores of known radium contents have also been prepared by the Bureau of Uranium Geology in Beijing, China (Yang Zhenzhou and Liu Xichen, 1983).

In calibrating the U and Th energy windows of a laboratory spectrometer there is a self-absorption effect similar to that ob-

served in the K window when potassium salts of different densities are used as counting standards. To assess the effect it is necessary to prepare eU and eTh calibration standards of different weights. Grasty et al. (1982) diluted their primary thorium reference material with silica, flour, and a cellulose patching-compound in various proportions and measured a decrease of 0.028% in the normalized thorium sensitivity per gram increase in sample weight. The corresponding coefficient for the uranium window was determined by interpolation between the values recorded in the K and Th windows. At Risø the eU and eTh assay errors associated with self-absorption in the samples are taken into consideration in the form of fixed relative standard deviations of 2% and 1.5% respectively. These uncertainties include the estimated errors on the eU and eTh reference grades and have been assessed from calibration trials with NBL standards having a matrix of either dunite (the 70 and 80 series) or silica (the 100 series) (Løvborg, 1983).

The analytical agreement between counting laboratories involved with the assignment of radiometric grades to calibration pads or borehole models was checked in an intercomparison organized in 1981 by Dr. David George of the Technical Measurements Center at the Grand Junction Area Office of the US Department of Energy. Six laboratories analysed 3 powdered materials prepared by loading a concrete mix with two uranium grades and one thorium grade. Table 18 shows the results of this experiment, including for Soreq (Israel) only the data recorded with a 152 × 102 mm sodium-iodide detector. It should be noted that the results obtained by the TMC include splits that were taken after the other laboratories had received their splits for analysis. Since the TMC assay values are the largest ones recorded, the master mixtures may not have been blended to the stage where the radioactive particles are completely randomly distributed (D.C. George, personal communication). The experiment indicates a good agreement between eU assay values provided by the participating laboratories, while the thorium result must be regarded slightly discouraging.

In spectrometer assays of minor pad radioelement concentrations it is the background rather than the reference materials that de-

termine the reliability of the determinations. Table 19 shows a priori 10% determination limits calculated for the Risø spectrometer by means of the "$n_Q$" working expression in Table 8. These data are based on the assumption of a 16-hour background run executed with inert sample material (for example sugar) immediately before a sample run is initiated. The table serves as a guide to the time required to assay the radioelement contents in samples of mixes used for the manufacture of B pads. While a single sample of B mix of 3 ppm eU and 7 ppm eTh can be assayed with 10% precision in one hour, sixteen hours of counting time are needed to obtain a similar precision on mix contents of 0.8 ppm eU and 2 ppm eTh. It is interesting to note that a small content of 2 ppm eTh in exposed rock can be assayed just as precisely in 20 minutes by means of a portable spectrometer (Fig. 11).

The enormous difference in assay speed for field and laboratory spectrometers is a consequence of reducing the effective sample mass from 40-50 kg on the outcrop (subsection 2.4) to a few hundred grams in the laboratory. The net count rate produced by 2 ppm eTh in the Risø spectrometer only amounts to 17% of the background count rate in the thorium window. Most of this background originates from thorium in the concrete walls of the counting room. Wollenberg and Smith (1966b) showed that it may be profitable to make use of a low-radioactivity aggregate in the construction of concrete enclosures for gamma-ray counting. They were able to reduce the overall background by a factor of two by installing their spectrometer behind concrete manufactured from specially procured serpentinized ultramafic rock.

## 5.3. Radiation monitoring of calibration pads

In-situ pad radioelement concentrations estimated from wet mix samples or from a "dry" assay plus a moisture correction are not reliable calibration grades until the errors on these grades due to moisture variations and radon exhalation have been determined. Such a determination involves a monitoring of the radiation from the pads over a long period of time, preferably several years so that the possible seasonal variation pattern is fully disclosed

and can be taken into consideration as an additional calibration uncertainty. The airport pads at Walker Field have been monitored more systematically than any other existing facility, and the results of this effort clearly illustrate that a calibration procedure cannot be fixed forever in the moment the mix analyses are received from the laboratory.

The monitoring of the Walker Field pads was started in 1977, about one year after the facility had been constructed. The technique has been that to accumulate window counts at intervals of one to two months using a large and thermally insulated sodium-iodide detector positioned centrally over each of the five pads. Measurements carried out up to the end of 1978 were reported by Stromswold (1978) who noted a significant increase in the eU concentrations of the U and M pads between October 1977 and April 1978. The temporarily increased eU values seen during the winter months reminded of the observations previously made for the U pad at Risø (Løvborg et al., 1978), although the seasonal variation detected at Walker Field only amounted to $\pm$ 5% as opposed to a variation of $\pm$ 20% shown by the Risø pad. That this was another example of a radon effect was supported by data from the Walker Field weather office: There was a clear positive correlation between the relative air humidity and the recorded eU concentrations, so that a high output of $^{214}Bi$ radiation could be explained by absorbed pad moisture acting as an internal radon barrier.

Continued monitoring of the Walker Field pads over the years 1979, 1980, and 1981, executed by TMC staff, has revealed an annual periodicity in all the pad concentrations (B.N. Key, personal communication). The cyclic variation shown by the radiation from the pads is a consequence of the regular climate in Grand Junction where the relative humidity exhibits a strong negative correlation with the air temperature. The seasonal temperature variation is essentially sinusoidal with a low of ~ 0°C in January and a high of ~ 36°C in July; the pad grades are accordingly found to oscillate in a sinusoidal manner. While the increased pad moisture in the winter produces the greatest eU concentrations, the same moisture attenuates the calibration radi-

ation so that the K and eTh reference grades are reduced. This situation is reversed in the summer when the pads have a depleted moisture content. Data recorded since May 1980 are based on a very well temperature-stabilized detector contained in a monitoring vehicle and suggest an annual variation of ± 3% on the eU calibration grades and a corresponding variation of between ± 0.6 and ± 1.9% on the K and eTh calibration grades. There is a direct negative correlation between the air temperature and the eU grades, while the K and eTh grades show a phase lag of one to two months with respect to the temperature cycle. This may be taken as evidence that the radon barrier is formed by easily evaporable pad surface moisture. Gamma-ray attenuation, on the other hand, is controlled by a more slow exchange of moisture between the air and greater parts of the pads volumes.

In conjunction with the IAEA intercomparison experiment reported in the next chapter, the spectrometer calibration pads at Risø were monitored 27 times with a portable GR-410 between March 1980 and August 1984. Most of the readings were taken during the period from spring to autumn which is the normal time for executing routine instrument calibrations. The relative standard deviations shown by the GR-410 window sensitivities recorded over this monitoring period were 2.1% (K), 2.8% (eU), and 1.9% (eTh). The highest sensitivities were measured in dry and warm weather. It should be mentioned that the radon exhalation from the U pad is without influence on these observations because the uranium sensitivity is obtained from the count rates on two M pads which do not exhibit a seasonal radon effect (Løvborg et al., 1981).

A diminuation of a potassium or thorium calibration grade by 1% corresponds to an absorption of 0.9% additional pad moisture (formula (32)). One might ask if it would be possible to seal a pad in order to prevent the pad from exchanging moisture with the air or releasing radon present in the concrete pore spaces. Silicone water-proofers exist which can be introduced as a mix ingredient or applied as a surface coating (Rixom, 1978). It is however unsafe how durable the sealing action will be over a time span of years. Calibration pads might alternatively be

stored under water to keep them saturated with moisture, but this precaution would only come into question in a frost-free climate.

## 5.4. The processing of calibration counts

Spectrometer window counts recorded on a series of P calibration pads require the same kind of processing whether the equipment to be calibrated is a portable unit, an airborne detector package, or a complete detector system installed in a geophysical aircraft. The basis of getting the stripping ratios and window sensitivities is the series of P linear equations contained in formula (38) which provides the pad count rates observed in a single energy window. One can extend (38) to include all three energy windows by making use of the window numbers introduced in chapter 2 (Table 1). One then arrives at the general matrix equation

$$\underline{\underline{N}} = \underline{\underline{X}} \cdot \underline{\underline{G}} + \underline{\underline{B}} \qquad (55)$$

with

$$\underline{\underline{G}} = \begin{bmatrix} g_{11} & g_{12} & g_{13} \\ g_{21} & g_{22} & g_{23} \\ g_{31} & g_{32} & g_{33} \end{bmatrix} .$$

The matrix element $g_{ij}$ represents the net count rate in window "i" from a unit concentration of radioelement "j", so that for example $g_{13}$ is the signal in the potassium window produced by 1 ppm eTh. Beforehand one will expect that $g_{21}$ and $g_{31}$ are zero since a sodium-iodide detector of acceptable energy resolution does not generate potassium counts in the uranium and thorium windows (subsection 2.2). $\bar{\bar{G}}$ is the spectrometer response matrix for the counting geometry used in the calibration trial. Stripping ratios and window sensitivities for use in field assays are derived as:

$$\alpha = g_{23}/g_{33} \qquad s_K = g_{11}/F_g$$

$$\beta = g_{13}/g_{33} \qquad s_U = g_{22}/F_g$$

$$\gamma = g_{12}/g_{22} \qquad s_{Th} = g_{33}/F_g$$

$$a = g_{32}/g_{22}$$

where $F_g$ is the geometry factor estimated for the calibration trial. Consequently, to perform a spectrometer calibration is essentially a question of solving the Eq. (55) with respect to $\overline{\overline{G}}$.

For a calibration facility based on four pads, typically a KUTB configuration, it may be decided to eliminate the $\overline{B}$ term as described in subsection 4.1. The resulting 3 × 3 matrix equation is

$$\overline{\overline{\Delta}}_n = \overline{\overline{\Delta}}_x \cdot \overline{\overline{G}} \tag{56}$$

which is analogous to formula (39) and has the solution

$$\overline{\overline{G}} = \overline{\overline{\Delta}}_x^{-1} \cdot \overline{\overline{\Delta}}_n \ . \tag{57}$$

The elements of $\overline{\overline{G}}$ are here obtained by successive row-column multiplications of the inverse matrix of pad concentration differences and the associated matrix of count rate differences. The B pad of the facility is used as a base in calculating these differences. Such a procedure is used to process calibration counts recorded with the five pads of the Walker Field facility. Since only four sets of calibration counts can be processed at a time, the calculation is performed for each of the combinations KUTB, MUTB, KMTB, and KUMB. Stromswold and Kosanke (1978) incorporated the estimated errors on the pad grades and the statistical errors on the count rates and demonstrated how sub-sets of calibration constants can be weighted together into a final calibration result of known standard deviations.

A more sophisticated and generally applicable solution method is based on the least squares principle applied directly to the Eq. (55). In this approach the elements of $\bar{\bar{G}}$ and $\bar{\bar{B}}$ with accompanying uncertainties are estimated through a weighted regression analysis in three dimensions (one dimension per radioelement). It is beyond the scope of this report to give a comprehensive presentation of the associated mathematics, whereas the essential features of the technique can be highlighted by considering the corresponding one-dimensional case in which there is only one independent variable. This case is approximated in the recording of thorium window counts on a series of T pads. The problem of fitting a line to experimental points with uncertainties on both co-ordinates was recently discussed by Zijp (1984). Since the same problem occurs in another context in the following chapter, it is relevant to discuss the general case of N points $(x_i,y_i)$ with the regression line

$$y = a + bx \quad . \tag{58}$$

The weight factor $w_i$ expressing the statistical significance of $(x_i,y_i)$ in the regression of y on x must include all variance associated with $(x_i,y_i)$ in the y direction. This variance is the square sum of $\sigma_{yi}$ and $b \cdot \sigma_{xi}$ where $\sigma_{yi}$ and $\sigma_{xi}$ are the standard deviations of $y_i$ and $x_i$. Since the resulting weight factor

$$w_i = (\sigma_{yi}^2 + b^2 \cdot \sigma_{xi}^2)^{-1} \tag{59}$$

contains the unknown regression slope b, it is necessary to make an initial guess of b and then to perform a series of regressions until b does not show an appreciable change any longer. The formulas for executing this iteration are presented in Table 20 which can be used to set up a program on a calculator such as the HP-41. (The "i" index is omitted in Table 20). It is convenient to guess a start value of b from an unweighted regression of $w_i = 1$.

The inequality of regression slopes obtained from weighted and unweighted linear fits is demonstrated in Fig. 44 which is a plot of thorium count rates recorded with two hypothetical T pads

plus a B pad. The eTh reference grades are supposed to be 40, 80, and 10 ppm with standard deviations of 1, 3, and 0.5 ppm respectively. It has furthermore been assumed that these grades produced count rates of 5.1, 10.9, and 1.45 counts/s with standard deviations of 0.1, 0.4, and 0.05 counts/s due to counting statistics. In the plot the uncertainties on the abscissa and ordinate of each data point is shown as a resulting elliptical 68% confidence area. Since the data point for the most active pad (the T-2) is ascribed the smallest statistical weight, the weighted regression line is mainly controlled by the positions of the two other data points. In this example the weighted and the unweighted regression slopes, which represent experimental thorium sensitivities, are not significantly different from each other (this is seen from their estimated standard deviations). That the weighted regression line is the one to be preferred follows from the fact that its intercept with the ordinate axis, i.e. the background count rate, is of the expected positive sign.

The three-dimensional regression case can be handled with the computer program PADWIN developed by Dr. P. Kirkegaard of Risø National Laboratory (Løvborg et al., 1981). Unlike several similar programs used other places for the processing of calibration counts, PADWIN provides a set of deterministic stripping ratios and window sensitivities which do not depend on a random number generator for simulating the effects of counting statistics and uncertainties on the calibration grades. PADWIN is available in Fortran-77 and has been installed on various computers at the I.R.D. (Rio de Janeiro), Soreq (Israel), the CSIRO Division of Mineral Physics (Sydney), and the GSC (Ottawa).

## 5.5. Theoretical accuracy of field determinations

Suppose that a recording of counts with a portable spectrometer on a set of calibration pads has resulted in the stripping ratios $\alpha$, $\beta$, $\gamma$, a and window sensitivities $s_K$, $s_U$, $s_{Th}$ with accompanying standard deviations. The spectrometer is now used in a field assay where window count rates of $n_1$, $n_2$, $n_3$ are recorded. Assuming that the corresponding background count rates

$b_1$, $b_2$, $b_3$ have been determined, the Eq. (4) are used for calculating three stripped count rates $n_{1,K}$, $n_{2,U}$, $n_{3,Th}$. These are then divided by $s_K$, $s_U$, $s_{Th}$ to furnish the radioelement concentrations in the ground, $x_K$, $x_U$, $x_{Th}$. What are the estimated standard deviations of these concentrations?

A partial answer to this problem was given in subsection 2.6 where experimental precision was discussed in terms of the statistical fluctuations shown by a background-corrected and stripped window count rate. A few modest approximations made it possible to write $n_{1K}$, $n_{2,U}$, and $n_{3,Th}$ in the common form

$$n \approx p - (k \cdot q + b) \tag{60}$$

where the meaning of the individual symbols were explained in Table 7. The variance $\sigma_n^2$ resulting from the counting statistics of p, q, and b was given in formula (8). It follows from the latter that a measured radioelement concentration $x = n/s$ has an absolute precision of

$$P_x = \frac{1}{s} \sqrt{p/t + k^2\, q/t + \sigma_b^2} \tag{61}$$

where s is the window sensitivity and t the counting time on the assay spot. In this derivation the main stripping ratio "k" is regarded as a fixed number of zero error.

The subject now is to estimate the accuracy of x, i.e. the deviation between the true radioelement concentration of the ground and the concentration recorded as an average of a large number of repeat measurements. Accuracy may be stated as a standard deviation $A_x$ which represents a systematic error originating from the uncertainties of the calibration constants required for the determination of x. When $A_x$ is known, it may be combined with the standard deviation $P_x$ due to counting statistics so as to provide an overall experimental standard deviation of

$$\sigma_x = \sqrt{P_x^2 + A_x^2}\ . \tag{62}$$

To calculate the $A_x$ associated with a particular energy window one must know the standard deviations $\sigma_s$ and $\sigma_k$ of the window sensitivity and the stripping ratio k which is identical to "a" in the thorium window, "α" in the uranium window, and "γ" in the potassium window ("β" is of negligible statistical importance as explained in subsection 2.6). With x = n/s and n given by formula (60) one obtains the estimate

$$A_x = x \cdot \sqrt{(\sigma_n/n)^2 + (\sigma_s/s)^2} \qquad (63)$$

where

$$\sigma_n = q \cdot \sigma_k \ . \qquad (64)$$

A useful working expression is provided by replacing the interfering count rate q·k by the known count rate "r" produced by the two other assayed radioelements. The same substitution was done in subsection 2.6 in deriving a priori detection and determination limits, and the calculation of "r" in each energy window was shown in Table 8. One can then get the accuracy of x from the formula

$$A_x = x \cdot \sqrt{(F \cdot \sigma_k/k)^2 + (\sigma_s/s)^2}$$

with (65)

$$F = \frac{r}{s \cdot x} \ .$$

The procedure for calculating $A_x$ in each spectrometer window is summarized in Table 21. It should be noticed that (65) is an approximative formula which disregards the possible covariances of the calibration constants. With a calibration facility that includes at least one pure T pad and one pure U pad the errors on the stripping ratios can be reduced to any desired level by accumulating calibration counts for a sufficiently long time. For such a calibration, formula (65) gives the simple result that the relative error on an assayed radioelement concentration equals the relative error on the window sensitivity used in the assay. It would be very convenient if field accuracy could be

estimated in this manner in a number of practical situations, and it is therefore relevant to investigate under which circumstances the first term under the square root sign in (65) may be disregarded.

If one demands that

$$F \cdot \frac{\sigma_k}{k} < 0.5 \frac{\sigma_s}{s} \quad , \tag{66}$$

then one commits a maximum error of 11% in setting $A_x/x = \sigma_s/s$. The intercomparison experiment reported in the next chapter indicates that, in practice, the relative standard deviations of stripping ratios and window sensitivities do not differ substantially from each other, so that (66) can be reduced into the condition: $F < 0.5$. For a portable GR-410 spectrometer with stripping ratios $\alpha = 0.6$ and $a = 0.03$ and a ratio of 2.5 between the uranium and thorium sensitivities one finds that the Th/U ratio of the assayed formation must be between 0.2 and 2. Therefore, in a typical granitic environment of Th/U ≈ 3 or greater, the estimated eU concentrations will be less accurate than suggested by the relative error on the uranium sensitivity. One should consequently not omit the "F" term in the calculation of field accuracy.

## 6. THE IAEA PADS INTERCOMPARISON EXPERIMENT 1980-84

### 6.1. Outline of the experiment

As stated in the Introduction, the present investigation was started with the primary objective of executing calibration trials with pads facilities available in 1979 in order to see to what extent stripping ratios and window sensitivities recorded with these facilities were in agreement with each other. If highly consistent calibration results could be provided, then there would be rather strong evidence that the radiometric grades

adopted at each facility are reliable. The instrument chosen for the recording of calibration counts was a Geometrics GR-410 purchased by Risø National Laboratory in 1977. This particular unit had been used for many field assays in Greenland and Denmark without ever showing any electronic malfunctioning or failure. It should therefore be qualified for use in an experiment that would involve several air travels to pads facilities abroad. Calibration counts taken on the spectrometer pads at Risø before and after each visit to a facility in another country would be a means of controlling whether it should be possible to avoid that the calibration constants of the instrument changed during the experiment. Such changes might be expected since the GR-410 carrying case was too voluminous to be brought along as hand baggage on international flights and therefore would be exposed to unavoidable bumps in airport baggage areas.

This originally planned exercise with calibration pads incorporated the airport facilities in Borlänge, Helsinki, Ottawa, and Grand Junction plus the series of smaller pads in Malå and at Bells Corners. These older calibration sites were visited with the portable GR-410 between February 1980 and June 1981, and the recorded stripping ratios and window sensitivities were presented at the OECD/NEA Symposium on Uranium Exploration Methods held in Paris in June 1982 (Løvborg, 1982). Calibration results from the pads at Bells Corners were not available at that time since the Geological Survey of Canada had not finished the evaluation of the pad grades when the symposium paper was written. The Risø pads were included in this first processing of the experimental data. However, in the final report on the Risø facility it was noticed that the eU grades for the two M pads of the facility were 18% greater than the grades suggested by the average uranium sensitivity determined for the GR-410 spectrometer (Løvborg et al., 1981). In view of this observation the idea arose to use the internationally calibrated GR-410 as a tool for testing the reliability of pad radioelement concentrations. The data recorded with the instrument on the Risø pads were actually used to revise the complete series of K, eU, and eTh reference levels in these pads, so that the Risø facility from now on can be regarded as a secondary calibration site

where the grades are tied to facilities in Canada, Finland, Sweden, and the USA.

A further opportunity to use the GR-410 as a testing and grade-assignment device became actual in the period from October 1982 to March 1984 during which time the facilities at Rio de Janeiro, Villa 25 de Mayo, Lanseria, Soreq, and Sydney either were completed or were in the stage of being assigned radioelement concentrations based on laboratory assays. The pads here plus three new pads added to the facility in Malå were all visited with the instrument while rigorously using the Risø pads to verify that the calibration constants of the instrument remained the same as recorded during the preceding calibration phase. As illustrated in subsection 6.6, it has been attempted to test a facility by plotting the "dry" pad concentrations measured by sealed-can gamma-ray counting against the concentrations determined with the GR-410 spectrometer. In view of the more or less pronounced seasonal dependence exhibited by in-situ pad grades (subsection 5.3), it is quite obvious that the observed regression slopes can be no more than a crude test of the grades suggested by laboratory determinations. On the other hand, the experiment has given a fair idea of what a "normal" regression slope should be, and in one particular case (the U pad at Lanseria) the in-situ assay with the GR-410 turned out to give the answer to a grade-assignment problem caused by inconsistent laboratory results (Corner and Smit, 1983).

In both the calibration phase and the assay part of the experiment it was attempted to perform the counting on the pads in a geometry corresponding to 90% of $2\pi$ or greater. Pads for portable spectrometers were counted with the GR-410 detector probe standing centrally as illustrated in Fig. 25 in the case of the pads at Villa 25 de Mayo. The various airport pads were most often counted with the detector in a slightly elevated position in order to enhance the signal from the more distant parts of the pad surfaces. The elevation was provided by placing the detector on a cardboard box or by suspending it on a tripod (Fig. 45). In all measurements a geometry factor was estimated by means of formula (21) with "h" taken as the distance from the pad sur-

face to the centre of the sodium-iodide crystal. It lasted one or two days to perform a counting trial with a facility, depending on the number of pads to be counted and the grades of the pads. Each pad was counted repeatedly using manual adjustments of the spectrometer gain between the readings whenever such adjustments were prompted by the error signal from the $^{133}Ba$ source attached to the detector (subsection 2.4). Readings taken on K, U, T, and M pads were not stopped until between 10,000 and 20,000 counts had been accumulated in the relevant energy window. A survey of the entire experimental program is presented in Table 22.

## 6.2. Statistical processing method

When several facilities are used for calibrating a spectrometer, one is faced with the problem that the individually recorded calibration factors have different uncertainties, mainly because the concentration matrix $\bar{\bar{X}}$ in Eq. (55) varies from one facility to another with respect to size, internal structure, and standard deviations on the matrix elements. In the subsequent application of the spectrometer for establishing a "normal" correlation between monitored and analysed pad grades there is the similar problem that the regression slopes obtained with the tested facilities have statistical errors which vary in accordance with the goodness of the linear fit. These problems are solved by forming a weighted average of the involved experimental data and by using a variance test to decide how an associated standard deviation should be calculated. The procedure was summarized by Løvborg (1982) and is explained here in somewhat greater detail.

Let $(x_1, x_2, \ldots, x_N)$ represent N observations of estimated standard deviations $(\sigma_1, \sigma_2, \ldots, \sigma_N)$. It is assumed that a histogram of x would furnish a normal distribution for $N \to \infty$, and the task is to assess the mean value $\bar{x}$ and the standard deviation $\sigma$ by which the normal distribution is defined. In calculating these two parameters, a single observation is ascribed a weight factor of

$$w_i = 1/\sigma_i^2 \qquad (67)$$

which is the inverse variance of the observation (cf. formula (59)). The mean value is obtained as

$$\bar{x} = \frac{\Sigma\, w_i x_i}{\Sigma\, w_i} \quad , \tag{68}$$

while an estimate of $\sigma^2$ may be provided in two different ways: 1) As a variance $V_1$ describing the actual dispersion of the observations around $\bar{x}$; 2) as an expected variance $V_2$ suggested by the known variances $\sigma_i^2$. The weighted expressions for the calculation of $V_1$ and $V_2$ are

$$V_1 = \frac{N}{N-1} \left\{ \frac{\Sigma\, w_i x_i^2}{\Sigma\, w_i} - \bar{x}^2 \right\} \tag{69}$$

and

$$V_2 = \frac{N}{\Sigma w_i} \quad . \tag{70}$$

If $V_1$ comes out smaller than $V_2$, the reason may be that the standard deviations ($\sigma_1$, $\sigma_2$,..., $\sigma_N$) contain a fixed uncertainty which did not show up as dispersion on the recorded data. Such an uncertainty might be represented by a laboratory assay error in repeat calibrations with one and the same pad facility. In general a small observed variance $V_1$ cannot be taken as evidence that $\sigma^2$ then must be small, so it is the $V_2$ variance which is adopted to begin with. Only if $V_1$ is significantly greater than $V_2$, in the statistical sense, one is forced to skip $V_2$ in favour of $V_1$ since the experiment disclosed variability not included in ($\sigma_1$, $\sigma_2$,..., $\sigma_N$).

The test of $V_1$ against $V_2$ is performed in terms of the ratio

$$F = \frac{V_1}{V_2} \tag{71}$$

whose nominator and denominator are characterized by N-1 and N degrees of freedom respectively. In the present study the null hypothesis "$V_1$ is not significantly greater than $V_2$" is tested

at a confidence level of 90%, i.e. there is a 10% chance of accepting the null hypothesis when it is actually false. The corresponding critical level $F_{10}$ (N-1, N) is taken from a standard tabulation, for example that presented by Koch and Link (1970). Whenever $F < F_{10}$ (N-1, N) $\sigma$ is estimated as $\sqrt{v_2}$, otherwise it is estimated as $\sqrt{v_1}$.

## 6.3. Result of calibration trials in 1980-81

The grades assigned to the pads used for calibrating the GR-410 spectrometer are shown on the relevant data sheets in the Appendix. For two of the facilities, Bells Corners and Walker Field, the pad grades are based on assays of cured and sealed mix samples, suggesting that the resulting window sensitivities essentially represent count rate per unit of "wet" radioelement concentration (subsection 5.1). The grades available for the pads of the four other facilities (Uplands airport, Helsinki-Vantaa, Borlänge, and Malå) originate from assays of powdered sample material and would consequently be expected to produce window sensitivities slightly greater than those recorded at Bells Corners and Walker Field. Therefore, it was not beforehand anticipated that the data generated in the experiment would result in an unambiguous calibration of the instrument.

GR-410 window counts recorded in each performed calibration trial were processed using the computer program PADWIN, so that the stated uncertainties on the pad grades were taken into consideration as described in subsection 5.4. The geometry factor estimated in each trial was used for normalizing the set of calculated window sensitivities into $2\pi$ measuring geometry. It can be seen from Table 22 that the Walker Field pads were visited twice, in February and August 1980. The two counting dates nearly coincide with the times of the year where the pad concentrations reach their extreme values in the seasonal cycle established for the facility (subsection 5.3). The expected radon exhalation from the U and M pads in August manifested itself as a uranium window sensitivity that was 6% smaller than the value measured in February. The smaller gamma-ray attenuation due to the evaporation

of pad moisture in the summertime was also noticed, namely as 4 to 5% increased potassium and thorium window sensitivities from the first to the second calibration trial. However, when the variance test was applied to the two single trials, neither the stripping ratios or the window sensitivities were found to vary more than suggested by the standard deviations on the pad grades. Consequently, it was possible to combine each pair of experimental calibration constants into an average value whose standard deviation was taken as the square root of the calculated $V_2$ variance.

The calibration performed in Sweden included two trials with the airport pads in Borlänge and one trial with the original version of the Malå facility. Since the four older pads at Malå were constructed from the supply of concrete bricks used for making the Borlänge pads and therefore possess the same grades as the latter, the trial at Malå was regarded as a repeat of the calibrations done at Borlänge. In merging the three sets of data into a single set of calibration constants the variance test gave statistical significance on the stripping ratio $\alpha$ and the normalized uranium sensitivity $s_U$. The standard deviations of these two calibration constants were accordingly chosen as the square root of the $V_1$ variance.

Having combined the repeat calibrations in the USA and Sweden, the recorded spectrometer counts produced five calibration results obtained in four countries. The series of experimental stripping ratios and window sensitivities are presented in Tables 23 and 24 respectively. Because the pad grades of the facilities at Uplands airport and Bells Corners are based on different laboratory reference materials, the two Canadian results have not been merged together. As opposed to what was expected beforehand, the window sensitivities recorded at Bells Corners and Walker Field are not consistently smaller than the sensitivities measured with the other facilities. This result shows that the distinction between "wet" and "dry" pad grades may be obscured by experimental uncertainties, in particular laboratory assay error and errors on the estimated geometry factors. The bottom of each table shows the estimated mean

calibration constants with associated standard deviations $\sqrt{V_1}$ and $\sqrt{V_2}$ and variance ratio F. Since none of the F ratios exceed the critical value $F_{10}$ stipulated by the number of single observations, $\sigma$ is estimated as $\sqrt{V_2}$ in all cases. It therefore appears that the errors ascribed to the pad grades used for calibrating the instrument are realistic, i.e. they have not been appreciably underestimated. (This statement may not be valid for the error of ± 0.5 ppm eU assumed for the U pads in Sweden). The most valuable information is contained in the recorded window sensitivities $s_K$, $s_U$, and $s_{Th}$ because these calibration constants are referencing absolute radiometric concentration levels. Table 24 shows that the window sensitivities measured with the Walker Field facility are the least uncertain (except for the $s_K$ result obtained in Sweden), so that this facility is given a strong weight in ascribing a representative set of average sensitivities to the spectrometer. Since the reference grades for the Walker Field pads include the effect of pad moisture, the trials presumably resulted in a calibration that can be classified as "wet".

The five single calibration results can be assumed to be completely independent of each other because they are provided by pad grades which have been estimated by procedures and reference materials that were not the same from one calibration to the next. It therefore makes sense to regard the data as the outcome of an experiment in which all the uncertainty is due to random error sources. In an experiment of this kind it is permissible to estimate the standard deviation of $\bar{x}$ as $\sigma/\sqrt{N}$, and this has been done for each determined calibration constant in Tables 23 and 24 where $\sigma/\sqrt{N}$ is given both absolutely and in percent of $\bar{x}$. It can be seen that the window sensitivities and main stripping ratios determined for the spectrometer are 1 to 2% uncertain. The question is whether it would be safe to adopt these small calibration uncertainties in the monitoring program executed after the calibration period. This problem is dealt with in subsection 6.5.

## 6.4. Calibration checks

Chapter 2 included a description of computer-simulated pulse spectra which were based on the combined use of terrestrial flux calculations and a detector response model providing the spectral components generated by a 76 × 76 mm sodium-iodide scintillator (full-energy peak, annihilation escape peaks, and Compton continuum). Such spectra were used to predict the stripping ratios and window sensitivities of a GR-410 spectrometer whose detector was ascribed an energy resolution of 7.6, 8.8, or 10.0 percent. These theoretical data, listed in Tables 2 and 3, may serve as a check on the experimental GR-410 calibration constants evaluated in the preceding subsection. As far as the stripping ratios are concerned, the measured values of $\beta$ and $\gamma$ are considerably smaller than their calculated counterparts. This observation may suggest that the potassium window of the instrument was narrower than the 0.21 MeV aimed at by the manufacturer when he adjusted the voltages which control the window widths. The calculated values of $\alpha$, on the other hand, are in the range from 0.577 to 0.595 which is in very good agreement with the experimental mean value of 0.583 ± 0.009. Assuming an intermediate energy resolution of 8.8% for the calibrated detector probe, the ratios between calculated and experimental window sensitivities amount to 1.18 (K window), 1.14 (U window), and 1.13 (Th window). One would expect a set of slightly overestimated theoretical window sensitivities because the gamma-ray absorption in the metal sheath and other parts of the detector unit was disregarded in the spectrum calculations. It is very satisfactory that the experiment indicated a ratio of 2.54 ± 0.06 between the U and Th sensitivities since this value is completely consistent with a theoretical ratio of between 2.52 (10.0% resolution) and 2.59 (7.6% resolution).

An entirely different kind of check was performed by measuring the gamma-ray exposure rates on the pads of two of the used calibration facilities, namely those at Walker Field and Borlänge. Table 4 showed factors for calculating the exposure rates one meter above an infinite soil medium of known radioelement concentrations. If similar factors were available for calibration

pads of various dimensions, it would be possible to get an idea of the validity of the pad grades from monitoring trials with radiological instruments or radiation dosimeters. A gamma-ray transport calculation for the finite geometry on a calibration pad is more complicated than the corresponding calculation for infinite sources. The exposure rates per radioelement concentration unit shown in Table 25 are based on the Monte-Carlo transport code GAMO used to get the theoretical exposure rates for the pads at Risø (Løvborg et al., 1981). It should be noted that large calibration pads (2R = 8 to 10 m) produce surface expose rates that are about 15% smaller than the exposure rates from an infinite source at 1 m. This is because the atmospheric backscatter contribution of low-energy gamma rays is distributed over a very large area, independently of the source dimensions, so that this contribution remains undetected when the source is less than several tens of meters across (Løvborg et al., 1980).

The exposure rates on the pads at Walker Field and Borlänge were recorded with Reuter-Stokes high-pressure argon ionization chambers placed centrally on the pad surfaces. These instruments are based on a design developed by the former US Health and Safety Laboratory and permit a reliable determination of environmental exposure rates down to a few microroentgens per hour (DeCampo et al., 1972). Both chambers used were 25 cm in diameter and mounted in 30 × 30 × 30 cm aluminium boxes so that the readings should be comparable to the exposure rates at 15 cm suggested by the dimensions and radioelement concentrations of the pads. Each chamber was calibrated by means of platinum-encapsulated $^{226}Ra$ sources of certified activity and an estimated gamma-ray constant of 0.825 $R \cdot m^2 \cdot h^{-1} \cdot g^{-1}$ (Nachtigall, 1969). In the Walker Field experiment this was done using the "shadow-shield" method, while the calibration performed in conjunction with the Borlänge trial was based on the flux of direct and ground-scattered gamma rays obtained with the radium source supported by a thin pole. The two calibration techniques were discussed by Bøtter-Jensen (1982). In using these calibrations for measuring the exposure rates on concrete pads, it is relevant to correct the ionization-chamber readings by +3% on K pads and by -2% on U, T, and M pads. These corrections are suggested from runs with the GAMO code in which the slightly en-

hanced energy response of the chambers between 0.06 and 0.3 MeV was taken into consideration.

The exposure rates on the Walker Field pads were measured three times between February and July 1980, while only one measurement was performed with the Borlänge facility. The result of these experiments is shown in Table 26 where calculated and experimental exposure rates are stated as difference values with respect to the B pads of the two facilities. Calculated exposure rates include the standard deviations on the pad grades as well as Monte Carlo statistics and uncertainties on the gamma-ray emissions from the radioelements. The experimental data for the Walker Field facility are averages of the three single determinations; no result is given for the K pad because this result was very imprecise and therefore contained no usable information. From the ratios given in the last column of the table it can be seen that, when the uncertainties are taken into consideration, the calculated and measured exposure rates do not deviate significantly from each other. This observation supports the validity of the grades ascribed to the six pads tested in the trial. However, it cannot be denied that the calculated average values systematically exceed their experimental counterparts by several percent. A deviation like this would be expected if the pad grades did not include all the moisture present in the pads, and it might be suggested that the experiment was on the point of revealing an unnoticed additional moisture content in the Walker Field pads.

## 6.5. Instrumental long-term stability

Figure 46 is a plot of the thorium window sensitivity and "$\gamma$" stripping ratio recorded with the GR-410 spectrometer in the 27 control calibrations executed on the Risø pads in the course of the entire experiment. Calibration constants measured in these trials are based on the revised pad grades obtained by processing the first 13 control measurements (those from 1980-81) with the evaluated calibration data in Tables 23 and 24. The revised grades for the Risø facility were presented by Løvborg (1983);

they include the uncertainties due to the varying amount of pad moisture over the year and the associated variable radon exhalation from the U pad. The use of $s_{Th}$ ("$s_T$" in Fig. 46) and $\gamma$ to give a visual impression of the instrumental long-term stability stems from the fact that these two calibration constants are positively correlated with the photomultiplier gain (Table 5). Accordingly, if the gain monitoring circuit of the instrument should begin to offset the energy calibration in the positive or negative direction, $s_{Th}$ and $\gamma$ should both reflect such a malfunction by changing their values in the same direction. From the plot of $\gamma$ it is not possible to see any systematic variation in the data. In fact, the fluctuations shown by the three main stripping ratios were not greater than suggested by counting statistics and the standard deviations assigned to the pad concentrations. Only the small "a" stripping ratio showed a surplus variability which may be explained by the radon effect in the U pad and therefore is inconclusive.

For the thorium window sensitivity it is possible to distinguish a seasonal influence, especially over the coherent data-recording period from mid 1982 to mid 1983. The first data point in 1983 (recorded on 11 February) corresponds to an almost 6% reduction of the thorium sensitivity typically measured in the summer months. This is an example of how much an instrument calibration can be biassed when the readings are taken with the pad surfaces exposed to an outdoor moisture such as that existing in Denmark in the winter months. In the present context the task is to assess the maximum variability exhibited by the thorium sensitivity due to instrumental factors. From Fig. 46 it appears that the summer readings taken with the instrument in the years from 1980 to 1983 have a high degree of consistency. The resulting 14 data points were analysed for dispersion using the assumption that the calculated $V_1$ variance could be explained by counting statistics alone, i.e. the uncertainties on the pad grades were not included in estimating the $V_2$ variance. The variance test was not significant, and it was concluded that the relative standard deviation on $s_{Th}$ from sources other than counting statistics was smaller than 0.5%. This contribution is insignificant as compared to the relative error of 1.2% adopted for the thorium window sensitivity of the instrument (Table 24).

In total the test calibrations undertaken from the beginning of the experiment and up to August 1983 have not revealed any change in the performance of the monitoring instrument. It is actually surprising that a portable spectrometer can maintain its calibration characteristics during more than four years of repeated airline transport between destinations where the climatic conditions often were extremely different from each other. Such a calibration cannot of course last forever. From Fig. 46 one observes that the last determination of thorium sensitivity, from August 1984, did not give the expected value of about 0.129 counts/s per ppm eTh, but rather suggested a 2% lower value of 0.126 counts/s per ppm eTh. This break in the pattern from the preceding years might be a first indication of an irreversible change in the instrument performance (possibly reduced energy resolution), but it could also be an indirect effect of the moist Danish summer in 1984.

## 6.6. Measurement of pad in-situ grades

In using the GR-410 as a tool for measuring pad radioelement concentrations, the B pad of each monitored facility was ascribed concentrations of zero. Counts recorded on a B pad were accordingly regarded as background signals, so that the concentrations measured in the other pads were derived relatively to the concentrations in the B pad. This way of stating pad grades corresponds to specifying the basic $\Delta_x$ matrix of the facility (subsection 4.1). The precision and accuracy of each in-situ assay were evaluated using the working expressions in Tables 7 and 21 and were then combined into overall standard deviation on the measured grades by means of formula (62). No attempt was made to estimate the accuracy of the geometry factors used for calculating the $2\pi$ window sensitivities of the instrument back into actual pad geometries. The recorded concentration differences are shown on the relevant data sheets in the Appendix together with the corresponding absolute grades suggested by sealed-can gamma-ray counting of powdered pad material. Grade differences stated for the Risø facility are based on the 13 monitoring trials executed in 1980-81, i.e. during the period when the in-

strument was calibrated. Uncertainties on these grade differences are either represented by $\sqrt{V_1}$ or $\sqrt{V_2}$, depending on the outcome of the associated variance test. The F ratio for the eU concentrations of the U pad was highly significant as one could expect from the strong seasonal radon effect established for this particular source.

The result of applying weighted, linear regression fits to the series of experimental in-situ grades and laboratory grades is presented in Table 27. Associated K, eU, and eTh regression plots are shown in Figs. 47 to 49 using the data from the CSIRO facility in Sydney as examples. Since the calibration of the GR-410 is believed to reference "wet" pad radioelement concentrations, the monitored grades should include the moisture contents in the pads under test. Furthermore, for all facilities with the possible exception of Soreq and Lanseria the laboratory assays were performed with concrete powder that had been dried for 24 hours at 105 to 110°C. A calculated regression slope, i.e. the ratio between analysed and monitored pad grades, should therefore provide the ratio

$$x_d/x = 1 + w \qquad (72)$$

where w is the absorbed pad moisture (subsection 3.4). In subsection 5.1 it was argued that the extreme limits for moisture absorption in concrete of ~ 20% porosity amount to 2% (low) and 10% (high). Consequently, one would expect experimental dry-to-wet concentration ratios of between 1.02 and 1.10.

Many of the ratios reported in Table 27 match the predicted variation range, but there are several noticeable exceptions from the general pattern. The fact that some of the U and Th dry-to-wet ratios are smaller than unity shows that the variability of the data cannot be explained from the moisture hypothesis alone. It must rather be concluded that the uncertainties contributed by analytical sampling and assay error as well as error on the estimated geometry factors tend to obscure the plain moisture effect. Also, as intimated by the calibration checks in subsection 6.4, it cannot be guaranteed that the GR-

410 was truly calibrated in terms of "wet" pad radioelement concentrations. One can easily imagine that the combined effect of the experimental uncertainties may push a recorded dry-to-wet ratio upwards, although it is hard to believe that this is the reason why a few of the ratios are considerably greater than 1.10.

To obtain an identification of the real outsiders in the data material, the variance test was applied iteratively to the ratios provided by each radioelement. This was done so that the most suspicious ratio was left out in a test prompted by a preceding test which revealed statistical significance. The procedure resulted in the mean dry-to-wet concentration ratios presented at the bottom of Table 27. In view of the error sources involved one cannot use these results to assess the average moisture contents in the tested pads, whereas it is quite possible to establish an upper limit of about 1.10 for the ratio between an analysed and a monitored pad grade. Consequently, facilities characterized by a ratio which exceeds ~ 1.10 must contain pads of either overestimated laboratory grades or underestimated in-situ grades.

The greatest diverging concentration ratios are observed for the facility at Villa 25 de Mayo. This is the only example of unsually large potassium and thorium dry-to-wet ratios derived from the experiment. One can explain the results for these two radioelements as a geometry error on the estimated in-situ grades. The Argentine pads are only one meter in diameter which is the smallest source dimension involved in the monitoring experiment. They were monitored using a geometry factor of 0.86 which is the value obtained from formula (21) with "h" taken as the distance of 70 mm from the bottom face of the GR-410 detector unit to the centre of the sodium-iodide crystal. In subsection 3.2 it was pointed out that formula (21) is inadequate for estimating geometry factors over sources whose radii are equal to ~ 0.5 m or smaller. The availability of the curves in Fig. 30 makes it possible to estimate an improved geometry factor of 0.80 for the monitoring of the Villa 25 de Mayo facility (using a value of $h/R = 0.14$ and interpolating between the curves for

h/R = 0.10 and h/R = 0.15). This correction step reduces the dry-to-wet concentration ratios for potassium, uranium, and thorium to 1.15 ± 0.05, 1.70 ± 0.03, and 1.08 ± 0.02, respectively. At least the thorium result is now consistent with the observations from the other facilities.

The interesting outcome of the test are three uranium concentration ratios which exceed the suggested upper limit of 1.10. The first anomalous U result is the corrected ratio of 1.70 ± 0.03 obtained for the pads at Villa 25 de Mayo. The two additional high U ratios are recorded for the facilities at Risø and Rio de Janeiro; they amount, respectively, to 1.25 ± 0.03 and 1.14 ± 0.03. A ratio of 1.14 is not conspicuously high. However, a plot of the laboratory eU grades for the eight Brazilian pads against the measured in-situ grades makes it possible to identify two of the M pads, number 3 and 5 (Fig. 36), as producers of anomalously low U radiation with an associated dry-to-wet ratio of 1.25 ± 0.03. As far as the Risø facility is concerned, the U concentration ratio is provided by two M pads plus a U pad of seasonally varying radon exhalation. In the 13 monitoring trials performed with the Risø pads in 1980-81, the eU grade of the U pad varied between 131 to 194 ppm, corresponding to a relative grade fluctuation of ± 19%. Over the same period the eU grades of the M pads showed a variability of less than ± 4%. The U pad therefore had a much smaller statistical weight than the M pads in calculating the regression slope used for estimating an average dry-to-wet uranium ratio for the facility.

It lays near at hand to conclude that a radon effect has been detected for the U pads at Villa 25 de Mayo and the M pads at Rio de Janeiro and Risø. One can make a conservative estimate of the suggested exhalation by calculating a relative radiation loss of

$$-\frac{\Delta\phi}{\phi} = \frac{b - 1.10}{b} \qquad (73)$$

where "b" is the dry-to-wet ratio (regression slope) recorded for the eU pad grades. Based on this expression, the monitoring revealed an exhalation of 35% for the Argentine U pads. Pads M-3 and M-5 at Rio de Janeiro and pads M-1 and M-2 at Risø similarly appear to exhibit an exhalation of 12%.

Having been presented to the result for the facility at Villa 25 de Mayo, staff of the C.N.E.A. in Mendoza flooded a similar U pad with water and noticed that the gamma radiation from the pad increased by 34% over a period of four weeks (F.J. Muñiz, personal communication). The moisture supplied to the pad in the experiment was estimated to be 12%, corresponding to a gamma-ray attenuation factor of 1.13 for the pad in the soaked condition (formula (32)). Consequently, the pad became 38% rather than 34% more radioactive when the radon flow through the pad surface was stopped by water in the concrete porespaces. This increase suggests an exhalation of 38/138 = 28%, in reasonable agreement with the monitored exhalation of 35%.

The applicability of U or M pads which emanate radon all depends on the seasonal variability of the exhalation. The U pad at Risø is only applicable for determining "a" and $\gamma$ stripping ratios because of the variable radiation output from it, while the two M pads of the facility permit a reliable determination of uranium window sensitivities by virtue of essentially constant eU calibration grades which include the radiation diminuation due to radon exhalation. A nearly constant exhalation rate probably results from a partly permeable radon barrier formed by excessive concrete surface moisture which is sustained all the year round by air humidity.

ACKNOWLEDGEMENTS

During the visits to calibration facilities abroad the author was met with great hospitality, scientific enthusiasm, and willingness to help and supply information. It is impossible to thank all the individuals who contributed to the success of the pads intercomparison experiment. Their respective organizations are or were: Comisión Nacional de Energía Atómica (Argentina); CSIRO Institute of Energy and Earth Resources (Australia); Comissão Nacional de Energia Nuclear (Brazil); Geological Survey of Canada; Geological Survey of Finland; Israel Atomic Energy Commission; Nuclear Development Corporation of South Africa; Swedish Geological; US Department of Energy; and Bendix Field Engineering Corporation (USA). Special thanks are due to Robert L. Grasty of the Geological Survey of Canada for a very inspiring exchange of views and information at meetings and by correspondence. The author is furthermore grateful to his colleagues in the Nuclear Geophysics Group, in particular Erik Mose, for their assistance in this research project. The exposure rate measurements on the Borlänge pads were performed by Lars Bøtter-Jensen of Risø's Health Physics Department. Sam Marutzky of Bendix Field Engineering Corporation monitored the exposure rates on the airport pads in Grand Junction. Lis Vang Christensen typed the manuscript with assistance from Kirsten Hansen, and Tora Skov, Agnete Michelsen, and Anna Taboryska made the drawings. The International Atomic Energy Agency was always very responsive and flexible in negotiating the renewal contracts.

REFERENCES

ADAMS, J.A.S. and FRYER, G.E. (1964). Portable γ-ray spectrometer for field determination of thorium, uranium, and potassium. The Natural Radiation Environment (Univ. Chicago Press, Chicago) 577-596.

ADAMS, J.A.S. and GASPARINI, P. (1970). Gamma-Ray Spectrometry of Rocks (Elsevier, Amsterdam) 295 pp.

AUSTIN, S.R. (1975). A laboratory study of radon emanation from domestic uranium ores. Radon in Uranium Mining (International Atomic Energy Agency, Vienna) 151-163.

AVIV, R. and VULKAN, U. (1983). Airborne gamma-ray survey over Israel: The methodology of the calibration of the airborne system. Rep. No. Z.D. 58/82 (Soreq Nuclear Research Center) 65 pp.

BARRETTO, P.M.C., CLARK, R.B., and ADAMS, J.A.S. (1972). Physical characteristics of radon-222 emanation from rocks, soils and minerals: Its relation to temperature and alpha dose. The Natural Environment II (USERDA, Springfield, Virginia) vol. 2, 731-740.

BECK, H.L. (1972). The absolute intensities of gamma rays from the decay of $^{238}U$ and $^{232}Th$. HASL-262 (US Atomic Energy Comm.) 14 pp.

BERGER, M.J. and SELTZER, S.M. (1972). Response functions for sodium iodide scintillation detectors. Nucl. Instrum. Meth. 104, 317-332.

BØTTER-JENSEN, L. (1982). Calibration and standardization of instruments for background radiation monitoring. Proc. Third Int. Symp. on Radiation Protection - Advances in Theory and Practice (Society for Radiological Protection, Inverness, Scotland, 6-11 June 1982) 685-690.

BRISTOW, Q. (1983). Airborne γ-ray spectrometry in uranium exploration. Principles and current practice. Int. J. Appl. Rad. and Isot. 34, 199-229.

CORNER, B., TOENS, P.D., RICHARDS, D.J., VAN AS, D., and VLEGGAAR, C.M. (1979). The Pelindaba facility for calibrating radiometric field instruments. Atomic Energy Board, Pretoria, Rep. PEL-268, 23 pp.

CORNER, B. and SMIT, C.B.J. (1983). The construction of a radiometric calibration facility at Lanseria airport, Republic of South Africa. Nucl. Develop. Corp. South Africa, Rep. PER-77, 24 pp.

CROUTAMEL, C.E. (1970). Applied Gamma-Ray Spectrometry. Second revised and enlarged edition by F. Adams and R. Dams (Pergamon, Oxford) 753 pp.

CULOT, M.V.J., OLSON, H.G., and SCHIAGER, K.J. (1976). Effective diffusion coefficient of radon in concrete, theory and method for field measurements. Health Phys. 30, 263-270.

CURRIE, L.A. (1968). Limits for qualitative detection and quantitative determination - application to radiochemistry. Analytical Chemistry 40, 586-593.

DARNLEY, A.G., BRISTOW, Q., and DONHOFFER, D.K. (1969). Airborne gamma-ray spectrometer experiments over the Canadian shield. Nuclear Techniques and Mineral Resources (International Atomic Energy Agency, Vienna) 163-186.

DARNLEY, A.G. and GRASTY, R.L. (1971). Mapping from the air by gamma-ray spectrometry. Geochemical Exploration (The Canadian Institute of Mining and Metallurgy, special volume 11) 485-500.

DARNLEY, A.G. (1973). Airborne gamma-ray survey techniques - present and future. Uranium Exploration Methods (International Atomic Energy Agency, Vienna) 67-108.

DARNLEY, A.G. (1977). The advantages of standardizing radiometric exploration measurements, and how to do it. Can. Min. Metallurg. Bull., February 1977, 1-5.

DECAMPO, J.A., BECK, H.L., and RAFT, P.D. (1972). High pressure argon ionization chamber systems for the measurement of environmental exposure rates. HASL-260 (US Atomic Energy Comm.) 69 pp.

DICKSON, B.H., BAILEY, R.C., and GRASTY, R.L. (1981). Utilizing multi-channel airborne gamma-ray spectra. Can. J. Earth Sci. 18, 1793-1801.

DICKSON, B.L., CLARK, G.J., and McGREGOR, B.J. (1979). Technique for correcting for overburden effects in ground level radiometric surveys of uranium ore bodies. Geophys. 44, 89-98.

DICKSON, B.L., CHRISTIANSEN, E.M., and LØVBORG, L. (1982). Reference materials for calibration of laboratory gamma-ray analyses. Uranium Exploration Methods (OECD, Paris) 687-698.

DICKSON, B.L. and LØVBORG, L. (1984). An Australian facility for the calibration of portable gamma-ray spectrometers. Bull. Aust. Soc. Explor. Geophys. (in press).

DOIG, R. (1968). The natural gamma-ray flux: in-situ analysis. Geophys. 33, 311-328.

ENDT, P.M. and VAN DER LEUN, C. (1973). Energy levels of A = 21-44 nuclei (V). Nucl. Phys. A214, p. 436.

EVANS, R.D. (1955). The Atomic Nucleus (McGraw-Hill, New York) 972 pp.

EWBANK, W.B. (1980). Status of transactinium nuclear data in the Evaluated Nuclear Structure Data File. IAEA-TECDOC-232 (International Atomic Energy Agency, Vienna) 109-141.

FAYE, G.H., BOWMAN, W.S., and SUTARNO, R. (1979). Uranium ore BL-5 - a certified reference material. CANMET Report 79-4, 11 pp.

FOOTE, R.S. (1978). Development of a USERDA calibration range for airborne gamma radiation surveys. Aerial Techniques for Environmental Monitoring (Am. Nucl. Soc., La Grange Park, Illinois) 158-174.

GEORGE, D.C. and KNIGHT, L. (1982). Field calibration facilities for environmental measurement of radium, thorium, and potassium. GJ/TMC-01(82), UC-70A (US Department of Energy, Technical Measurements Center, Grand Junction Area Office) 10 pp. + Appendix.

GEORGE, D.C., NOVAK, E.F., and PRICE, R.K. (1984). Calibration-pad parameter assignments for in-situ gamma-ray measurements of radium, thorium and potassium. GJ/TMC-17, UC-70A (US Department of Energy, Technical Measurements Center, Grand Junction Area Office) 105 pp.

GRASTY, R.L. and DARNLEY, A.G. (1971). The calibration of gamma-ray spectrometers for ground and airborne use. Geol. Surv. Canada, Paper 71-17, 27 pp.

GRASTY, R.L. and CHARBONNEAU, B.W. (1974). Gamma-ray spectrometer calibration facilities. Geol. Surv. Canada, Paper 74-1B, 69-71.

GRASTY, R.L. (1975a). Uranium measurement by airborne gamma-ray spectrometry. Geophys. 40, 503-519.

GRASTY, R.L. (1975b). Atmospheric absorption of 2.62 MeV gamma-ray photons emitted from the ground. Geophys. 40, 1058-1065.

GRASTY, R.L. (1976). A calibration procedure for an airborne gamma-ray spectrometer. Geol. Surv. Canada, Paper 76-16, 9 pp.

GRASTY, R.L. (1979). Gamma ray spectrometric methods in uranium exploration - theory and operational procedures. Geophysics and Geochemistry in the Search for Metallic Ores (P.J. Hood, ed.; Geol. Surv. Canada, Econ. Geol. Rep. 31) 147-161.

GRASTY, R.L. (1982). Utilizing experimentally derived multi-channel gamma-ray spectra for the analysis of airborne data. Uranium Exploration Methods (OECD, Paris) 653-669.

GRASTY, R.L., BRISTOW, Q., CAMERON, G.W., DYCK, W., GRANT, J.A., and KILLEEN, P.G. (1982). Primary calibration of a laboratory gamma-ray spectrometer for the measurement of potassium, uranium and thorium. Uranium Exploration Methods (OECD, Paris) 699-712.

GRASTY, R.L. (1984). Airborne gamma-ray surveys and radon emanation. Newsletter on R & D in Uranium Exploration Techniques (OECD Nuclear Energy Agency, Paris) No. 5, 16-18.

GRASTY, R.L., CARSON, J.M., CHARBONNEAU, B.W., and HOLMAN, P.B. (1984). Natural background radiation in Canada. Geol. Surv. Canada, Bull. 360, 39 pp.

GYURCSAK, J. and LENDA, A. (1979). On the response functions of NaI(Tl) detectors to terrestrial gamma-radiation. Int. J. Appl. Rad. and Isot. 31, 169-177.

HERHOLDT, A.D., JUSTESEN, C.F.P., NEPPER-CHRISTENSEN, P., and NIELSEN, A. (1979). Beton-Bogen (Aalborg Portland) 719 pp (in Danish).

HUBBELL, J.H. (1982). Photon mass attenuation and energy-absorption coefficients from 1 keV to 20 MeV. Int. J. Appl. Rad. and Isot. 33, 1269-1290.

IAEA (1974). Recommended instrumentation for uranium and thorium exploration. Techn. Rep. Ser. No. 158 (International Atomic Energy Agency, Vienna) 93 pp.

IAEA (1976). Radiometric reporting methods and calibration in uranium exploration. Techn. Rep. Ser. No. 174 (International Atomic Energy Agency, Vienna) 57 pp.

IAEA (1979). Gamma-ray surveys in uranium exploration. Techn. Rep. Ser. No. 186 (International Atomic Energy Agency, Vienna) 90 pp.

IAEA (1982). Borehole logging for uranium exploration - a manual. Techn. Rep. Ser. No. 212 (International Atomic Energy Agency, Vienna) 275 pp.

IVANOVICH, M. and HARMON, R.S. (1982). Uranium Series Disequilibrium: Applications to Environmental Problems (Clarendon, Oxford) 571 pp.

KILLEEN, P.G. and CARMICHAEL, C.M. (1970). Gamma-ray spectrometer calibration for field analysis of thorium, uranium and potassium. Can. J. Earth Sci. 7, 1093-1098.

KILLEEN, P.G. (1978). Gamma-ray spectrometer calibration facilities - a preliminary report. Geol. Surv. Canada, Paper 78-1A, 243-247.

KILLEEN, P.G. (1979). Gamma ray spectrometric methods in uranium exploration - application and interpretation. Geophysics and Geochemistry in the Search for Metallic Ores (P.J. Hood, ed.; Geol. Surv. Canada, Econ. Geol. Rep. 31) 163-229.

KIRKEGAARD, P. and LØVBORG, L. (1979). Program system for computation of the terrestrial gamma-radiation field. Risø-R-492, 31 pp.

KIRKEGAARD, P. and LØVBORG, L. (1980). Transport of terrestrial γ radiation in plane semi-infinite geometry. J. Comput. Phys. 36, 20-34.

KOCH, G.S. and LINK, R.F. (1970). Statistical Analysis of Geological Data (Wiley, New York) 375 pp.

KOCHER, D.C. (1981). Radioactive decay data tables (Technical Information Center, US Department of Energy) 221 pp.

KOGAN, R.M., NAZAROV, I.M., and FRIDMAN, Sh.D. (1976). Fundamentals of Gamma Spectrometry of Natural Media (Atomizdat, Moscow) 368 pp (in Russian).

LARSON, R.E. and BRESSAN, D.J. (1980). Radon-222 as an indicator of continental air masses and air mass boundaries over ocean areas. Natural Radiation Environment III (Technical Information Center, US Department of Energy) vol. 1, 308-326.

LINDÉN, A.H. and ÅKERBLOM, G. (1977). Method of detecting small or indistinct radioactive sources by airborne gamma-ray spectrometry. Geology, Mining and Extractive Processing of Uranium (Inst. of Mining and Metallurgy, London) 113-120.

LØVBORG, L., KUNZENDORF, H., and HANSEN, J. (1969). Use of field gamma-spectrometry in the exploration of uranium and thorium deposits in South Greenland. Nuclear Techniques and Mineral Resources (International Atomic Energy Agency, Vienna) 197-211.

LØVBORG, L., WOLLENBERG, H., SØRENSEN, P., and HANSEN, J. (1971). Field determination of uranium and thorium by gamma-ray spectrometry, exemplified by measurements in the Ilímaussaq alkaline intrusion, South Greenland. Econ. Geol. 66, 368-384.

LØVBORG, L., KIRKEGAARD, P., and ROSE-HANSEN, J. (1972). Quantitative interpretation of the gamma-ray spectra from geologic formations. The Natural Radiation Environment II (USERDA, Springfield, Virginia) vol. 1, 155-180.

LØVBORG, L. and KIRKEGAARD, P. (1974). Response of 3" × 3" NaI(Tl) detectors to terrestrial gamma radiation. Nucl. Instrum. Meth. 121, 239-251.

LØVBORG, L. and KIRKEGAARD, P. (1975). Numerical evaluation of the natural gamma radiation field at aerial survey heights. Risø Report No. 317, 52 pp.

LØVBORG, L., KIRKEGAARD, P., and CHRISTIANSEN, E.M. (1976). Design of NaI(Tl) scintillation detectors for use in gamma-ray surveys of geological sources. Exploration for Uranium Ore Deposits (International Atomic Energy Agency, Vienna) 127-148.

LØVBORG, L., BØTTER-JENSEN, L., and KIRKEGAARD, P. (1978). Experiences with concrete calibration sources for radiometric field instruments. Geophys. 43, 543-549.

LØVBORG, L., GRASTY, R.L., and KIRKEGAARD, P. (1978). A guide to the calibration constants for aerial gamma-ray surveys in geoexploration. Aerial Techniques for Environmental Monitoring (Am. Nucl. Soc., La Grange Park, Illinois) 193-206.

LØVBORG, L., BØTTER-JENSEN, L., KIRKEGAARD, P., and CHRISTIANSEN, E.M. (1979). Monitoring of natural soil radioactivity with portable gamma-ray spectrometers. Nucl. Instrum. Meth. 167, 341-348.

LØVBORG, L., BØTTER-JENSEN, L., CHRISTIANSEN, E.M., and NIELSEN, B.L. (1980). Gamma-ray measurements in an area of high natural radioactivity. Natural Radiation Environment III (Technical Information Center, US Department of Energy) vol. 2, 912-926.

LØVBORG, L. (1982). Error analysis of calibration and field trials with spectrometers and counters. Uranium Exploration Methods (OECD, Paris) 671-680.

LØVBORG, L. (1983). Total-count calibration blocks for use in uranium exploration. Risø-R-490, 47 pp.

MATHERON, G. (1963). Principles of geostatistics. Econ. Geol. 58, 1246-1266.

MATHEWS, M.W. and KOSANKE, K.L. (1978). Gross gamma-ray calibration blocks. GJBX-59(78) (Bendix Field Eng. Corp.) 89 pp.

MINATO, S. (1980). Some observations of the variations in natural gamma radiation due to rainfall. Natural Radiation Environment III (Technical Information Center, US Department of Energy) vol. 1, 370-382.

MULTALA, J. (1981). The construction of gamma-ray spectrometer calibration pads. Geoexpl. 19, 33-46.

NACHTIGALL, D. (1959). Table of specific gamma-ray constants (Karl Thiemig Verlag, München) 98 pp.

NEVILLE, A.M. (1981). Properties of Concrete (Pitman, London) 779 pp.

NIELSEN, B.L. (1981). Exploration of the Kvanefjeld uranium deposit, Ilímaussaq intrusion, South Greenland. Uranium Exploration Case Histories (International Atomic Energy Agency, Vienna) 353-388.

OECD (1981). Reporting and calibration of total-count gamma radiation measurements. Newsletter on R&D in Uranium Exploration Techniques (OECD Nuclear Energy Agency, Paris) No. 3, 16-19.

PEREIRA, E.B. (1980). Reconnaissance of radon emanation power of Poços de Caldas, Brazil, uranium ore and associated rocks. Natural Radiation Environment III (Technical Information Center, US Department of Energy) vol. 1, 117-123.

RICHARDSON, K.A. (1964). Thorium, uranium, and potassium in the Conway granite, New Hampshire, U.S.A. The Natural Radiation Environment (Univ. Chicago Press, Chicago) 39-50.

RIXOM, M.R. (1978). Chemical Admixtures for Concrete (Spon Ltd., London) 234 pp.

ROHDE, R.E. (1965). Gain vs temperature effects in NaI(Tl) photomultiplier scintillation detectors using 10 and 14 stage tubes. IEEE Trans. Nucl. Sci. NS-12 (1), 16-23.

ROJKO, R. (1976). Calibration centre for field gamma spectrometers. Geol. Pruzkum 18, 336-339 (in Czech).

SCHROEDER, G.L., KRANER, H.W., and EVANS, R.D. (1965). Diffusion of radon in several naturally occuring soil types. J. Geophys. Res. 70, 471-474.

SCHWARZER, T.F. and ADAMS, J.A.S. (1973). Rock and soil discrimination by low altitude airborne gamma-ray spectrometry in Payne Country, Oklahoma. Econ. Geol. 68, 1297-1312.

SMITH, C.W. and STEGER, H.F. (1983). Radium-226 in certified uranium reference ores DL-1a, BL-4a, DH-1a and BL-5. CANMET Report 83-9E, 8 pp + appendices.

STROMSWOLD, D.C. (1978). Monitoring of the airport calibration pads at Walker Field, Grand Junction, Colorado for long-term radiation variations. GJBX-99(78) (Bendix Field Eng. Corp.) 35 pp.

STROMSWOLD, D.C. and KOSANKE, K.L. (1978). Calibration and error analysis for spectral radiation detectors. IEEE Trans. Nucl. Sci. NS-25, 782-786.

TANNER, A.B. (1964). Radon migration in the ground: A review. The Natural Radiation Environment (Univ. Chicago Press, Chicago) 161-190.

TANNER, A.B. (1980). Radon migration in the ground: A supplementary review. Natural Radiation Environment III (Technical Information Center, US Department of Energy) vol. 1, 5-56.

TRAHEY, N.M., VOEKS, A.M., and SORIANO, M.D. (1982). Grand Junction/New Brunswick Laboratory interlaboratory measurement program, part I: Evaluation, part II: Methods manual. US Department of Energy (Argonne, Illinois) 189 pp.

TROXELL, E.G., DAVIS, H.E., and KELLY, J.W. (1968). Composition and Properties of Concrete (McGraw-Hill, New York) 529 pp.

VAVILIN, L.N., VOROB'EV, V.P., EFIMOV, A.V., ZELENETSKIJ, D.S. et al. (1982). Aerogamma Spectrometry in Geology ("Nedra", Leningrad) 271 pp (in Russian).

WARD, D.L. (1978). Construction of calibration pads facility Walker Field, Grand Junction, Colorado. GJBX-37(78) (Bendix Field Eng. Corp.) 16 pp + appendices.

WOLLENBERG, H.A. and SMITH, A.R. (1966a). Radioactivity of cement raw materials. Proc. 2nd Forum on Geology of Industrial Minerals (Indiana Univ., Bloomington) 129-147.

WOLLENBERG, H.A. and SMITH, A.R. (1966b). A concrete low-background counting enclosure. Health Phys. 12, 53-60.

WOLLENBERG, H.A. (1977). Radiometric methods. Nuclear Methods in Mineral Exploration and Production (J.G. Morse, ed.; Elsevier, Amsterdam) 5-36.

WORMALD, M.R. and CLAYTON, C.G. (1976). Observations on the accuracy of gamma spectrometry in uranium prospecting. Exploration for Uranium Ore Deposits (International Atomic Energy Agency, Vienna) 149-171.

YANG ZHENZHOU and LIU XICHEN (1983). Seven standard ore samples of uranium, thorium and radium prepared by the Bureau of Uranium Geology (China). Geostandards Newsletter 7, 251-260.

ZIJP, W.L. (1984). Generalized least squares principle for straight line fitting. Rep. ECN-154 (Netherlands Energy Research Foundation, Petten) 38 pp.

# APPENDIX

## DATA SHEETS FOR CALIBRATION FACILITIES INCLUDED IN THE IAEA INTERCOMPARISON EXPERIMENT

The radioelement concentrations of pads used for calibrating the portable GR-410 spectrometer are listed under the heading "Assigned calibration grades". Pads tested in the experiment are described by two sets of radioelement concentrations: "Laboratory-assayed grades" which refer to powdered, dry pad material and "Monitored in-situ grades" which are relative to the B pad of the facility in question and believed to include most of the free moisture in the pads. Missing assay or monitoring results indicate that a grade determination was not attempted because of a highly probable spectral pile-up effect.

The calibration pads are labelled using the letter code introduced in subsection 4.2. For facilities in which the pads are numbered, the literal descriptor and the pad number are used hyphenated.

The global distribution of the visited pad facilities is shown in Fig. 50.

## ARGENTINA

Facility: Villa 25 de Mayo (near San Rafael, Mendoza province)
Operating organization: Comisión Nacional de Energía Atómica

Number of pads: 10 Pad configuration: $KU_5T_2MB$
Pad dimensions: 1 m in dia. × 0.5 m

| Pad | Laboratory-assayed grades [1] | | | Monitored in-situ grades | | |
|---|---|---|---|---|---|---|
| | % K | ppm eU | ppm eTh | % K | ppm eU | ppm eTh |
| K-9 | 5.46±0.09 | 2.7±0.4 | 1.9±0.3 | 2.57±0.05 | 1.4±0.2 | -5.9±0.3 |
| U-1 | 2.15±0.07 | 83.6±1.9 | 21.4±1.0 | 0.05±0.06 | 37.2±0.9 | 13.5±0.5 |
| U-2 | 1.91±0.13 | 274±6 | 8.2±1.0 | 0.34±0.14 | 151±4 | 2.7±0.7 |
| U-3 | 2.02±0.23 | 597±12 | 5.9±1.1 | 1.4±0.3 | 361±8 | 5.5±1.4 |
| U-4 | 1.3±0.5 | 1043±22 | 8.6±2.0 | - | - | - |
| U-5 | - | 2983±60 | - | - | - | - |
| T-6 | 2.32±0.07 | 34.7±0.9 | 213±4 | 0.12±0.07 | 17.4±0.8 | 168±3 |
| T-7 | 2.13±0.09 | 88.4±1.9 | 364±6 | 0.09±0.11 | 30.9±1.4 | 297±4 |
| M-8 | 1.5±0.5 | 570±11 | 144±3 | 1.3±0.4 | 350±8 | 129±3 |
| B-0 | 2.34±0.04 | 6.5±0.3 | 7.4±0.5 | 0±0 | 0±0 | 0±0 |

1) "Dry" assays performed at Risø National Laboratory

## AUSTRALIA

Facility: CSIRO, Sydney (located at North Ryde)
Operating organization: CSIRO Institute of Energy and Earth Resources (Division of Mineral Physics)

Number of pads: 5 Pad configuration: KUTMB
Pad dimensions: 2 m in dia. × 0.5 m

| Pad | Laboratory-assayed grades [1] | | | Monitored in-situ grades | | |
|---|---|---|---|---|---|---|
| | % K | ppm eU | ppm eTh | % K | ppm eU | ppm eTh |
| K | 4.15±0.11 | 0.97±0.53 | 2.6±1.1 | 3.68±0.04 | 0.24±0.10 | -1.0±0.2 |
| U | 0.15±0.20 | 89.5±5.1 | 2.6±1.5 | 0.20±0.08 | 87.4±1.8 | -0.9±0.4 |
| T | 0.14±0.16 | 7.8±1.5 | 166±4 | -0.12±0.05 | 9.56±0.70 | 158±2 |
| M | 0.15±0.17 | 38.9±1.6 | 95.7±2.6 | -0.02±0.06 | 39.1±1.0 | 88.8±1.3 |
| B | 0.19±0.07 | 0.77±0.63 | 2.3±1.2 | 0±0 | 0±0 | 0±0 |

1) "Dry" assays performed by the CSIRO Division of Mineral Physics

Reference: Dickson and Løvborg (1984)

## BRAZIL

Facility: I.R.D., Rio de Janeiro (located at Barra)
Operating organization: Instituto de Radioproteção e Dosimetrica of the C.N.E.N

Number of pads: 8 Pad configuration: $K_2TM_4B$
Pad dimensions: 3 m in dia. × 0.5 m

| Pad | Laboratory-assayed grades [1] | | | Monitored in-situ grades | | |
|---|---|---|---|---|---|---|
| | % K | ppm eU | ppm eTh | % K | ppm eU | ppm eTh |
| K-1 | 6.77±0.10 | 1.8±0.3 | 19.4±0.5 | 6.40±0.07 | 1.69±0.15 | 15.6±0.4 |
| K-2 | 4.76±0.07 | 2.4±0.4 | 32.0±0.7 | 4.62±0.05 | 2.44±0.20 | 27.6±0.5 |
| T-6 | 3.93±0.09 | 10.8±0.5 | 274±5 | 3.34±0.09 | 14.3±1.1 | 247±3 |
| M-3 | 3.40±0.04 | 72.9±2.1 | 39.3±0.8 | 3.37±0.06 | 55.5±1.2 | 37.7±0.6 |
| M-4 | 3.77±0.04 | 13.3±0.4 | 69.6±1.1 | 3.43±0.05 | 12.6±0.5 | 65.1±0.9 |
| M-5 | 3.63±0.08 | 45.9±1.0 | 175±4 | 3.27±0.09 | 37.7±1.0 | 155±2 |
| M-8 | 3.81±0.10 | 19.9±0.4 | 46.7±0.9 | 3.44±0.04 | 17.7±0.4 | 41.2±0.6 |
| B-7 | 0.08±0.01 | 0.58±0.06 | 1.46±0.04 | 0±0 | 0±0 | 0±0 |

[1] "Dry" assays performed at Risø National Laboratory

## CANADA

Facility: Uplands airport (Ottawa)
Operating organization: Geological Survey of Canada

Number of pads: 5 Pad configuration: $T_2M_2B$
Pad dimensions: 7.6 × 7.6 × 0.5 m

| Pad | Assigned calibration grades [1] | | |
|---|---|---|---|
| | % K | ppm eU | ppm eTh |
| T-3 | 2.21±0.08 | 3.0±0.3 | 26.1±0.9 |
| T-4 | 2.21±0.11 | 2.9±0.3 | 40.8±1.9 |
| M-2 | 2.27±0.09 | 7.3±0.2 | 12.6±0.7 |
| M-5 | 2.33±0.09 | 11.7±0.3 | 13.2±0.7 |
| B-1 | 1.70±0.08 | 2.4±0.2 | 8.9±0.6 |

[1] Based on laboratory assays of six drill cores from each pad (Grasty and Darnley, 1971)

## CANADA

Facility: Bells Corners (approx. 10 km west of Ottawa)
Operating organization: Geological Survey of Canada

Number of pads: 10 Pad configuration: $K_3U_3T_3B$
Pad dimensions: 3 m in dia. × 0.6 m

| Pad | Assigned calibration grades [1] | | |
|---|---|---|---|
| | % K | ppm eU | ppm eTh |
| K-1 | 1.05±0.03 | 0.21±0.06 | 1.42±0.14 |
| K-2 | 1.54±0.07 | 0.16±0.06 | 1.52±0.20 |
| K-3 | 3.16±0.08 | 0.24±0.07 | 1.23±0.22 |
| U-4 | 0.32±0.15 | 12.4±3.6 | 1.01±0.12 |
| U-5 | 0.39±0.03 | 42.6±4.7 | 0.79±0.21 |
| U-6 | 1.90±0.13 | 490±30 | 0.64±0.77 |
| T-7 | 0.22±0.02 | 0.86±0.05 | 10.4±0.3 |
| T-8 | 0.24±0.02 | 3.86±0.16 | 79.8±3.0 |
| T-9 | 0.59±0.04 | 16.1±0.9 | 382±23 |
| B-10 | 0.29±0.01 | 0.25±0.04 | 0.68±0.11 |

1) These are "wet" concentrations based on cured and sealed mix samples (P.G. Killeen, personal communication)

Reference: Killeen (1978)

## DENMARK

Facility: Risø (near Roskilde)
Operating organization: Risø National Laboratory

Number of pads: 6 Pad configuration: $KUTM_2B$
Pad dimensions: 3 m in dia. × 0.5 m

| Pad | Laboratory-assayed grades [1] | | | Monitored in-situ grades [2] | | |
|---|---|---|---|---|---|---|
| | % K | ppm eU | ppm eTh | % K | ppm eU | ppm eTh |
| K | 6.88±0.03 | 4.44±0.10 | 1.95±0.13 | 5.70±0.07 | 2.46±0.16 | 0.01±0.17 |
| U | 0.97±0.06 | 230.0±3.6 | 2.03±0.50 | 0.00±0.31 | 147±18 | -2.2±1.7 |
| T | 0.78±0.06 | 8.46±0.54 | 169±1 | 0.08±0.09 | 7.2±0.7 | 148±2 |
| M-1 | 1.40±0.06 | 59.9±1.1 | 156±1 | 0.53±0.11 | 48.4±1.2 | 142±4 |
| M-2 | 1.31±0.03 | 18.8±0.4 | 50.5±0.7 | 0.43±0.04 | 16.5±0.5 | 48.1±1.0 |
| B | 1.10±0.01 | 0.31±0.04 | 2.4±0.09 | 0±0 | 0±0 | 0±0 |

1) "Dry" assays (Løvborg et al., 1981)
2) Average grades provided by 13 monitoring trials in 1980-81

For finally adopted calibration grades: See Løvborg (1983)

## FINLAND

Facility: Helsinki-Vantaa airport
Operating organization: Geological Survey of Finland

Number of pads: 4 Pad configuration: KUTB
Pad dimensions: 8 × 8 × 0.5 m

| Pad | Assigned calibration grades [1] | | |
|---|---|---|---|
| | % K | ppm eU | ppm eTh |
| K | 3.51±0.17 | 2.3±0.2 | 2.4±0.5 |
| U | 2.30±0.15 | 53.2±3.7 | 7.7±0.6 |
| T | 2.55±0.13 | 11.3±0.8 | 104±9 |
| B | 2.54±0.11 | 4.1±0.3 | 9.1±0.6 |

[1] Based on assays of powdered, but undried mix samples (Multala, 1981)

## ISRAEL

Facility: Soreq (the pads are located at a military airfield)
Operating organization: Soreq Nuclear Research Center

Number of pads: 4 (5) Pad configuration: $KUTB_{(2)}$
Pad dimensions: 8 × 8 × 0.4 m

| Pad | Laboratory-assayed grades [1] | | | Monitored in-situ grades | | |
|---|---|---|---|---|---|---|
| | % K | ppm eU | ppm eTh | % K | ppm eU | ppm eTh |
| K | 0.58±0.01 | 1.04±0.03 | 3.79±0.05 | 0.410±0.010 | 0.50±0.06 | 2.74±0.10 |
| U | 0.03±0.01 | 12.77±0.05 | 1.88±0.05 | -0.160±0.015 | 12.8±0.3 | -0.33±0.09 |
| T | 0.00±0.01 | 0.72±0.05 | 34.1±0.1 | -0.159±0.013 | 1.18±0.15 | 33.2±0.5 |
| B | 0.17±0.01 | 0.55±0.03 | 0.86±0.03 | 0±0 | 0±0 | 0±0 |

[1] Assays performed at Soreq Nuclear Research Center

Reference: Aviv and Vulkan (1983)

## SOUTH AFRICA

Facility: Lanseria airport (north of Johannesburg)
Operating organization: Nuclear Development Corporation of South Africa (NUCOR)

Number of pads: 4 Pad configuration: KUTB
Pad dimensions: 8 m in dia. × 0.35 m

| Pad | Laboratory-assayed grades [1] | | | Monitored in-situ grades | | |
|---|---|---|---|---|---|---|
| | % K | ppm eU | ppm eTh | % K | ppm eU | ppm eTh |
| K | 5.06±0.17 | 0.8±0.2 | 1.7±0.2 | 4.71±0.05 | 0.21±0.09 | -0.21±0.15 |
| U | 0.20±0.04 | 56.8±3.4 | 6.5±0.5 | 0.09±0.05 | 52.2±1.1 | 6.4±1.0 |
| T | 0.22±0.05 | 3.6±0.3 | 139±6 | 0.05±0.04 | 4.1±0.6 | 138±2 |
| B | 0.17±0.03 | 1.1±0.1 | 1.7±0.2 | 0±0 | 0±0 | 0±0 |

1) Based on assays performed by 7 laboratories
Note: The eU grade of the U pad was assigned in situ by NUCOR using a spectrometer calibrated on the pads at Pelindaba

Reference: Corner and Smit (1983)

## SWEDEN

Facility: Borlänge (located at Dala airport, 150 km north-west of Stockholm)
Operating organization: Swedish Geological (Uppsala office)

Number of pads: 4 Pad configuration: KUTB
Pad dimensions: Approx. 10.7 m in dia. × 0.5 m

| Pad | Assigned calibration grades [1] | | |
|---|---|---|---|
| | % K | ppm eU | ppm eTh |
| K | 7.50±0.08 | 1.03±0.05 | 1.3±0.2 |
| U | 0.70±0.03 | 24.8±0.5 | 2.6±0.2 |
| T | 0.60±0.03 | 3.58±0.05 | 49.1±2.2 |
| B | 0.40±0.03 | 1.53±0.05 | 2.4±0.2 |

1) Based on the author's evaluation of assays performed by 3 Scandinavian laboratories

## SWEDEN

Facility: Malå (Västerbotten district)
Operating organization: Swedish Geological (Luleå office)

Number of pads: 7 Pad configuration: $KU_3T_2B$
Pad dimensions: Approx. 3 × 3 × 0.5 m

Pads "K", "U-1", "T-1", and "B" consist of concrete bricks identical to those used for constructing the airport pads at Borlänge. The following results were obtained for the 3 pads added to the Malå facility in 1982:

| Pad | Laboratory-assayed grades [1] | | | Monitored in-situ grades [2] | | |
|---|---|---|---|---|---|---|
| | % K | ppm eU | ppm eTh | % K | ppm eU | ppm eTh |
| U-2 | 0.4±0.1 | 355±13 | 6.4±0.5 | 0.93±0.30 | 327±7 | 6.7±1.3 |
| U-3 | 0.6±0.1 | 655±22 | 15.1±2.4 | - | 631±13 | - |
| T-2 | 2.4±0.1 | 18.4±1.1 | 384±7 | 1.6±0.2 | - | 378±5 |

1) "Dry" assays performed by Risø National Laboratory
2) Measured with respect to the B pad, as usual

USA

Facility: Walker Field airport (Grand Junction, Colorado)
Operating organization: Technical Measurements Center at the Grand Junction Area Office of the US Department of Energy

Number of pads: 5 Pad configuration: KUTMB
Pad dimensions: 9.1 × 12.2 × 0.5 m

| Pad | Assigned calibration grades [1] | | |
|---|---|---|---|
| | % K | ppm eU | ppm eTh |
| K-2 | 5.14±0.045 | 5.09±0.17 | 8.48±0.13 |
| U-4 | 2.03±0.025 | 30.29±0.80 | 9.19±0.14 |
| T-3 | 2.01±0.02 | 5.14±0.11 | 45.33±0.37 |
| M-5 | 4.11±0.03 | 20.39±0.64 | 17.52±0.17 |
| B-1 | 1.45±0.005 | 2.19±0.04 | 6.26±0.07 |

1) These are "wet" concentrations based on cured and sealed mix samples. The standard deviations equal half the 95% confidence ranges stated by Stromswold and Kosanke (1978)

Additional reference: Ward (1978)

# TABLES

Table 1. Radioelement assay based on spectrometer window counting

| Energy window | Radioelement selected | Window setting for Geometrics GR-410 (MeV) | Target events in the ground | |
|---|---|---|---|---|
| | | | Radioactive decay | Associated photon emissions (MeV) |
| 1 | Potassium | 1.37-1.55 | $^{40}K \rightarrow {}^{40}Ar$ | 1.4608 |
| 2 | Uranium | 1.66-1.87 | $^{214}Bi \rightarrow {}^{214}Po$ | 1.7296<br>1.7645<br>1.8474 |
| 3 | Thorium | 2.46-2.78 | $^{208}Tl \rightarrow {}^{208}Pb$ | 2.6146 |

Table 2. Calculated stripping ratios for GR-410 spectrometer

| Assumed energy resolution for detector unit (%) | Stripping ratio | | | |
|---|---|---|---|---|
| | $\alpha$ | $\beta$ | $\gamma$ | a |
| 7.6 | 0.577 | 0.617 | 0.983 | 0.022 |
| 8.8 | 0.584 | 0.625 | 0.983 | 0.023 |
| 10.0 | 0.595 | 0.635 | 0.988 | 0.023 |

Table 3. Calculated window sensitivities for GR-410 spectrometer

| Assumed energy resolution for detector unit (%) | Counts/s per radioelement concentration unit | | |
|---|---|---|---|
| | $s_K$ | $s_U$ | $s_{Th}$ |
| 7.6 | 4.02 | 0.375 | 0.145 |
| 8.8 | 3.96 | 0.371 | 0.145 |
| 10.0 | 3.87 | 0.365 | 0.145 |

Table 4. Calculated factors for converting radioelement concentrations in soil into gamma-ray exposure rates at 1 meter

| Reference | μR/h | | |
|---|---|---|---|
| | 1% K | 1 ppm eU *) | 1 ppm eTh |
| Løvborg et al. (1979) | 1.505 | 0.619 | 0.305 |
| This work | 1.505±0.014 | 0.653±0.005 | 0.287±0.007 |

*) Including a small contribution from $^{235}U$

A radiation exposure of 1 R corresponds to an absorbed dose of $8.69 \times 10^{-3}$ Gy in standard air

Table 5. Calculated influence of photomultiplier gain drift on the calibration constants of a GR-410 spectrometer

| % Drift | % Change | | | | | | |
|---|---|---|---|---|---|---|---|
| | $\alpha$ | $\beta$ | $\gamma$ | a | $s_K$ | $s_U$ | $s_{Th}$ |
| +2 | +4.4 | -8.8 | +5.6 | +81 | -1.5 | 0 | +4.8 |
| -2 | +2.3 | +16.5 | -6.0 | -70 | -4.7 | -5.1 | -4.8 |

Table 6. Background count rates recorded with GR-410 spectrometer over water

| Place | Elevation (m) | Counts/s | | |
|---|---|---|---|---|
| | | Window 1 (K) | Window 2 (U) | Window 3 (Th) |
| Roskilde Fjord Denmark | 0 | 0.546±0.009 | 0.160±0.005 | 0.108±0.004 |
| Hornavan Lake N. Sweden | 425 | 0.378±0.014 | 0.199±0.011 | 0.136±0.009 |
| St. Umevattnet N. Sweden | 520 | 0.435±0.010 | 0.201±0.007 | 0.137±0.006 |
| Helsinki Bay Finland | 0 | 0.420±0.011 | 0.233±0.008 | 0.139±0.006 |
| Highline Lake Colorado, USA | 1433 | 0.446±0.010 | 0.412±0.010 | 0.158±0.006 |
| Average values | | 0.46 ± 0.06 | 0.21 ± 0.08 | 0.13 ± 0.02 |

Standard deviations on the single determinations are calculated from counting statistics

Table 7. Symbols and working expressions for the calculation of critical signal levels $n_C$ and signal precision $\sigma_n$

| Quantity | General symbol | Signal or stripping ratio | | |
|---|---|---|---|---|
| | | Window 1 (K) | Window 2 (U) | Window 3 (Th) |
| Counting time | t | | | |
| Total signal | p | $n_1$ | $n_2$ | $n_3$ |
| Interfering signal | q | $n_2$ | $n_3$ | $n_2$ |
| Background | b | $b_1$ | $b_2$ | $b_3$ |
| Net signal | n | $n_{1,K}$ | $n_{2,U}$ | $n_{3,Th}$ |
| Stripping ratio | k | $\gamma$ | $\alpha$ | a |

n is obtained from Eq. (4)

$$n_C = 1.645\sqrt{\frac{k(1+k)q+b}{t} + \sigma_b^2}$$

$$\sigma_n = \sqrt{\frac{p+k^2q}{t} + \sigma_b^2}$$

If $n < n_C$ then $n_{max} = n + 2 \cdot \sigma_n$

Table 8. Symbols and working expressions for the calculation of a priori signal detection limits $n_D$ and determination limits $n_Q$

| Quantity | Symbol | Signal | | |
|---|---|---|---|---|
| | | Window 1 (K) | Window 2 (U) | Window 3 (Th) |
| Counting time | t | | | |
| Interfering contribution | r | $\beta s_{Th} \cdot x_{Th} + \gamma s_U \cdot x_U$ | $\alpha s_{Th} \cdot x_{Th}$ | $a s_U \cdot x_U$ |
| Background | b | $b_1$ | $b_2$ | $b_3$ |
| Net signal | n | $n_{1,K}$ | $n_{2,U}$ | $n_{3,Th}$ |

$$n_D = 2.71/t + 3.29 \sqrt{(2r + b)/t + \sigma_b^2}$$

$$n_Q = 50 \left\{ \frac{1}{t} + \sqrt{\frac{1}{t^2} + \frac{(2r + b)/t + \sigma_b^2}{25}} \right\}$$

Table 9. Suggested numerical data in the use of formula (14) for predicting the window sensitivities of an airborne gamma-ray spectrometer

| Energy window | $s$ (Counts/s per 1000 $cm^3$ of detector volume) | $\mu$ (Attenuation per meter of standard air) |
|---|---|---|
| 1 (K) | 6.7 | 0.0107 |
| 2 (U) | 0.62 | 0.0097 |
| 3 (Th) | 0.33 | 0.0088 |

Table 10. Experimental and calculated window sensitivities for the GSC airborne gamma-ray spectrometer

| Detector system | Survey height (m) | | Counts/s per concentration unit | | |
|---|---|---|---|---|---|
| | | | K | U | Th |
| 1) | 125 | a | 75.6 | 8.6 | 6.3 |
| | | b | 88.7 | 9.3 | 5.5 |
| 2) | 122 | a | 91.0 | 9.1 | 7.0 |
| | | b | 92.1 | 9.6 | 5.7 |

1) Twelve 229 × 102 mm cylindrical detectors
Experimental data from Løvborg et al. (1978)

2) Twelve 102 × 102 × 406 mm prismatic detectors
Experimental data from Bristow (1983)

a = experimental b = calculated from formula (14)

Table 11. Contributions to the mass attenuation coefficients of $SiO_2$ at the photon energies selected by a field spectrometer

| Interaction process | $\mu/\rho$ ($cm^2/g$) | | |
|---|---|---|---|
| | 1.46 MeV | 1.76 MeV | 2.61 MeV |
| Compton scattering | 0.05235 | 0.04729 | 0.03765 |
| Photoelectric absorption | 0.00001 | 0.00001 | ~ 0 |
| Pair production | 0.00007 | 0.00031 | 0.00117 |
| Total | 0.05243 | 0.04761 | 0.03882 |

Table 12. Total mass attenuation coefficients for chemical rock constituents plus concrete and air

| Substance | $\mu/\rho$ ($cm^2/g$) | | |
|---|---|---|---|
| | 1.46 MeV | 1.76 MeV | 2.61 MeV |
| $SiO_2$ | 0.0525 | 0.0477 | 0.0390 |
| $TiO_2$ | 0.0503 | 0.0458 | 0.0379 |
| $Al_2O_3$ | 0.0516 | 0.0468 | 0.0383 |
| $Fe_2O_3$ | 0.0503 | 0.0459 | 0.0384 |
| MnO | 0.0492 | 0.0450 | 0.0376 |
| MgO | 0.0522 | 0.0474 | 0.0387 |
| CaO | 0.0526 | 0.0479 | 0.0397 |
| $Na_2O$ | 0.0509 | 0.0462 | 0.0377 |
| $K_2O$ | 0.0515 | 0.0469 | 0.0389 |
| $H_2O$ | 0.0583 | 0.0529 | 0.0428 |
| Concrete | 0.0530 | 0.0482 | 0.0394 |
| Air | 0.0524 | 0.0476 | 0.0386 |

Table 13. Approximate radiometric grades of B pads in eight calibration facilities

| Country | Facility | Aggregate material | % K | ppm eU | ppm eTh |
|---|---|---|---|---|---|
| Argentina | Villa 25 de Mayo | River sand (orthose feldspar) | 2.3 | 6 | 7 |
| Brazil | I.R.D., Rio de Janeiro | Beach sand (mainly quartz) | 0.1 | 0.6 | 1.5 |
| Canada | Uplands airport | Glaciated derived gravel + hematite | 1.7 | 2.4 | 8.9 |
| Denmark | Risø | Beach sand | 1.1 | 0.3 | 2.4 |
| Israel | Soreq | Beach gravel[1)] | 0.2 | 0.6 | 0.9 |
| South Africa | Lanseria | Bushveld norite | 0.2 | 1.1 | 1.7 |
| Sweden | Borlänge | Limestone | 0.4 | 1.5 | 2.4 |
| USA | Walker Field | Masonry sand | 1.5 | 2.2 | 6.3 |

[1)]Used without a cement binder

Table 14. Uranium ores used in various countries for the manufacture of U and M pads

| Country | Facility | Ore material used or host rock | Origin | Ore grade (% U) |
|---|---|---|---|---|
| Argentina | Villa 25 de Mayo | Continental sandstone | Sierra Pintanda San Rafael district | 0.35 and 0.64 |
| Brazil | I.R.D., Rio de Janeiro | Albite-pyroxene gneiss | Lagoa Real State of Bahia | 0.46 |
| Canada | Uplands airport | Pitchblende ore (hand picked) | Eldorado Mine Saskatchewan | Several percent |
| Denmark | Risø (M pads) | Peralkaline nepheline syenite | Kvanefjeld South Greenland | 0.07 |
| Finland | Helsinki-Vantaa | Phosphate rock | Paltamo East Finland | 0.04 |
| South Africa | Lanseria | Witwatersrand quartz-pebble conglomerate | West Rand Consolidated Mine | 0.02 |
| Sweden | Borlänge | Alum shale | Ranstad Vestergötland | 0.03 |
| USA | Walker Field | Vein-type uranium ore | Schwartzwalder Mine Colorado | 2.6 |

Table 15. Relation between the Th/U grade ratios for U pads and the grades of the uranium ores used for loading the mixes

| Country | Facility | Ore grade[1)] | Th/U (Ratio between pad grades) |
|---|---|---|---|
| Argentina | Villa 25 de Mayo | High | 0.01 |
| Australia | CSIRO, Sydney | High | 0.03 |
| Canada | Bells Corners | High | 0.02 |
| Finland | Helsinki-Vantaa | Low | 0.14 |
| Israel | Soreq | Low | 0.15 |
| South Africa | Lanseria | Low | 0.11 |
| Sweden | Borlänge | Low | 0.10 |

[1)]The distinction between low and high ore grades is based on a grade of 0.1% U

Table 16. Thorium admixtures and resulting U/Th grade ratios for T pads

| Country | Facility | Thorium admixture | U/Th (Ratio between pad grades) |
|---|---|---|---|
| Australia | CSIRO, Sydney | Monazite | 0.05 |
| Brazil | I.R.D., Rio de Janeiro | Monazite | 0.04 |
| Canada | Uplands airport | Thorite | 0.07 |
| " | Bells Corners | Thorium oxide | 0.04 |
| Denmark | Risø | Monazite | 0.05 |
| Finland | Helsinki-Vantaa | Granitic rock | 0.11 |
| South Africa | Lanseria | Monazite | 0.03 |
| Sweden | Borlänge | Diorite | 0.07 |

Table 17. Calculated ratios between an analysed pad radioelement concentration and the corresponding radiometric in-situ grade for the pad

| Pad moisture (%) | Ratio laboratory grade/in-situ grade | |
|---|---|---|
| | Mix sample crushed and dried ($x_d/x$) | Mix sample sealed in assay can ($x'/x$) |
| 2 | 1.06 | 0.96 |
| 6 | 1.10 | 1.00 |
| 10 | 1.14 | 1.04 |

Table 18. Results of laboratory intercomparison experiment arranged by Dr. D.C. George of the Technical Measurements Center, Grand Junction

| Laboratory | Sample 1 (ppm eU) | Sample 2 (ppm eU) | Sample 3 (ppm eTh) |
|---|---|---|---|
| CSIRO Australia | 215 ± 2 | 2133 ± 20 | 523 ± 9 |
| CGS Canada | 215 ± 3 | 2182 ± 39 | 552 ± 7 |
| Risø Denmark | 216 ± 2 | 2099 ± 24 | 534 ± 11 |
| Soreq Israel | 214 ± 10 | 2123 ± 90 | 519 ± 25 |
| NUCOR South Africa | 211 ± 8 | 2102 ± 80 | - |
| TMC USA | 219 ± 9 | 2210 ± 70 | 574 ± 17 |
| Coefficient of variation (weighted value) | 0.5% | 1.6% | 3.2% |

Table 19. Examples of determination limits for the laboratory spectrometer in Fig. 42

| Counting time (hours) | Radioelement concentrations determined with 10% precision | | |
|---|---|---|---|
| | % K | ppm eU | ppm eTh |
| 1 | 0.34 | 3.0 | 6.8 |
| 2 | 0.23 | 2.0 | 4.6 |
| 4 | 0.15 | 1.4 | 3.3 |
| 8 | 0.11 | 1.1 | 2.4 |
| 16 | 0.09 | 0.8 | 1.9 |

Table 20. Application of weighted regression analysis to the expression $y = a + bx$ where a and b are unknowns (N observations, $N > 3$)

---

1. Make a qualified guess of b

2. For each paired observation (x,y) calculate the weight factor $w = (\sigma_y^2 + b^2 \cdot \sigma_x^2)^{-1}$

3. Compute the sums

$$S_w = \Sigma w \qquad S_{xx} = \Sigma wx^2$$
$$S_x = \Sigma wx \qquad S_{xy} = \Sigma wxy$$
$$S_y = \Sigma wy \qquad S_{yy} = \Sigma wy^2$$

4. Calculate

$$d = S_w \cdot S_{xx} - S_x^2$$
$$b = (S_w \cdot S_{xy} - S_x \cdot S_y)/d$$

5. If the new estimate of b deviates sufficiently little from the old estimate, proceed with step 6, otherwise repeat steps 2 to 5.

6. Calculate

$$a = (S_{xx} \cdot S_y - S_x \cdot S_{xy})/d$$

$$\chi^2 = S_{yy} - a \cdot S_y - b \cdot S_{xy}$$

$$\sigma_a = \sqrt{\chi^2 \cdot S_{xx}/d/(N-2)}$$

$$\sigma_b = \sqrt{\chi^2 \cdot S_w/d/(N-2)}$$

Table 21. Symbols and working expression for the calculation of assay accuracy $A_x$ obtained with spectrometer of known estimated calibration errors

| Quantity | Symbol | Signal, calibration constant, or assay result | | |
|---|---|---|---|---|
| | | Window 1 (K) | Window 2 (U) | Window 3 (Th) |
| Interfering contribution | r | $\beta s_{Th} \cdot x_{Th} + \gamma s_U \cdot x_U$ | $\alpha s_{Th} \cdot x_{Th}$ | $a s_U \cdot x_U$ |
| Sensitivity | s | $s_K$ | $s_U$ | $s_{Th}$ |
| Radioelement concentration | x | $x_K$ | $x_U$ | $x_{Th}$ |
| Stripping ratio | k | $\gamma$ | $\alpha$ | a |

$$F = \frac{r}{s \cdot x}$$

$$A_x = x \cdot \sqrt{(F \cdot \sigma_k/k)^2 + (\sigma_s/s)^2}$$

Table 22. Calibration trials and grade tests executed in the IAEA pads intercomparison experiment undertaken by the author

| Country | Monitored facility | Counting date(s) (yy mm dd) | Purpose |
|---|---|---|---|
| Argentina | Villa 25 de Mayo | 82-10-22 | Grade test |
| Australia | CSIRO, Sydney | 84-02-23 | " |
| Brazil | I.R.D., Rio de Janeiro | 82-10-15 | " |
| Canada | Uplands airport | 80-08-07 | Calibration |
| " | Bells Corners | 80-08-06 | " |
| Denmark | Risø | *) | Grade test |
| Finland | Helsinki-Vantaa | 80-05-05 | Calibration |
| Israel | Soreq | 83-04-19 | Grade test |
| South Africa | Lanseria | 82-10-29 | " |
| Sweden | Borlänge | 80-06-20 | Calibration |
| " | " | 81-06-15 | " |
| " | Malå (old pads) | 80-06-24 | " |
| " | Malå (new pads) | 83-07-27 | Grade test |
| USA | Walker Field | 80-02-25 | Calibration |
| " | " | 80-08-13 | " |

*) The Risø facility was monitored 27 times between March 1980 and August 1984

Table 23. Experimental GR-410 stripping ratios and resulting mean values with standard deviations *)

| Country | Facility used | Stripping ratio | | | |
|---|---|---|---|---|---|
| | | α | β | γ | a |
| Canada | Uplands airport | 0.661±0.053 | 0.618±0.126 | 0.755±0.243 | - |
| " | Bells Corners | 0.561±0.013 | 0.468±0.014 | 0.770±0.008 | 0.035±0.001 |
| Finland | Helsinki-Vantaa | 0.580±0.029 | 0.498±0.051 | 0.803±0.045 | 0.041±0.008 |
| Sweden | Borlänge and Malå | 0.602±0.025 | 0.543±0.026 | 0.779±0.021 | 0.040±0.005 |
| USA | Walker Field | 0.601±0.016 | 0.494±0.024 | 0.751±0.017 | 0.022±0.006 |
| | $\bar{x}$ | 0.583 | 0.488 | 0.769 | 0.035 |
| | $\sqrt{V_1}$ | 0.026 | 0.033 | 0.011 | 0.011 |
| | $\sqrt{V_2}$ | 0.020 | 0.024 | 0.015 | 0.002 |
| | F | 1.72 | 1.92 | 0.48 | 1.87 |
| | σ | 0.020 | 0.024 | 0.015 | 0.002 |
| | $\sigma/\sqrt{N}$ | 0.009 (1.5%) | 0.011 (2.3%) | 0.007 (0.9%) | 0.001 (2.9%) |

*) 5 observations: $F_{10}$ (4,5) = 3.52
4 " : $F_{10}$ (3,4) = 4.19

Table 24. Experimental GR-410 window sensitivities and resulting mean values with standard deviations *)

| Country | Facility | Window sensitivity ($2\pi$ geometry) | | |
|---|---|---|---|---|
| | | $s_K$ (Counts/s per % K) | $s_U$ (Counts/s per ppm eU) | $s_{Th}$ (Counts/s per ppm eTh) |
| Canada | Uplands airport | 3.15±1.16 | 0.285±0.032 | 0.1258±0.0110 |
| " | Bells Corners | 3.29±0.08 | 0.347±0.018 | 0.1186±0.0031 |
| Finland | Helsinki-Vantaa | 3.38±0.75 | 0.339±0.026 | 0.1259±0.0119 |
| Sweden | Borlänge and Malå | 3.40±0.04 | 0.339±0.026 | 0.1271±0.0061 |
| USA | Walker Field | 3.32±0.05 | 0.320±0.008 | 0.1314±0.0018 |
| | $\bar{x}$ | 3.358 | 0.3247 | 0.1280 |
| | $\sqrt{v_1}$ | 0.051 | 0.0149 | 0.0059 |
| | $\sqrt{v_2}$ | 0.065 | 0.0149 | 0.0033 |
| | F | 0.61 | 1.00 | 3.21 |
| | $\sigma$ | 0.065 | 0.0149 | 0.0033 |
| | $\sigma/\sqrt{N}$ | 0.029 (0.9%) | 0.0066 (2.0%) | 0.0015 (1.2%) |

*) 5 observations: $F_{10}$ (4,5) = 3.52

Table 25. Calculated factors for estimating the gamma-ray exposure rates on calibration pads of various diameters (elevation of detector point: h = 5 cm)

| Pad diameter (m) | μR/h | | |
|---|---|---|---|
| | 1% K | 1 ppm eU *) | 1 ppm eTh |
| 1 | 1.16±0.01 | 0.488±0.004 | 0.216±0.005 |
| 2 | 1.26±0.01 | 0.529±0.004 | 0.236±0.006 |
| 3 | 1.28±0.01 | 0.539±0.004 | 0.240±0.006 |
| 8 | 1.31±0.01 | 0.552±0.004 | 0.246±0.006 |
| 10 | 1.32±0.01 | 0.554±0.004 | 0.247±0.006 |

*) Including a small contribution from $^{235}U$

A radiation exposure of 1 R corresponds to an absorbed dose of $8.69 \times 10^{-3}$ Gy in standard air

Table 26. Calculated and experimental exposure rates for the airport facilities in the USA and Sweden *)

| Facility | Pad monitored | μR/h | | Ratio |
|---|---|---|---|---|
| | | Calculated | Experimental | |
| Walker Field | U | 16.6±0.5 | 14.9±1.2 | 1.11±0.10 |
| " | T | 11.8±0.3 | 10.9±0.9 | 1.08±0.09 |
| " | M | 16.0±0.4 | 14.9±1.1 | 1.07±0.08 |
| Borlänge | K | 8.7±0.2 | 8.3±0.8 | 1.04±0.11 |
| " | U | 13.0±0.3 | 12.5±0.8 | 1.04±0.07 |
| " | T | 12.6±0.6 | 11.5±0.8 | 1.10±0.09 |

*) Reported values are relative to the B pads of the two facilities

Table 27. Ratios between analysed and monitored radioelement concentrations for calibration pads in seven countries

| Country | Facility | Laboratory assay/in-situ assay | | |
|---|---|---|---|---|
| | | Potassium | Eq. uranium | Eq. thorium |
| Argentina [1] | Villa 25 de Mayo | 1.24±0.05 [2] | 1.83±0.03 [2] | 1.16±0.02 [2] |
| Australia | CSIRO, Sydney | 1.08±0.04 | 0.98±0.04 | 1.04±0.03 |
| Brazil [1] | I.R.D, Rio de Janeiro | 1.05±0.01 | 1.14±0.03 [2] | 1.08±0.01 |
| Denmark [1] | Risø | 1.01±0.02 | 1.25±0.03 [2] | 1.09±0.02 |
| Israel | Soreq | 1.00±0.04 | 0.95±0.02 | 1.02±0.02 |
| South Africa | Lanseria | 1.04±0.04 | 1.02±0.07 | 0.98±0.05 [2] |
| Sweden [1] | Malå (new pads only) | - | 1.06±0.03 | 1.01±0.03 |
| | $\bar{x}$ | 1.04 | 0.99 | 1.07 |
| | $\sqrt{V_1}$ | 0.02 | 0.05 | 0.03 |
| | $\sqrt{V_2}$ | 0.02 | 0.03 | 0.02 |
| | F | 1.30 | 3.19 | 3.23 |
| | $F_{10}$ | 3.52 | 4.19 | 3.52 |

[1] Laboratory analysis done at Risø

[2] Value excluded from $\bar{x}$ due to significance in the F test

# FIGURES

Fig. 1. Portable Geometrics GR-410 spectrometer on outcrop of the Galway granite, Ireland.

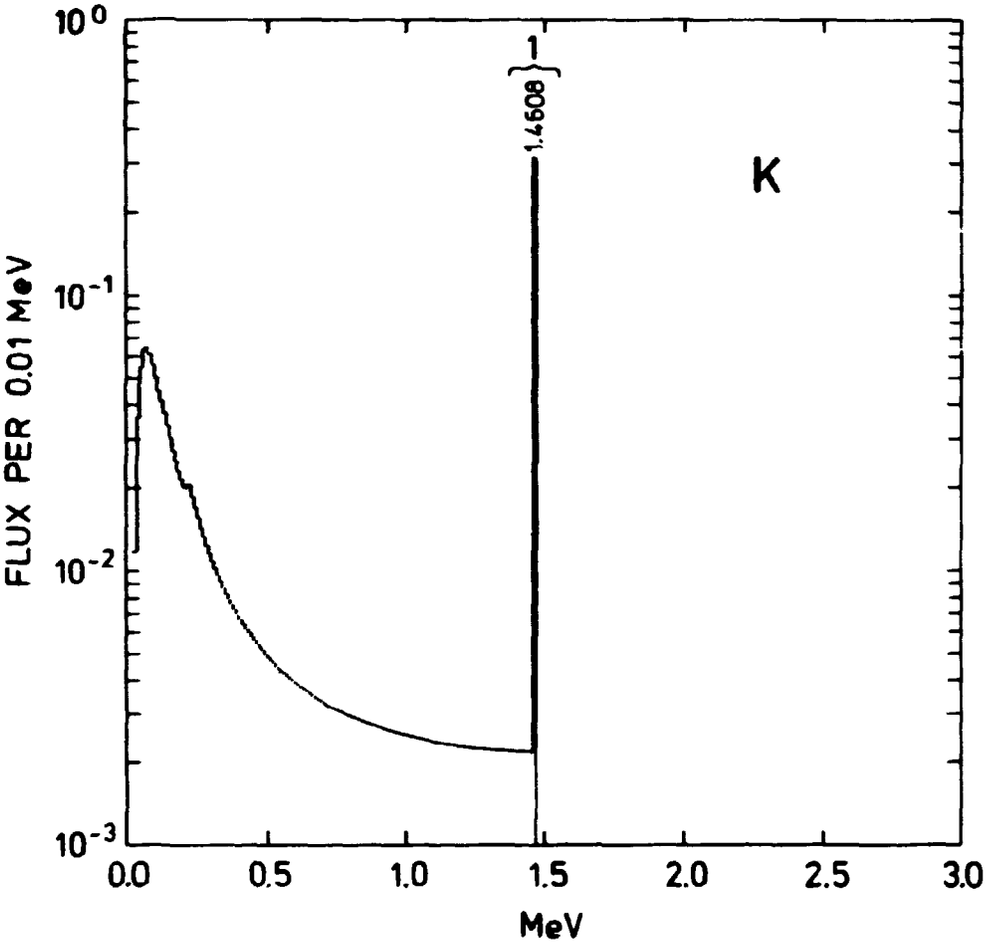


Fig. 2. Energy distribution of potassium gamma radiation on a ground with 1% K. The brace labelled "1" shows the potassium window of a GR-410 spectrometer.

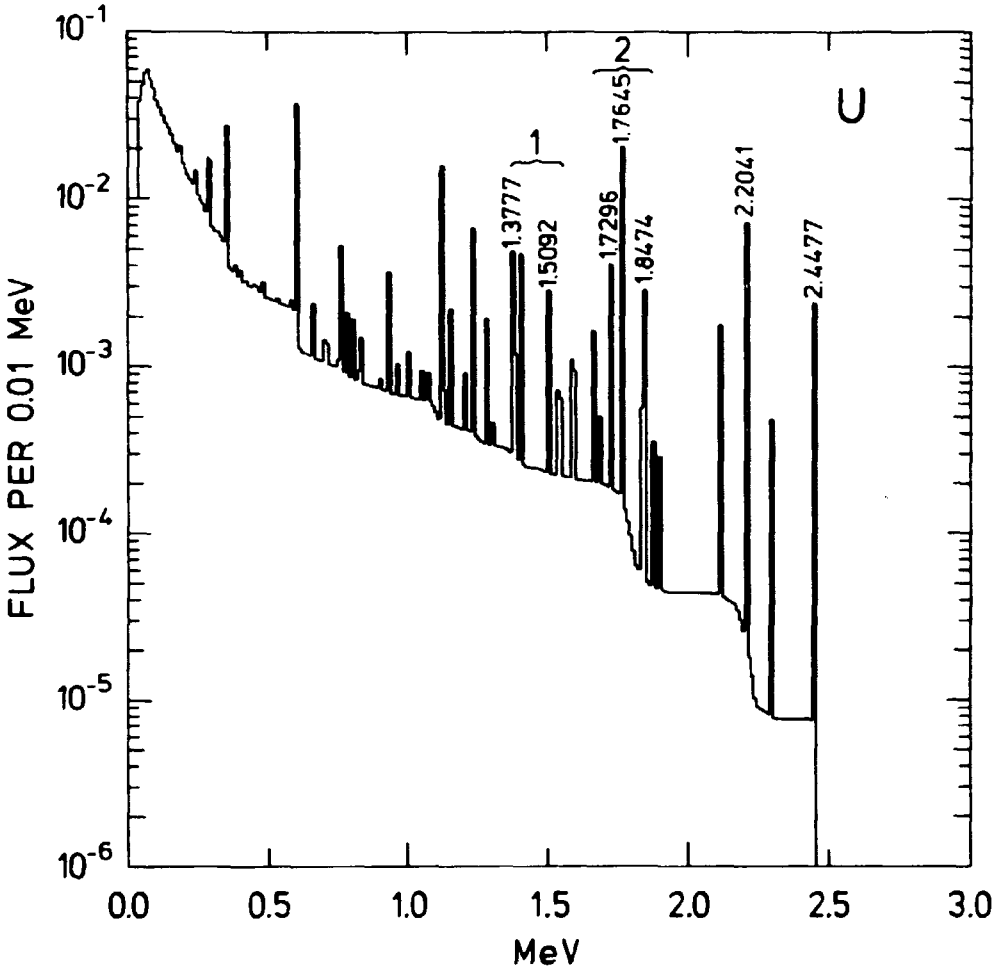


Fig. 3. Energy distribution of uranium (radium) gamma radiation on a ground with 1 ppm eU. The brace labelled "2" shows the uranium window of a GR-410 spectrometer.

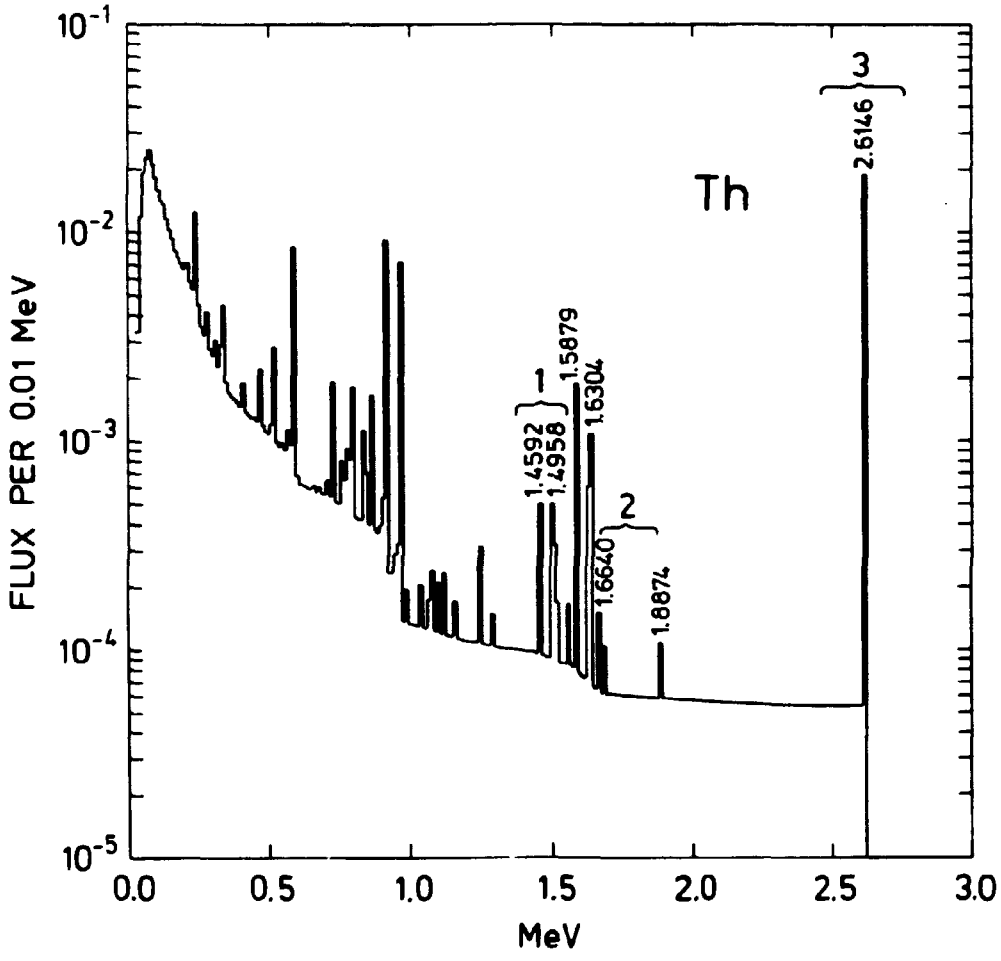


Fig. 4. Energy distribution of thorium gamma radiation on a ground with 1 ppm eTh. The brace labelled "3" shows the thorium window of a GR-410 spectrometer.

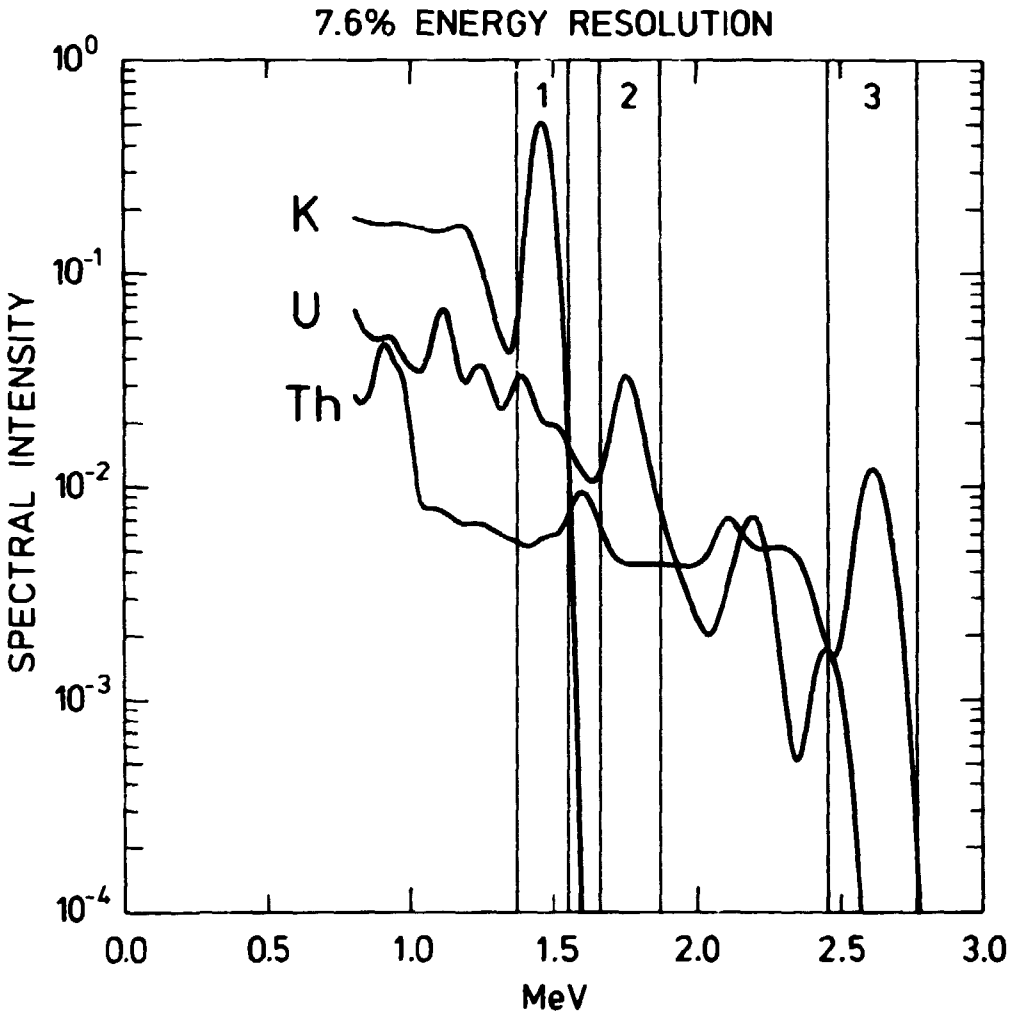


Fig. 5. Calculated pulse spectra for 76 × 76 mm sodium-iodide scintillator placed on a rock surface. An excellent energy resolution of 7.6% is assumed.

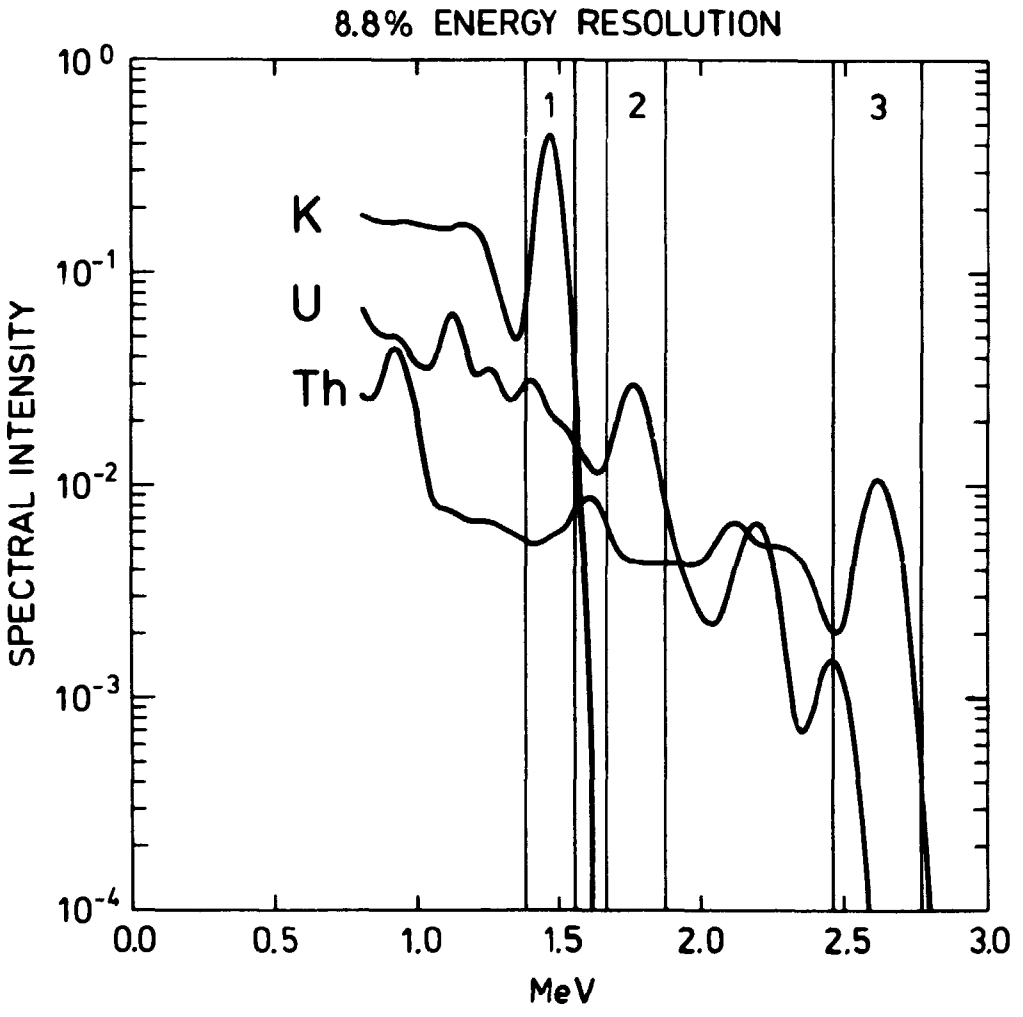


Fig. 6. Calculated pulse spectra for 76 × 76 mm sodium-iodide scintillator placed on a rock surface. An acceptable energy resolution of 8.8% is assumed.

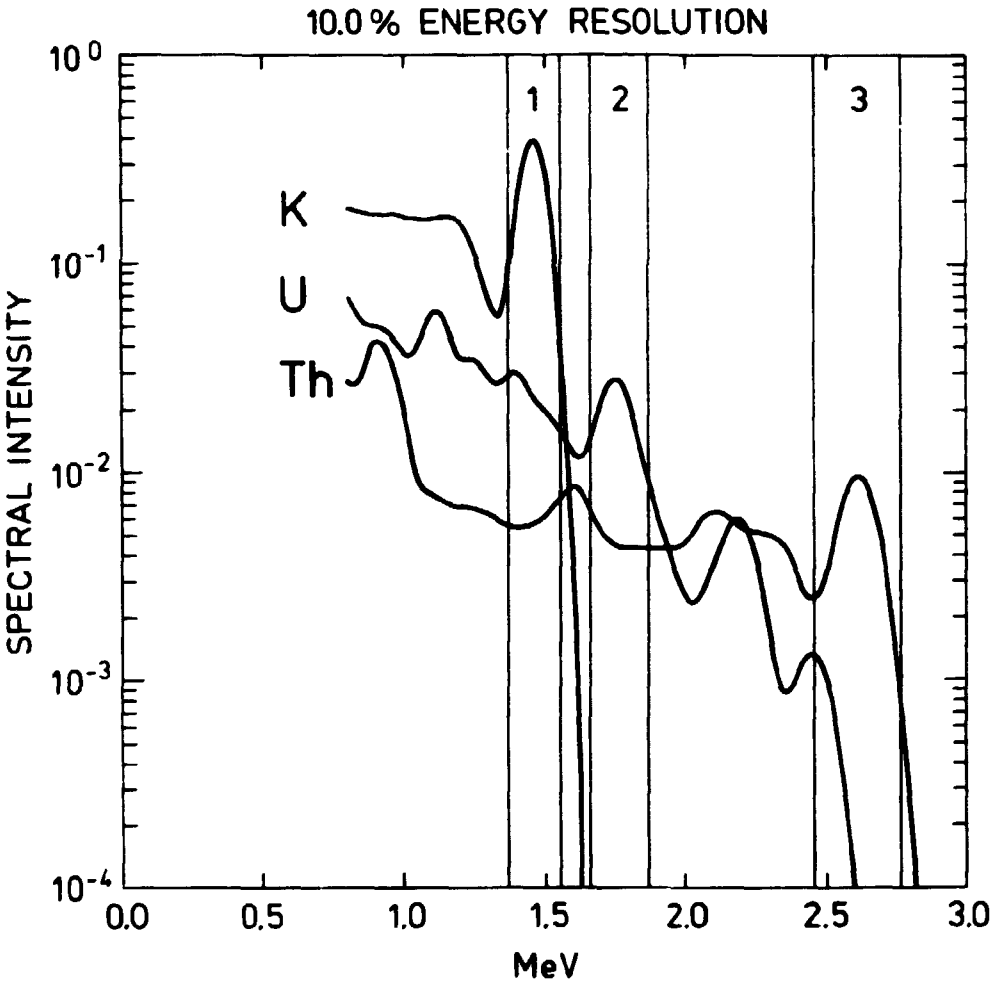


Fig. 7. Calculated pulse spectra for 76 × 76 mm sodium-iodide scintillator placed on a rock surface. A poor energy resolution of 10.0% is assumed.

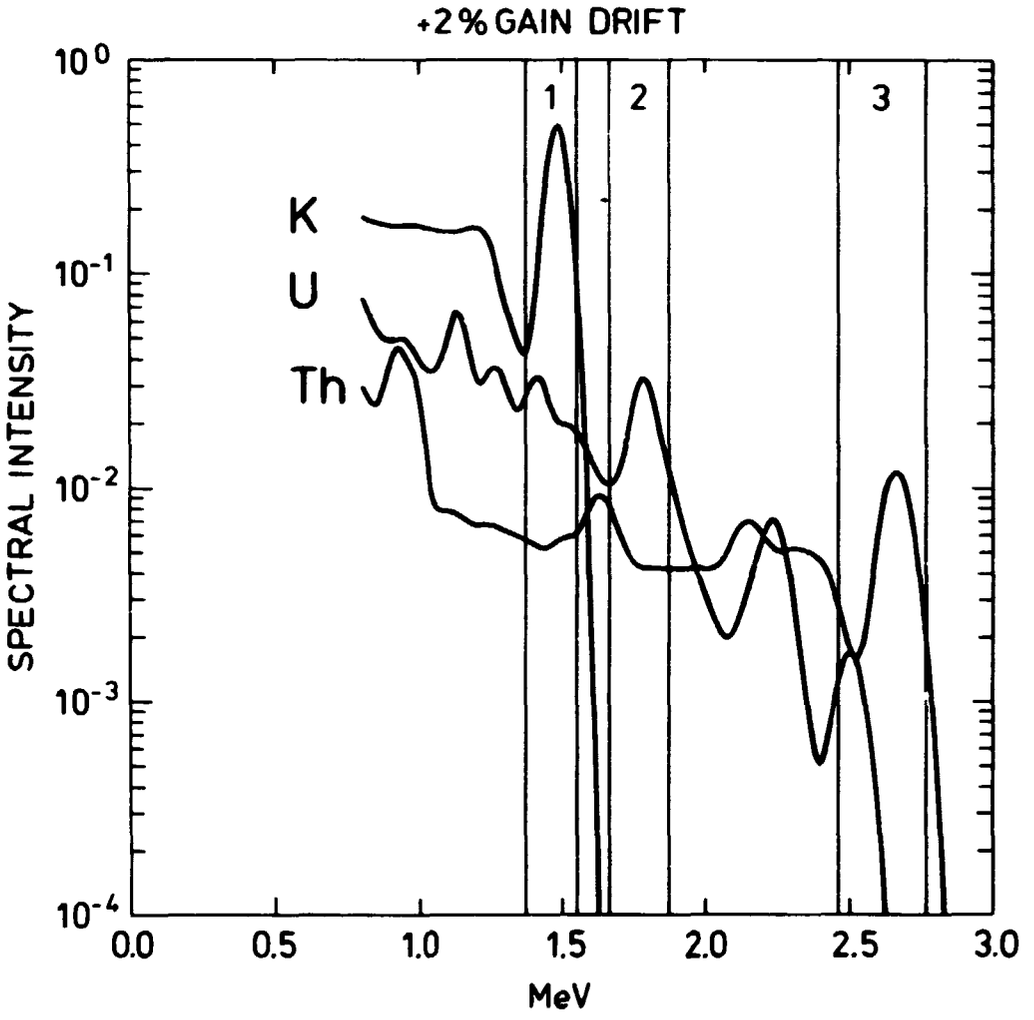


Fig. 8. Shifted peak positions in the energy windows resulting from +2% photomultiplier gain drift.

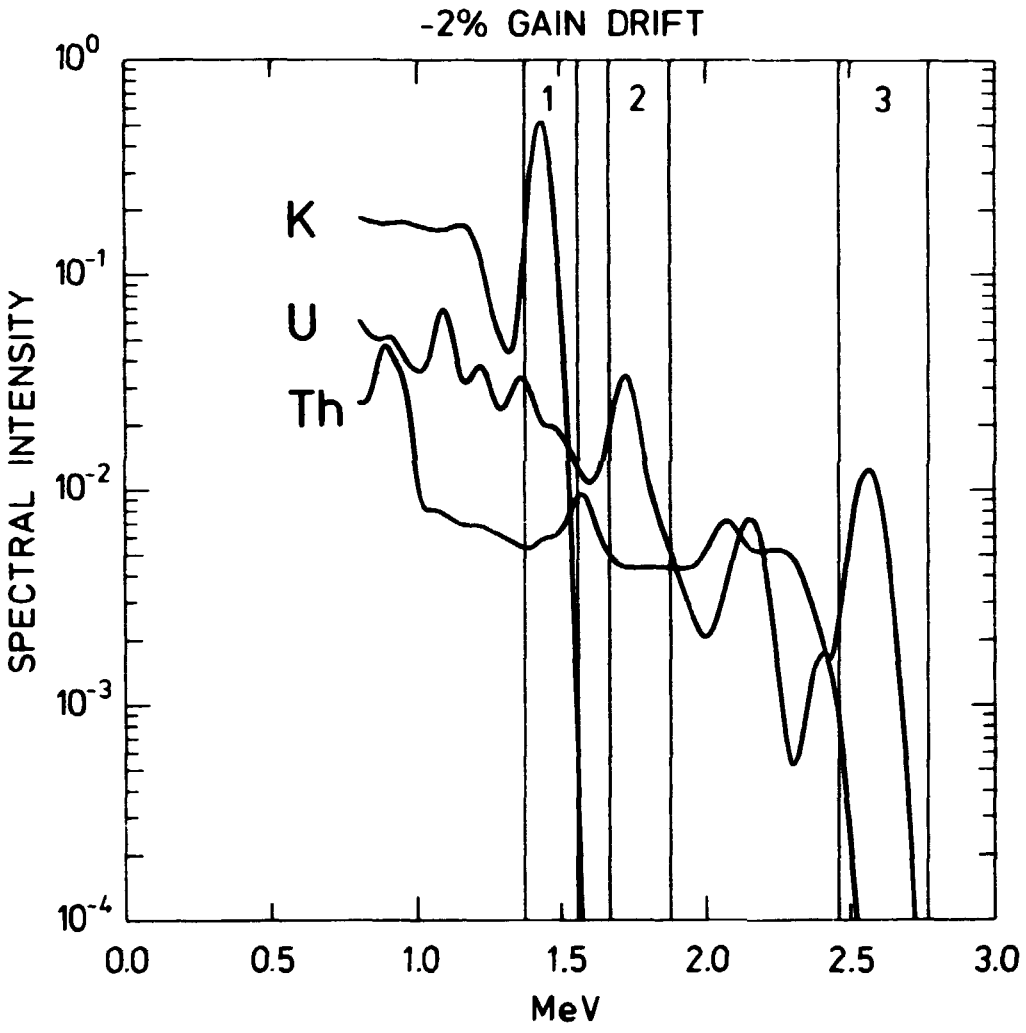


Fig. 9. Shifted peak positions in the energy windows resulting from -2% photomultiplier gain drift.

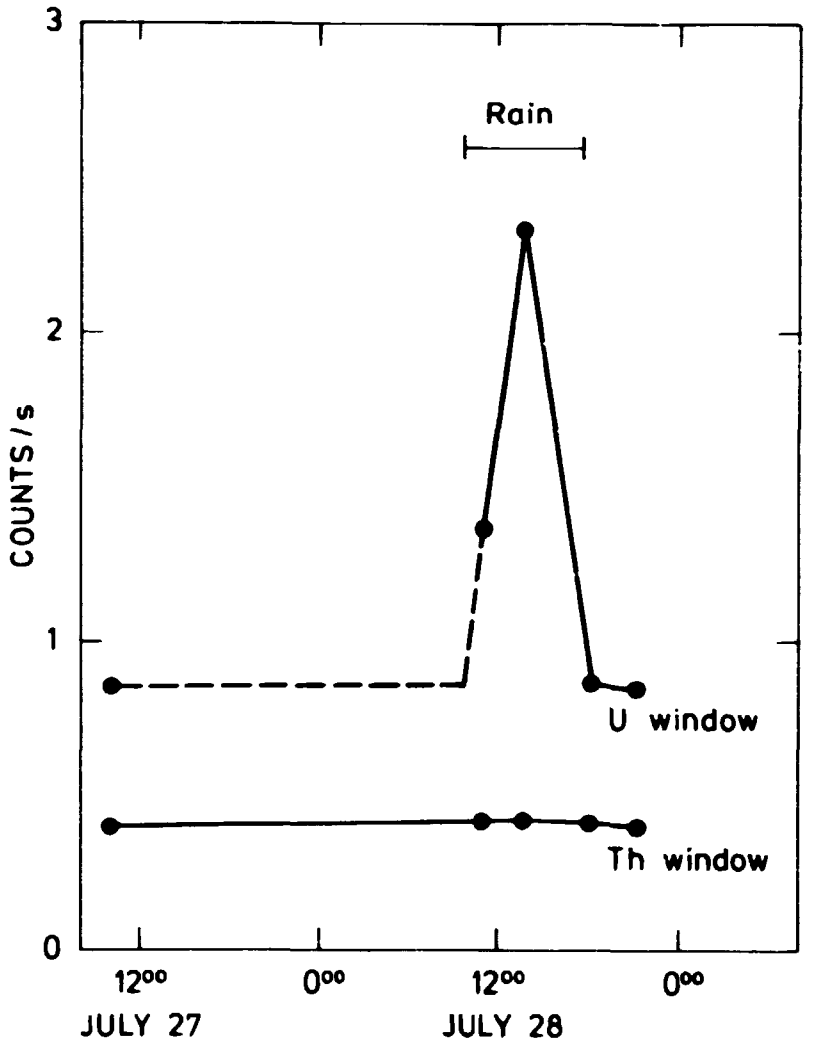


Fig. 10. Temporary increase in the uranium count rate of GR-410 spectrometer placed on "background" calibration pad at Malå, Sweden. The effect is attributed to $^{214}Bi$ deposited on the pad surface by rain drops.

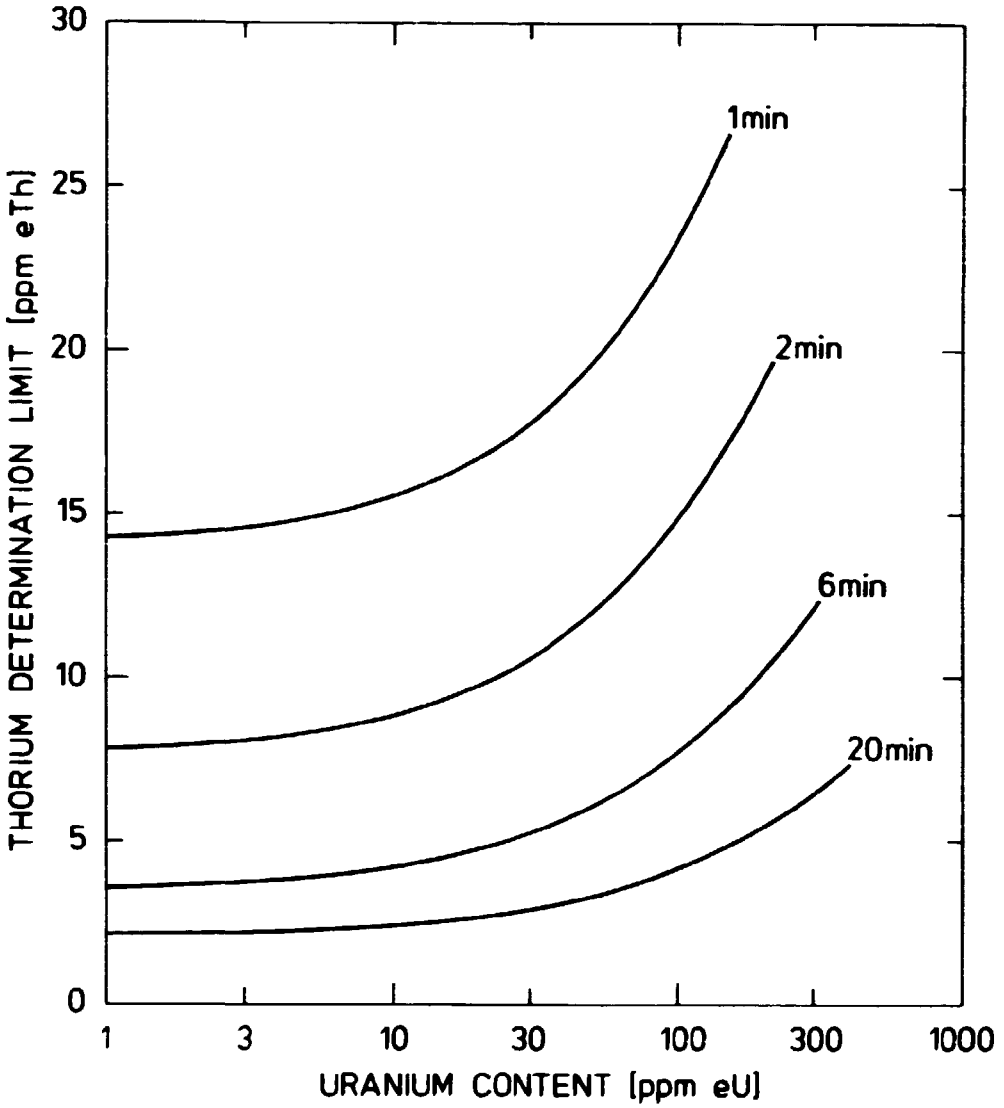


Fig. 11. Calculated curves providing the counting time required to determine a ground concentration of thorium with 10% precision. The graph pertains to the GR-410 spectrometer used in the IAEA pads intercomparison experiment.

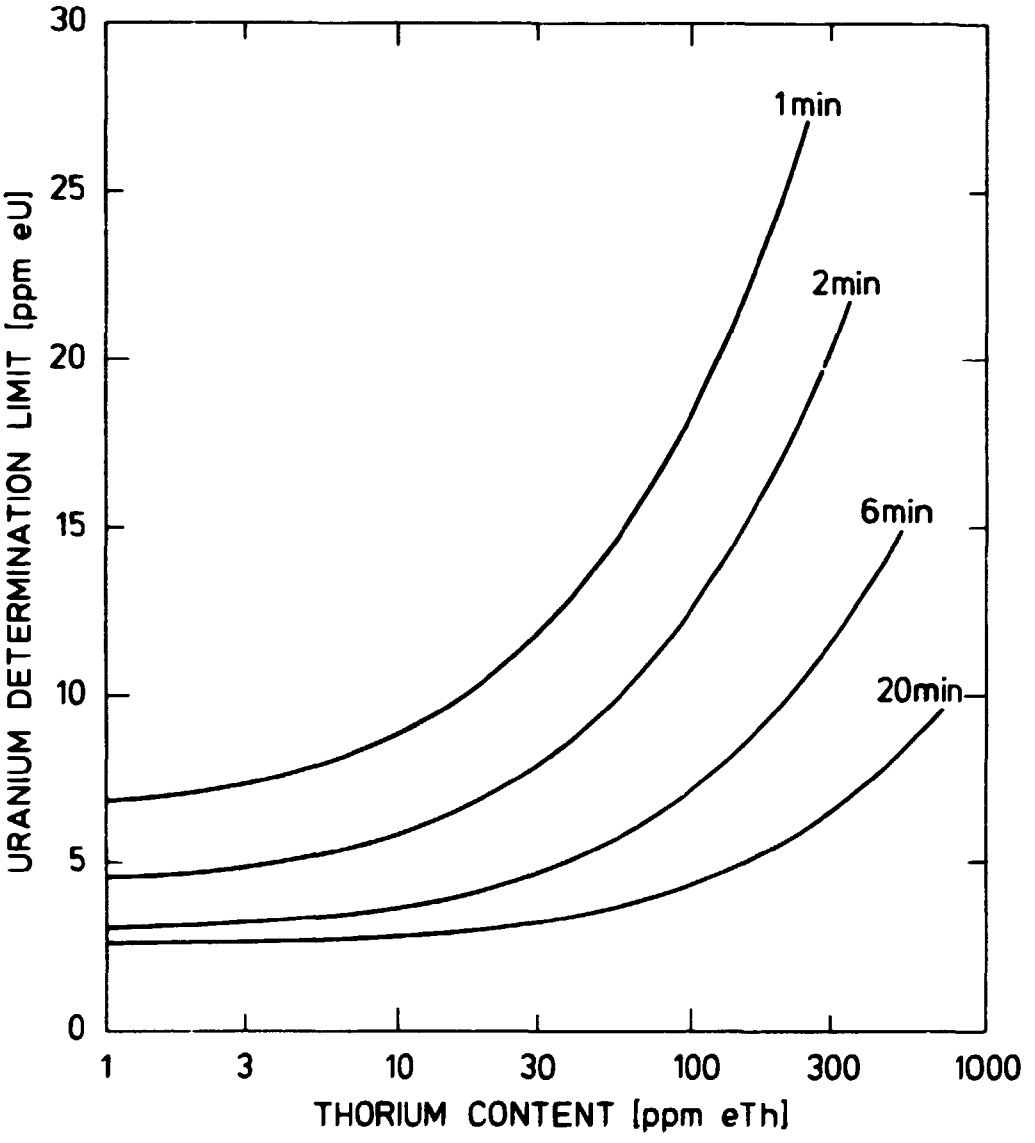


Fig. 12. Calculated curves providing the counting time required to determine a ground concentration of uranium (radium) with 10% precision. The graph pertains to the GR-410 spectrometer used in the IAEA pads intercomparison experiment.

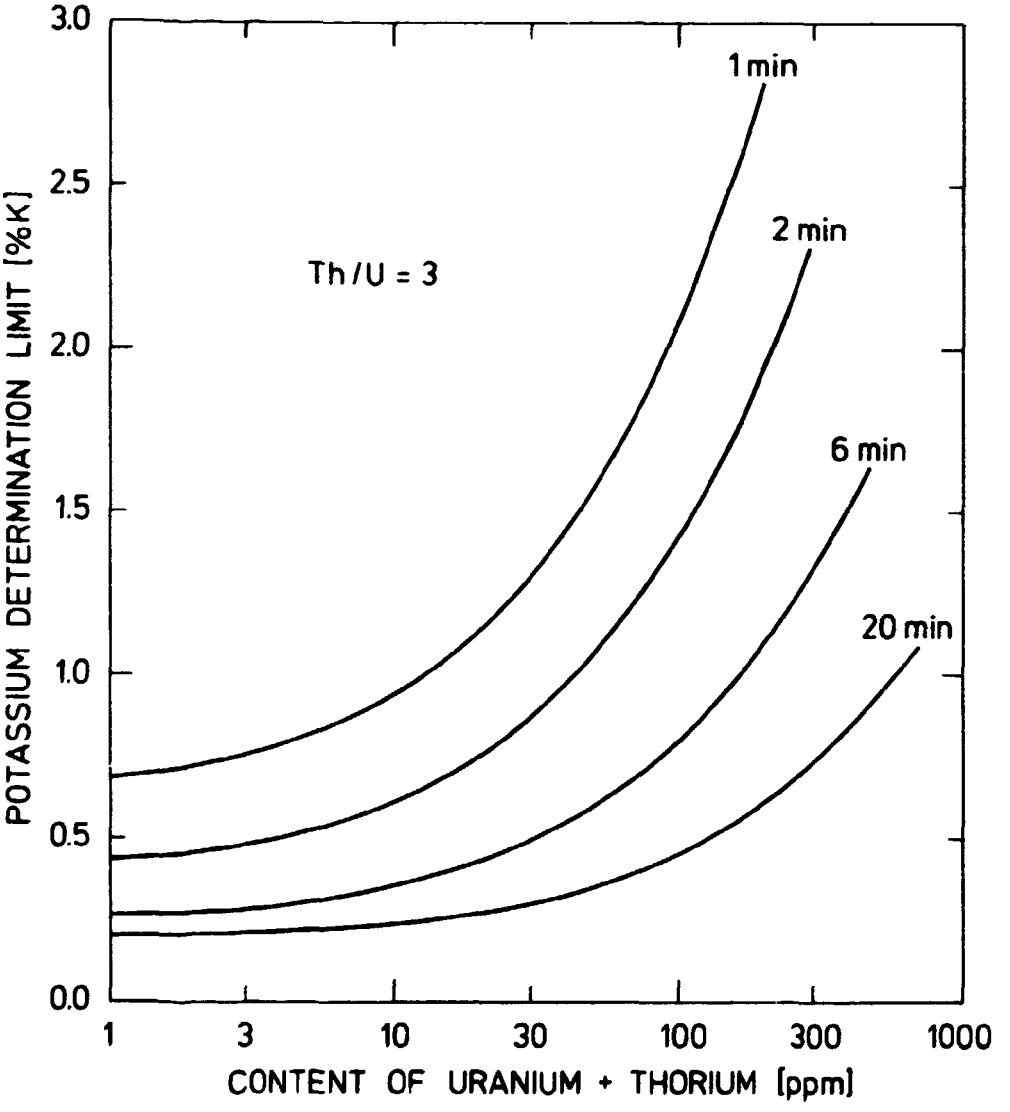


Fig. 13. Calculated curves providing the counting time required to determine a ground concentration of potassium with 10% precision. A thorium/uranium concentration ratio of 3 is assumed for the ground material. The graph pertains to the GR-410 spectrometer used in the IAEA pads intercomparison experiment.

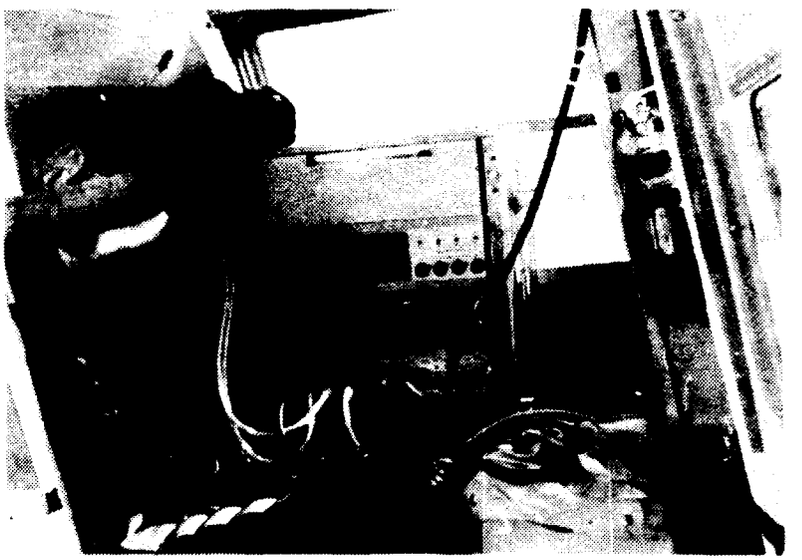

Fig. 14. Light airborne gamma-ray spectrometer designed by Risø National Laboratory and installed in Jet Ranger helicopter. Window counts are recorded with a Scintrex GAD-6 portable spectrometer.

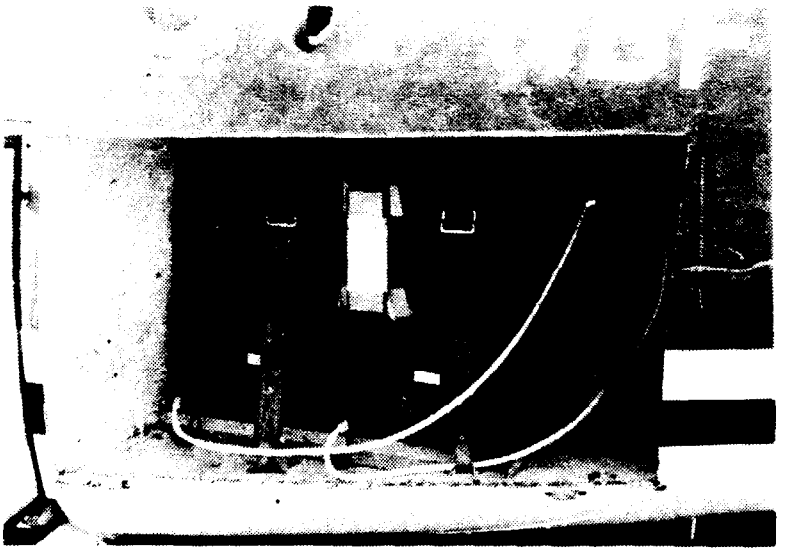

Fig. 15. Two detector packages of Risø's aerial survey system. Each package contains two thermally insulated 152 × 102 mm sodium-iodide scintillators, corresponding to a total detector volume of 7,400 $cm^3$.

Fig. 16. High-sensitivity detector system flown in fixed-wing Skyvan aircraft by the Geological Survey of Canada. The large containers house twelve prismatic sodium-iodide scintillators of the dimensions 102 × 102 × 406 mm which provide a total detector volume of 50,700 $cm^3$.

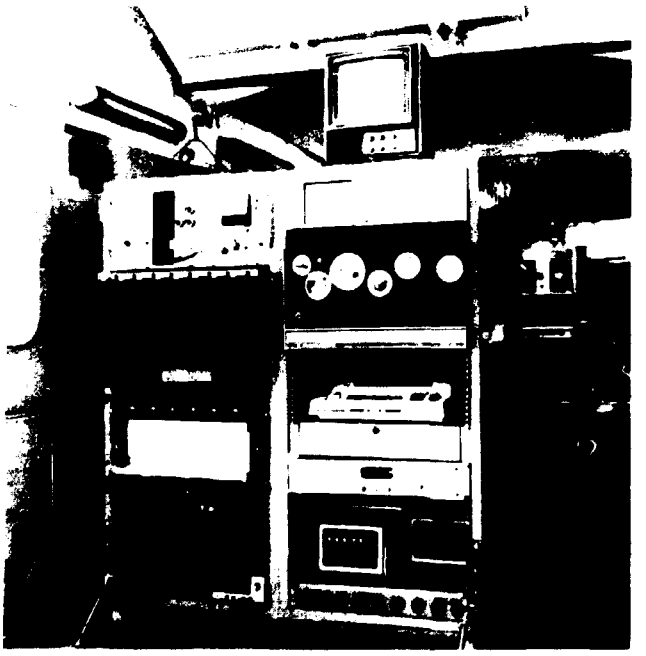

Fig. 17. The data acquisition panel of the Canadian airborne gamma-ray spectrometer. A NOVA minicomputer is used for the recording of 256-channel spectra at 1 second intervals along the flight lines.

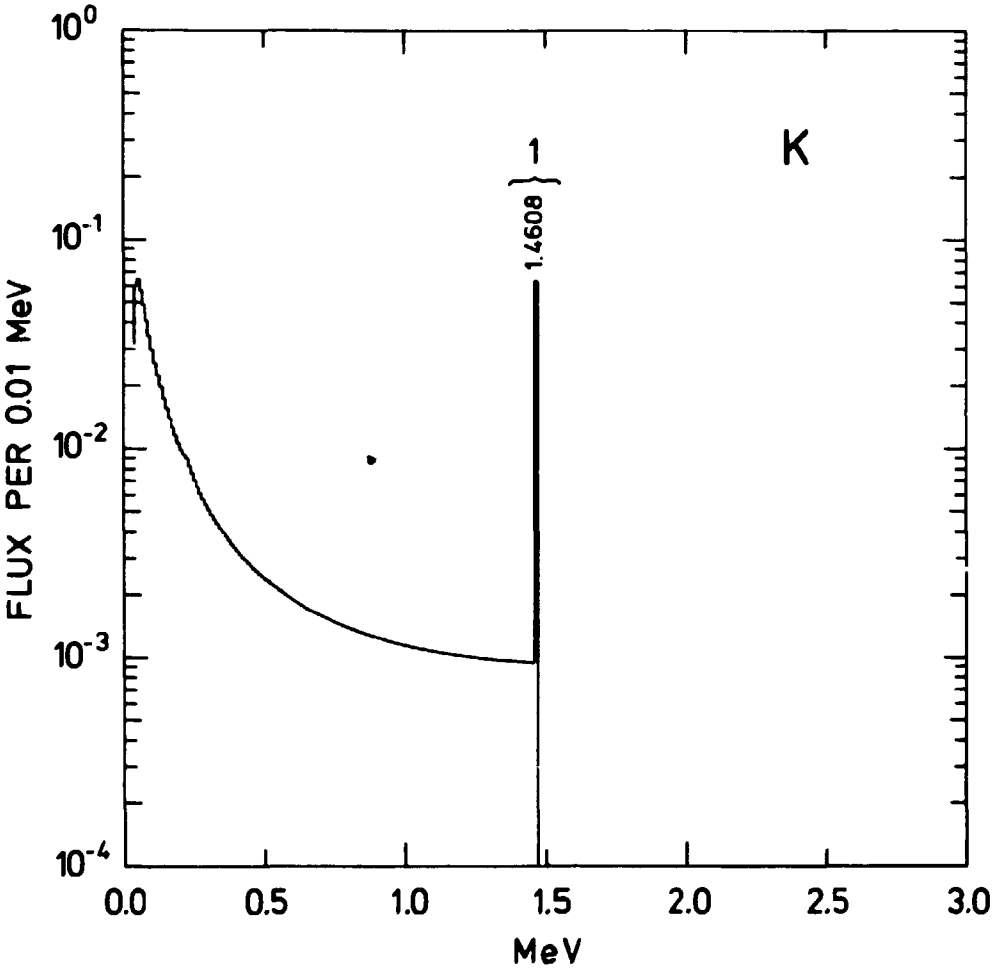


Fig. 18. Energy distribution of potassium gamma radiation 125 m over a ground with 1% K.

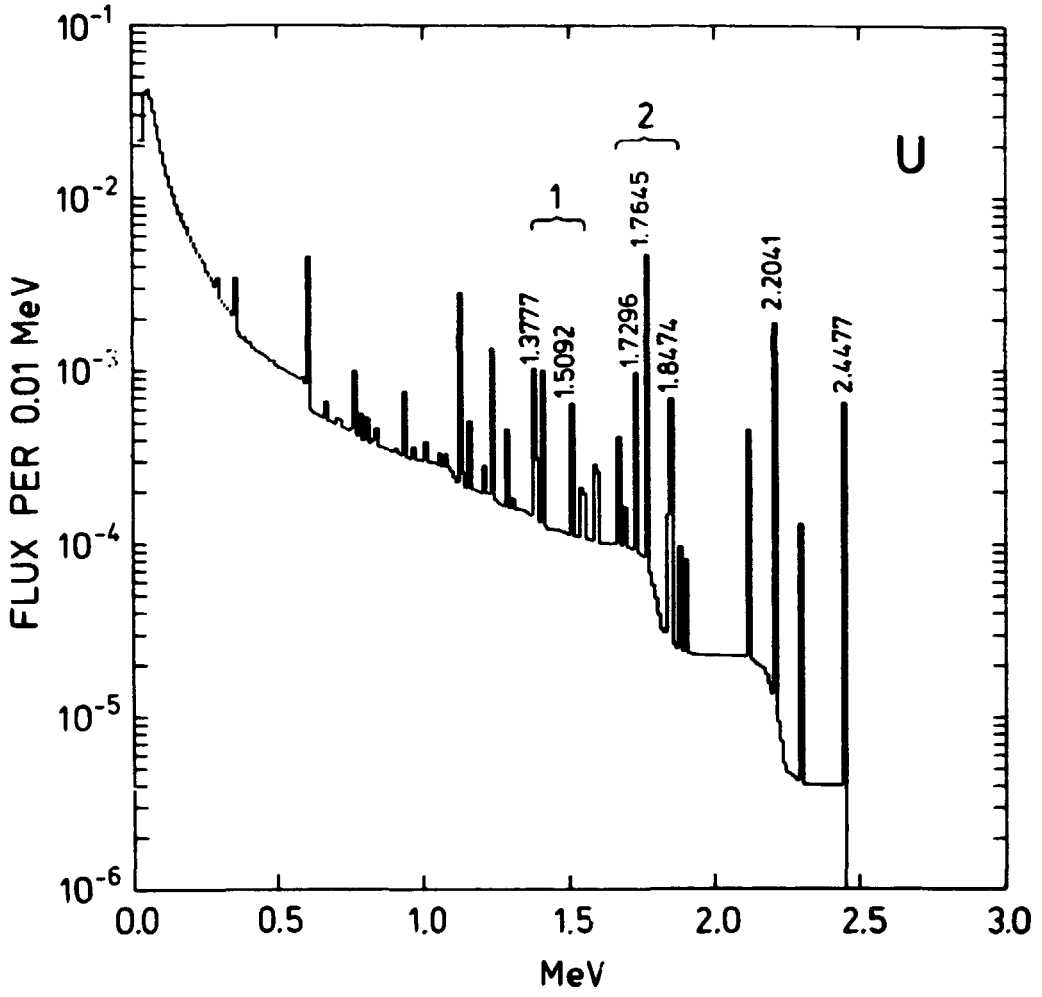


Fig. 19. Energy distribution of uranium (radium) gamma radiation 125 m over a ground with 1 ppm eU.

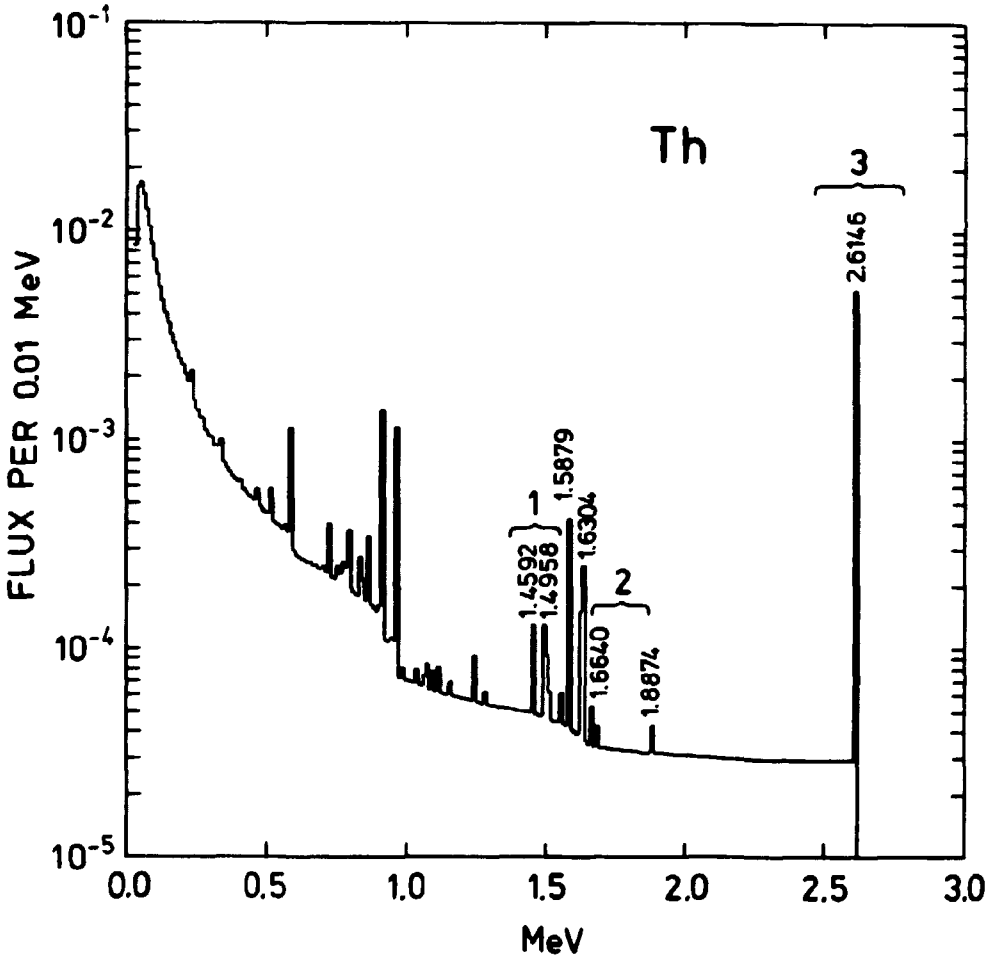


Fig. 20. Energy distribution of thorium gamma radiation 125 m over a ground with 1 ppm eTh.

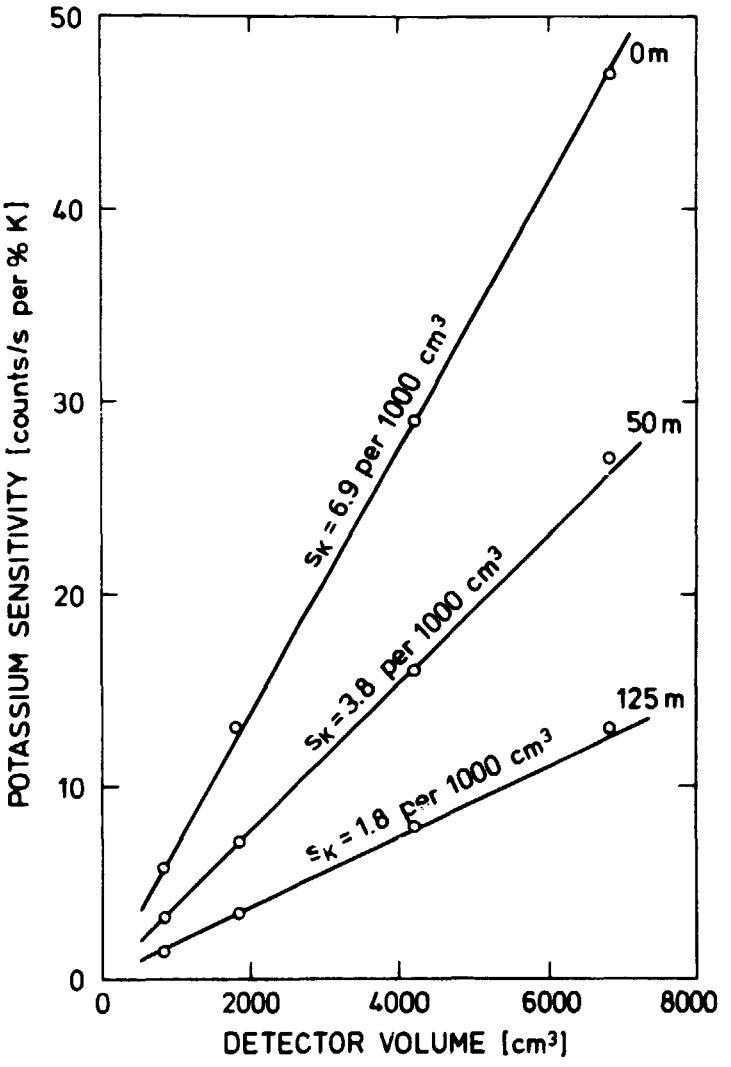


Fig. 21. Theoretical potassium window sensitivities for 102 mm thick sodium-iodide detectors in survey heights of 0, 50, and 125 m.

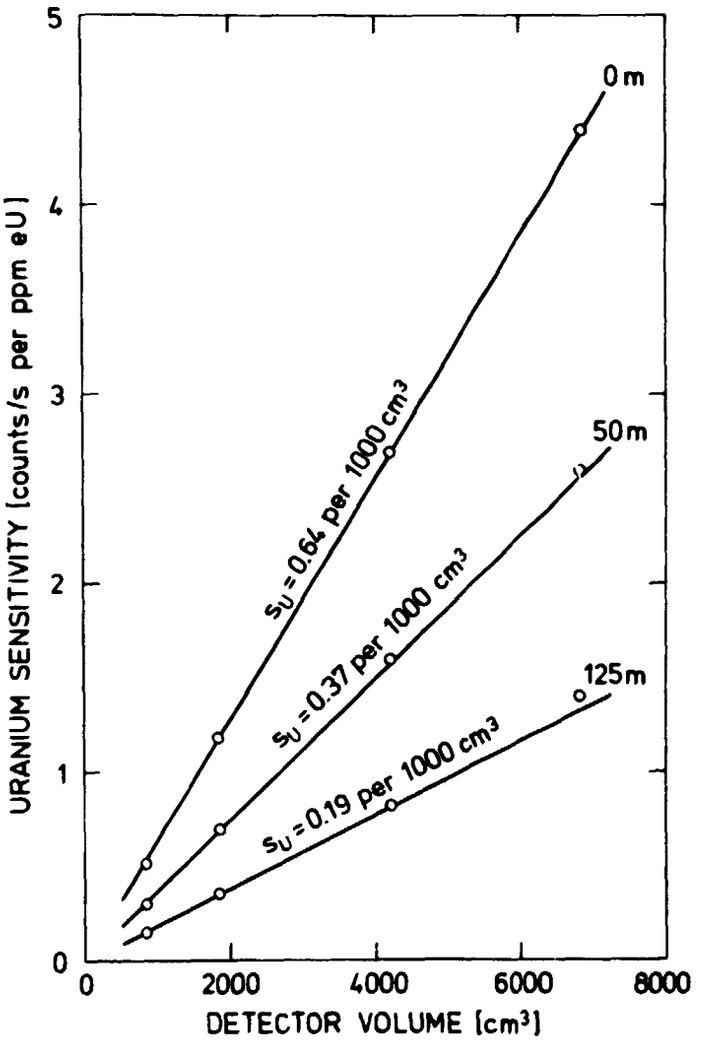


Fig. 22. Theoretical uranium window sensitivities for 102 mm thick sodium-iodide detectors in survey heights of 0, 50, and 125 m.

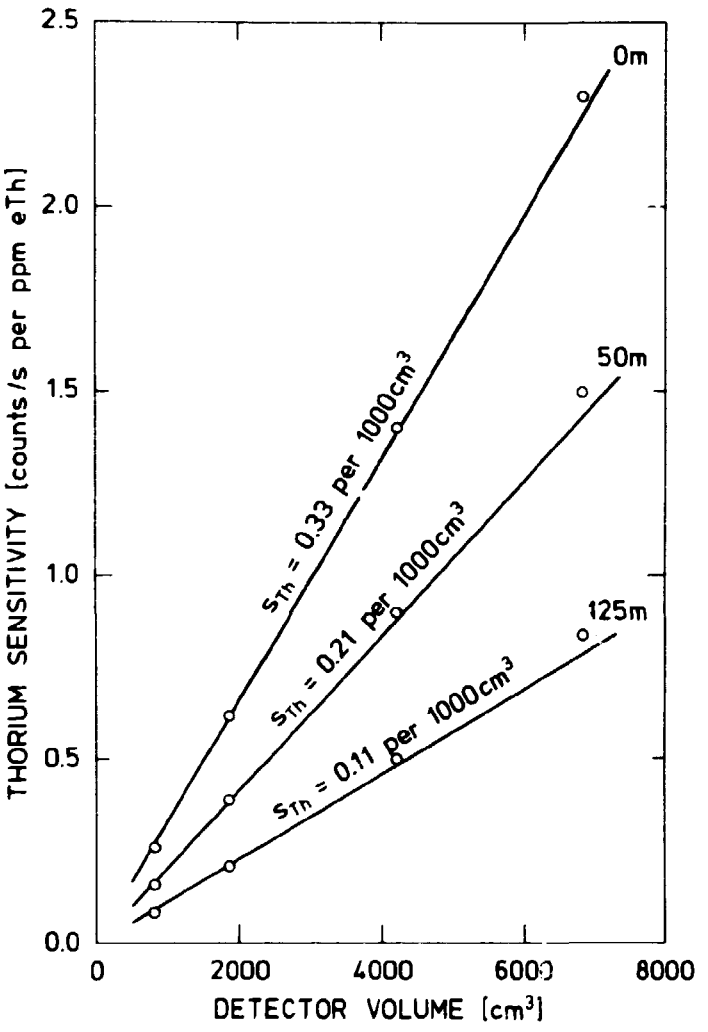


Fig. 23. Theoretical thorium window sensitivities for 102 mm thick sodium-iodide detectors in survey heights of 0, 50, and 125 m.

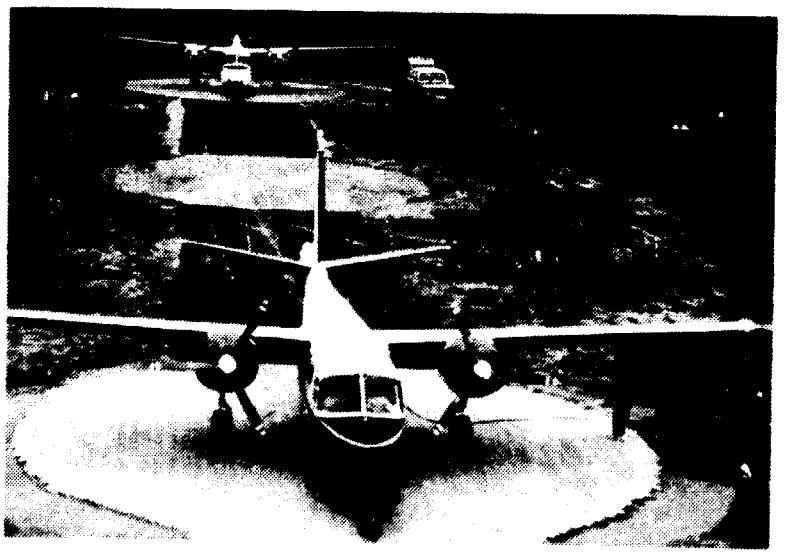

Fig. 24. Gamma-ray survey aircraft parked for the recording of calibration counts on concrete pads at the airport in Borlänge, Sweden.

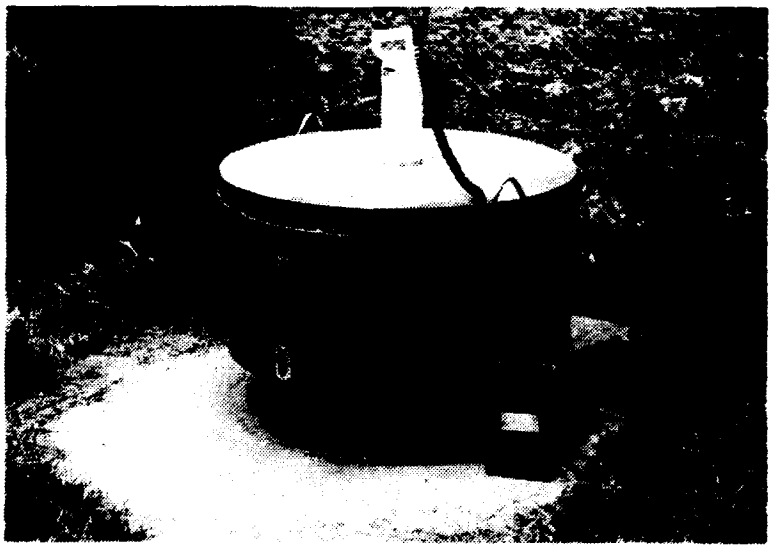

Fig. 25. Portable GR-410 spectrometer set up for monitoring of small calibration pad at Villa 25 de Mayo in the Mendoza province, Argentina.

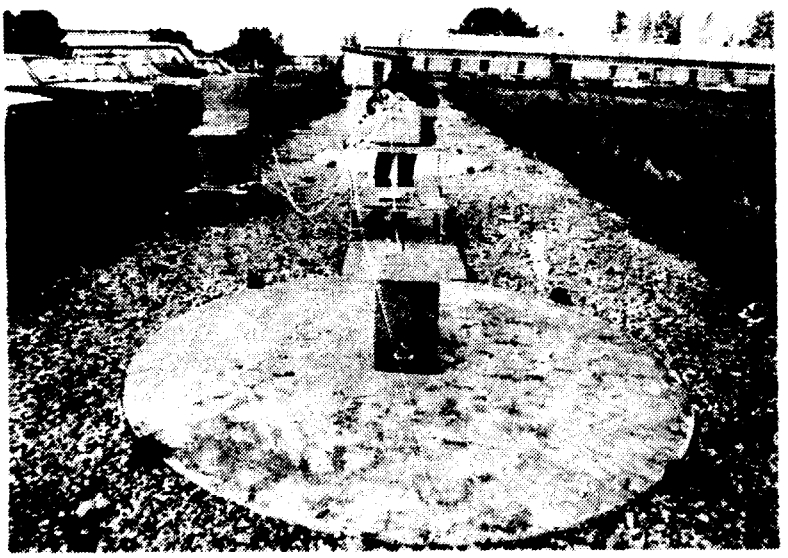

Fig. 26. Calibration of airborne detector package using pads available at Risø National Laboratory.

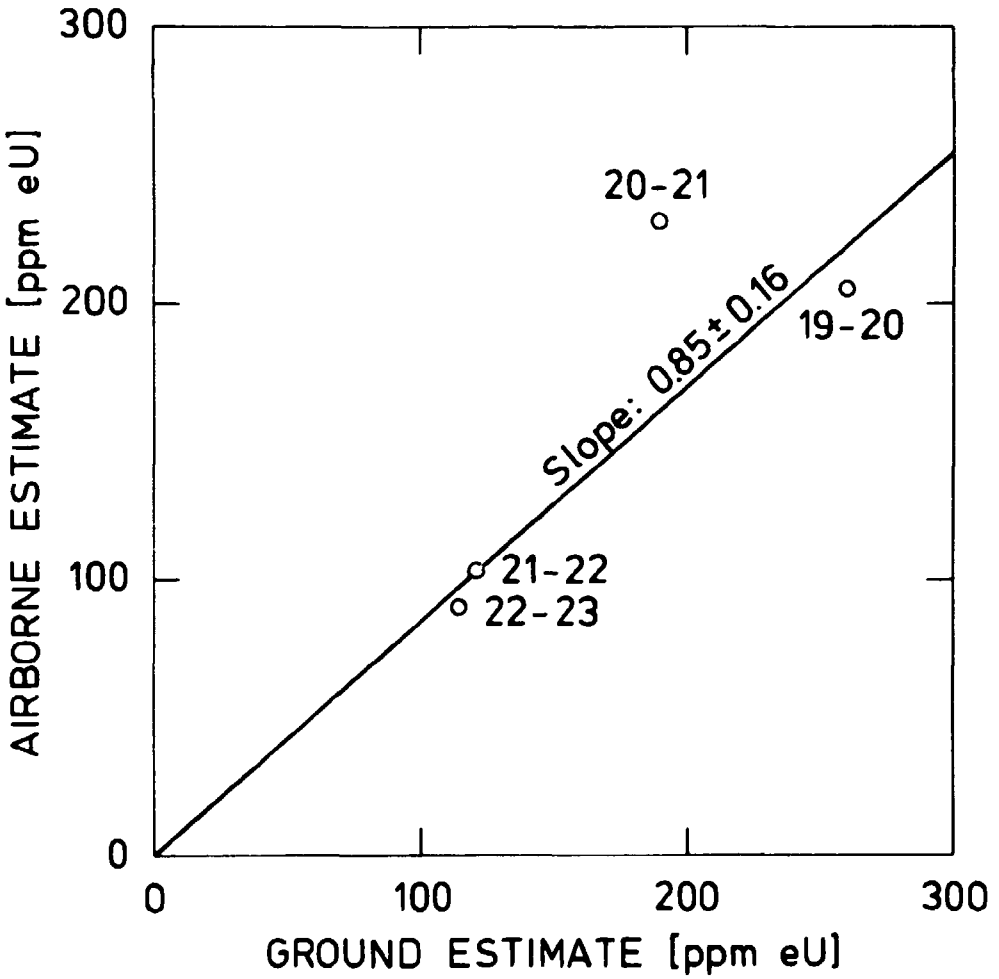


Fig. 27. The correlation between uranium concentrations measured from the air and recorded on the surface with portable spectrometers. These data originate from a 1.5 km long traverse across the plateau formed by the Kvanefjeld U-Th deposit, South Greenland. The four data points represent an average of concentrations assayed between five fiducial markers along the flight line.

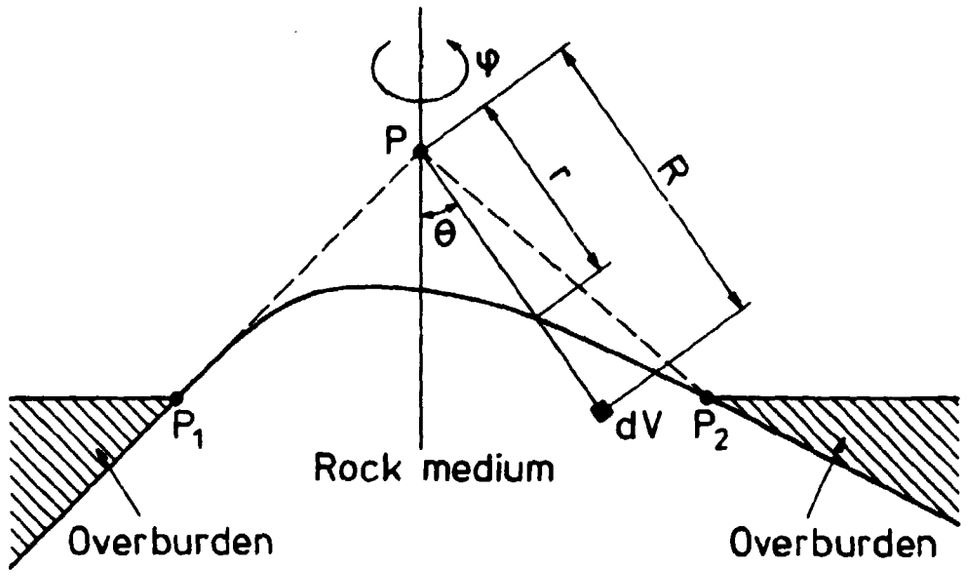


Fig. 28. Distances and angles required for calculating the gamma-ray flux at P from a homogeneous rock medium that crops out between $P_1$ and $P_2$.

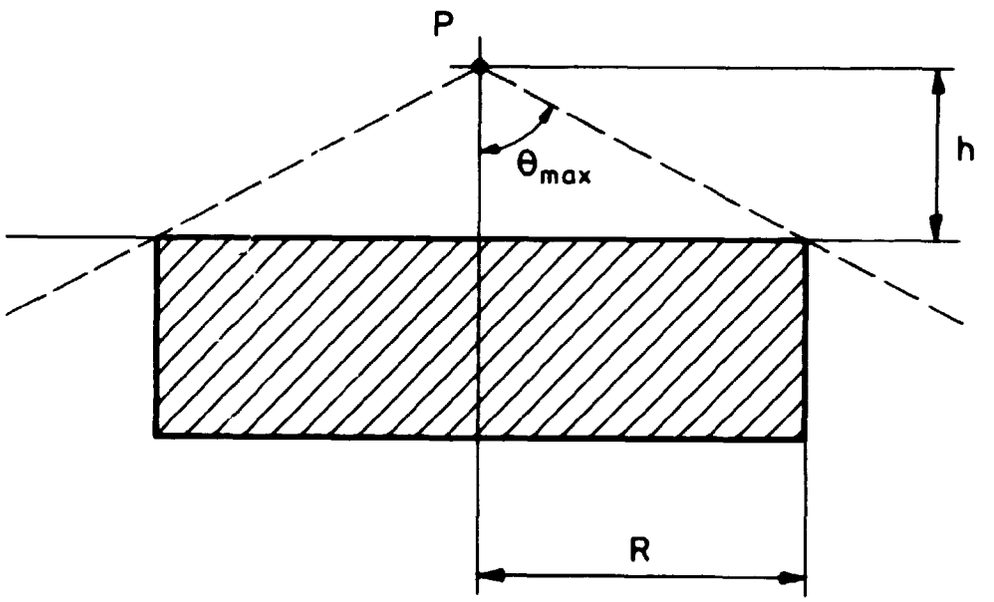


Fig. 29. Simplified representation of the counting geometry on a circular calibration pad. When h << R it is permissible to calculate the solid detection angle at P as $2\pi(1-h/R)$.

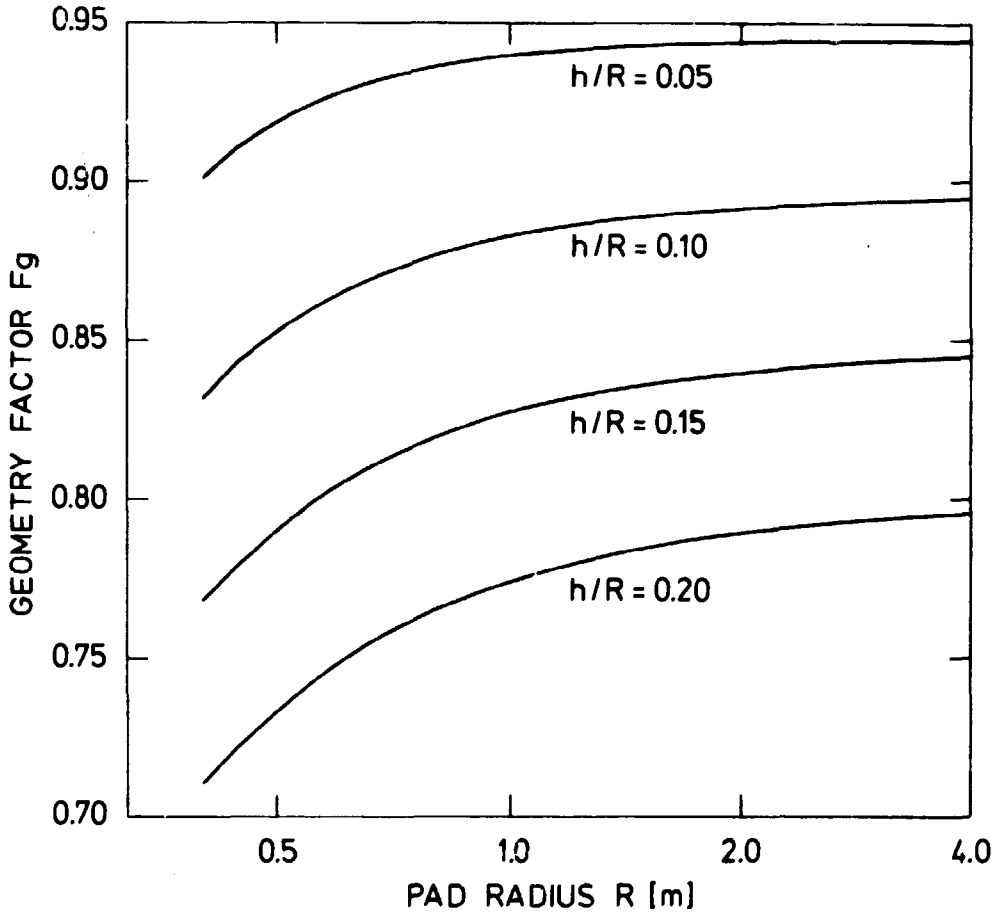


Fig. 30. Geometry factors calculated for circular calibration pads using numerical integration of the transport equation for ~ 2 MeV gamma rays. For $R \to \infty$ or $h \to 0$ the curves converge towards horizontal lines with the equation $F_g = 1 - h/R$.

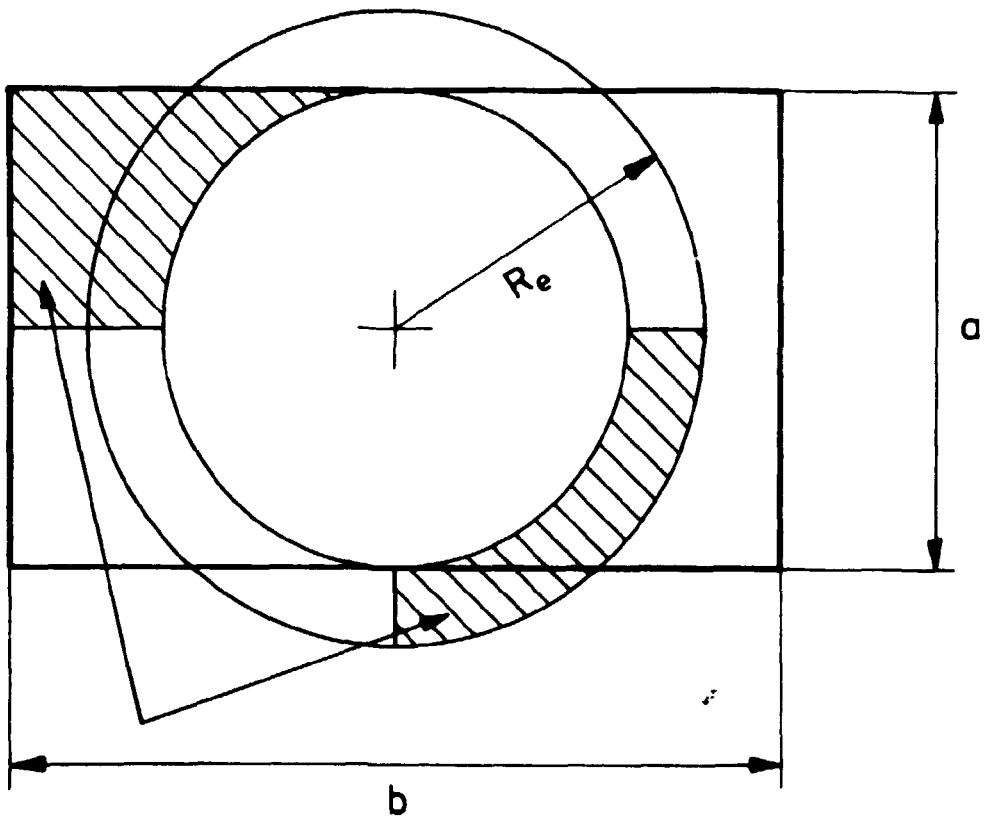


Fig. 31. Calculation of the equivalent radius $R_e$ of a rectangular calibration pad with side lengths a and b. The circle is determined by equating the solid angles in which the two shaded areas are viewed from a point on the pad axis.

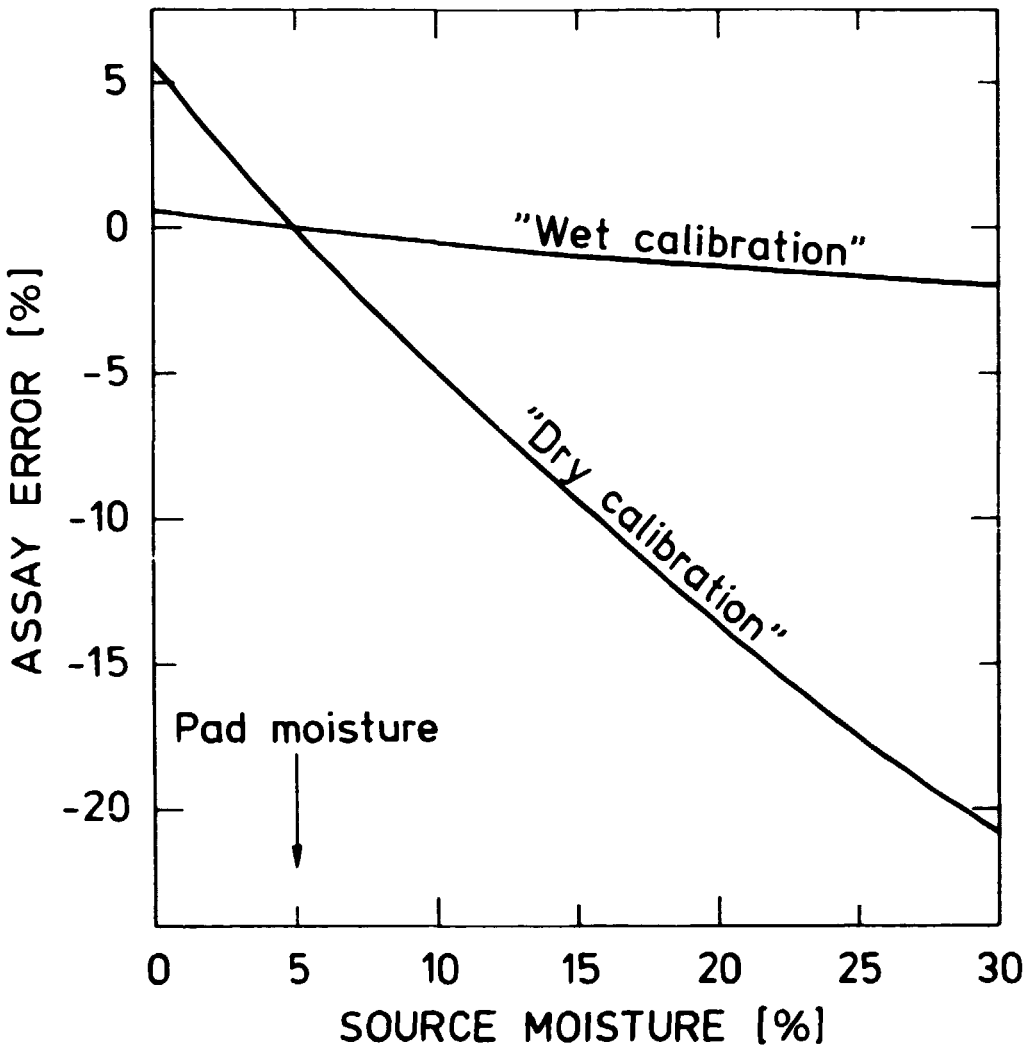


Fig. 32. Field assay errors on sources of various moisture contents. The error may be large if it is attempted to measure the radioelement content per dry weight of the ground material using a calibration against "dry" pad grades. By calibrating the spectrometer in terms of "wet' or "in-situ" pad grades, the radioelement content per wet weight of rock or soil is almost measured correctly.

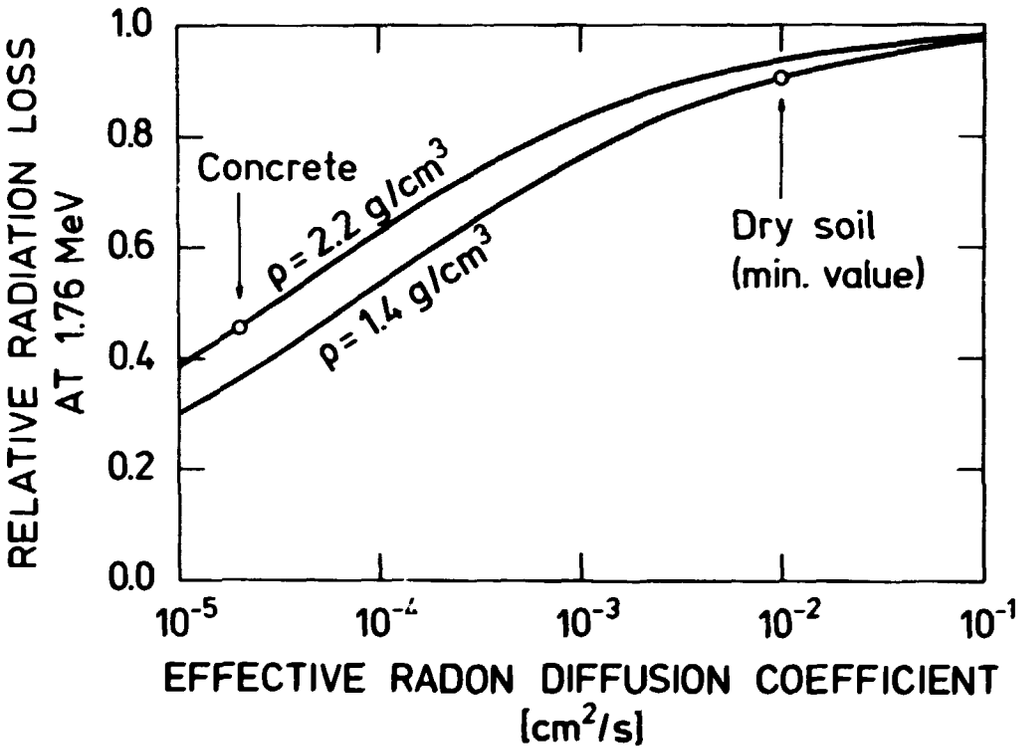


Fig. 33. Calculated radiation losses at 1.76 MeV due to radon exhalation from the source medium. The data are normalized to an emanation power of 100% for the uranium (radium) contained in the medium, and capillary diffusion is the only considered exhalation mechanism.

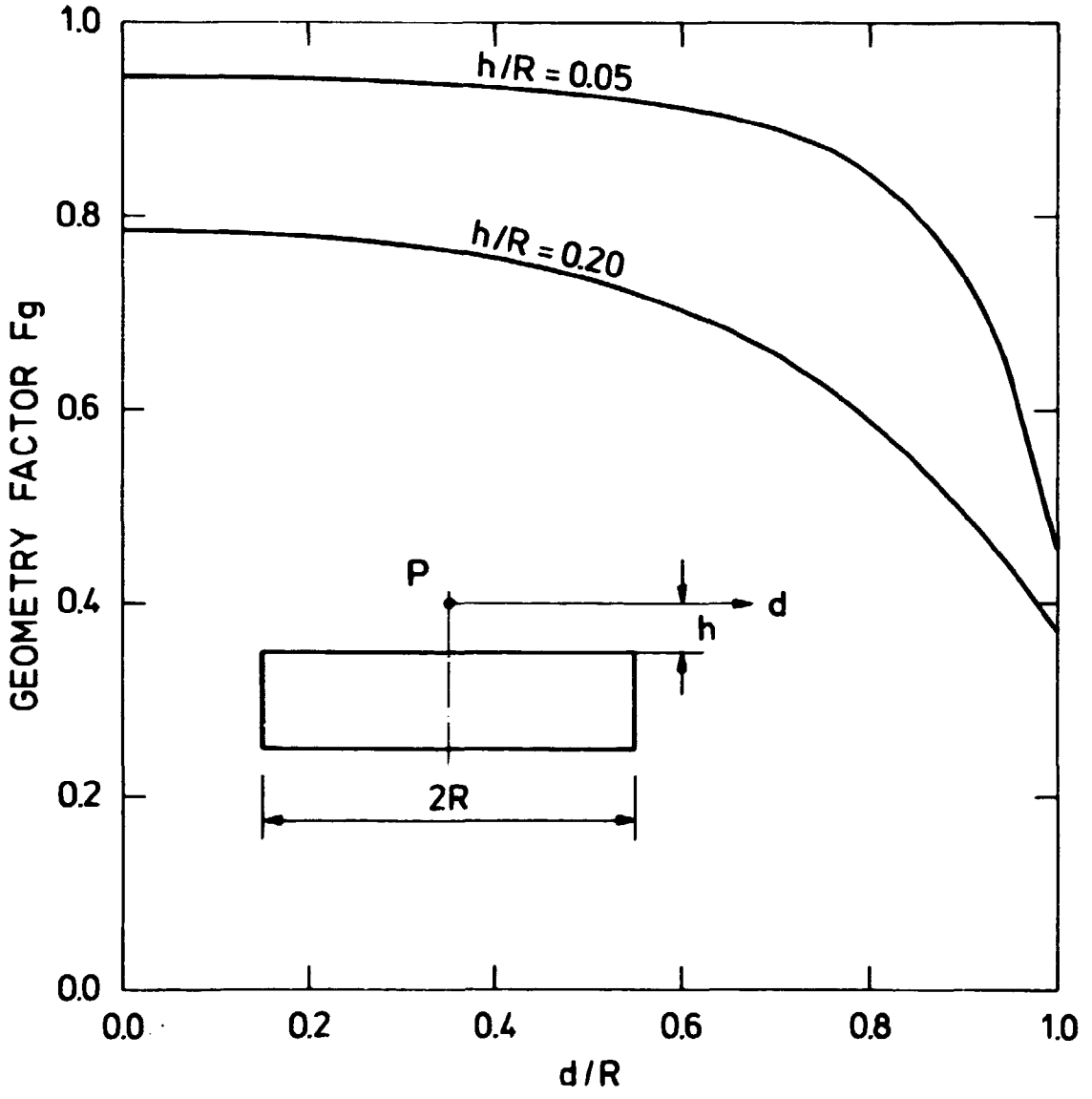


Fig. 34. Calculated decrease of the geometry factor with increasing distances to the axis of a circular calibration pad.

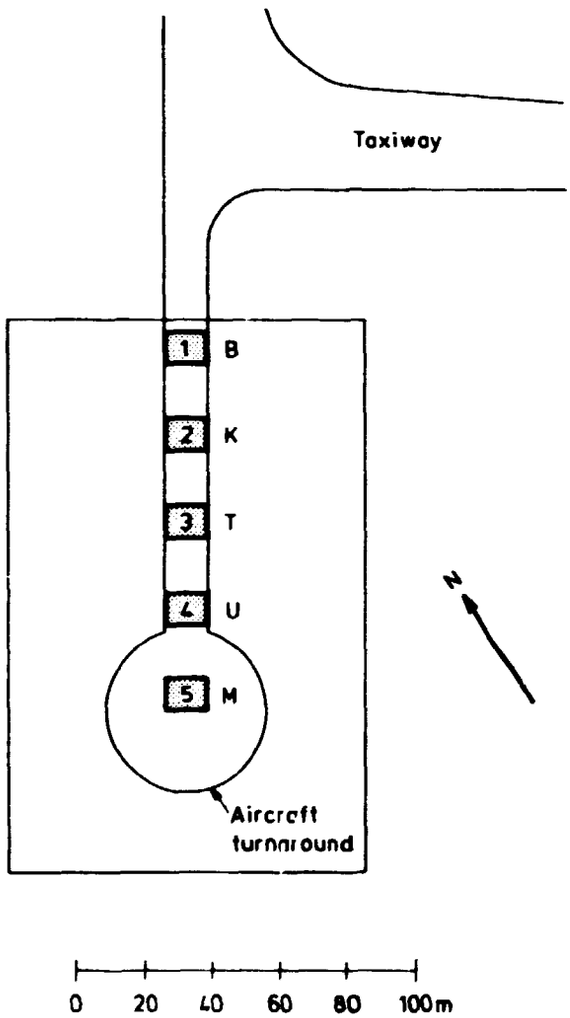


Fig. 35. The calibration pads at Walker Field airport, Grand Junction, Colorado (after Ward (1978)).
B = "blank", K = "potassium", T = "thorium", U = "uranium", M = "mixed".

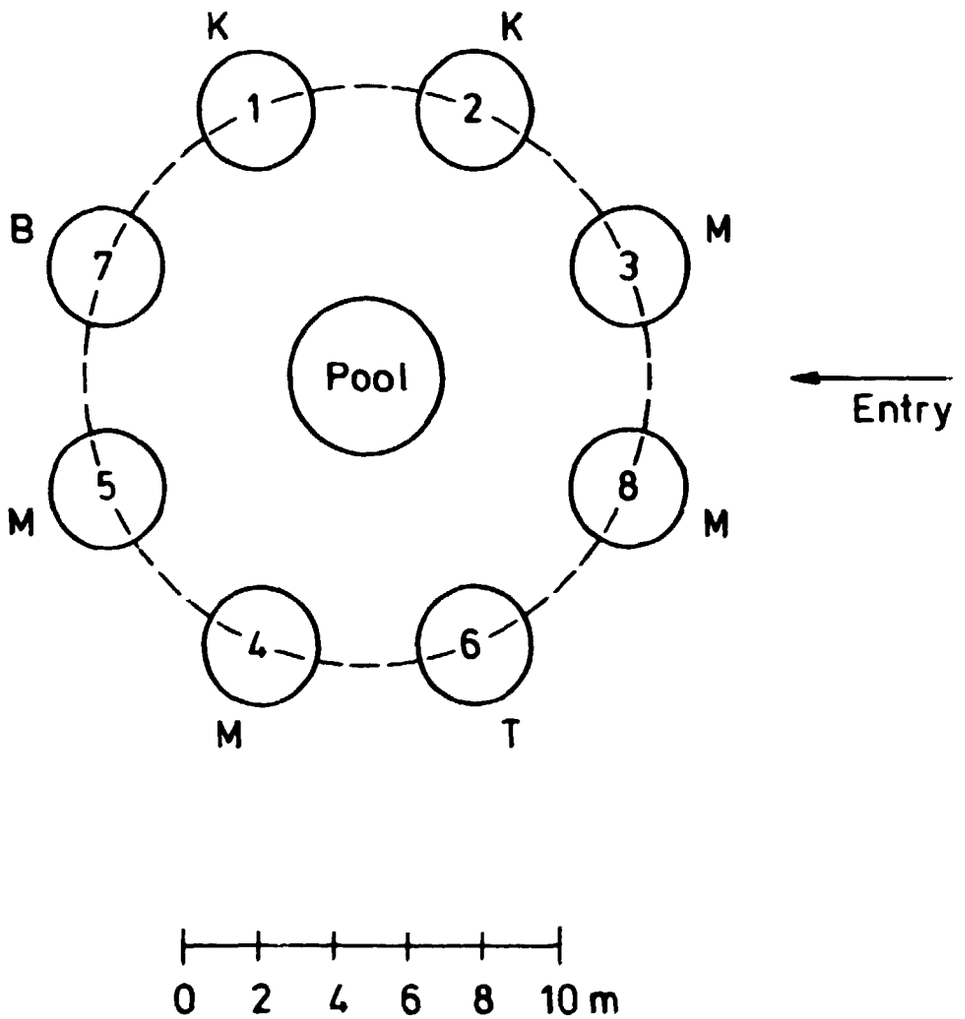


Fig. 36. The calibration pads at the Instituto de Radioproteção e Dosimetrica south of Rio de Janeiro, Brazil.

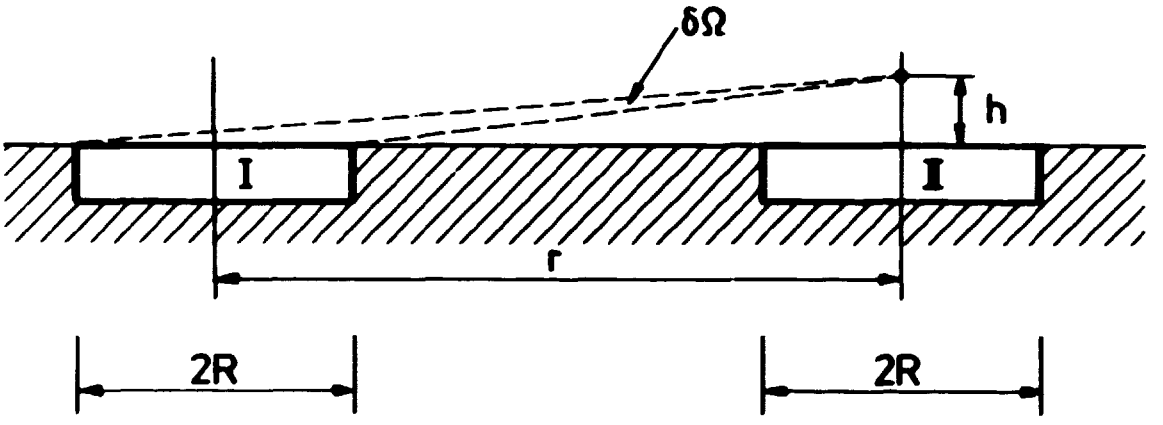


Fig. 37. Model for calculating the interference from a pad (I) on a neighbouring pad (II). The interfering radiation is proportional to the small solid angle δΩ.

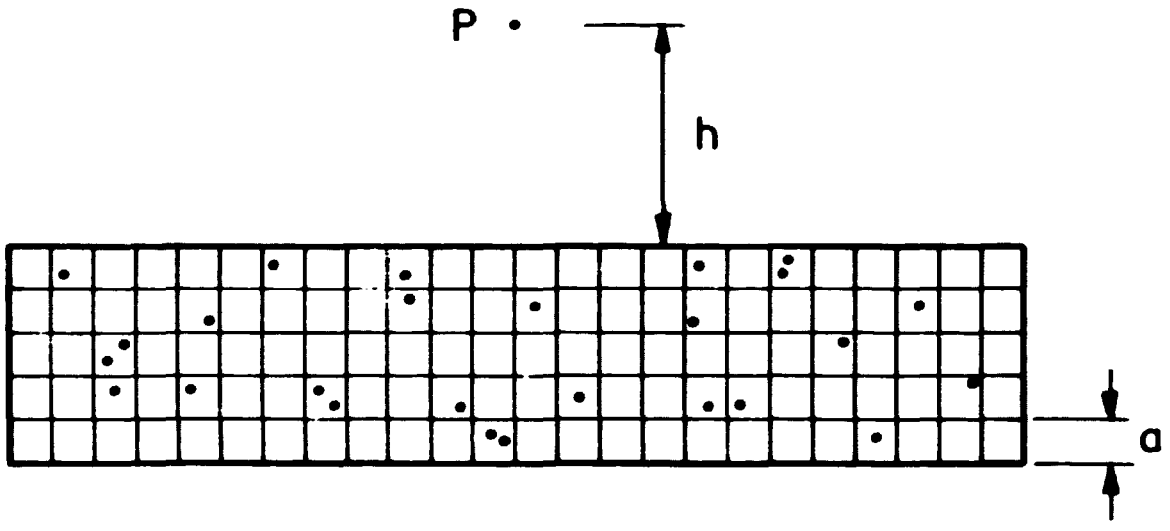


Fig. 38. Model for computer simulation of radioactive pad heterogeneity. A rectangular calibration pad is divided into cubic cells which may be inactive or contain one or more radioactive particles. From repeat calculations in which the spatial distribution of the particles is varied at random one can derive a standard deviation for the gamma-ray signal recorded at P.

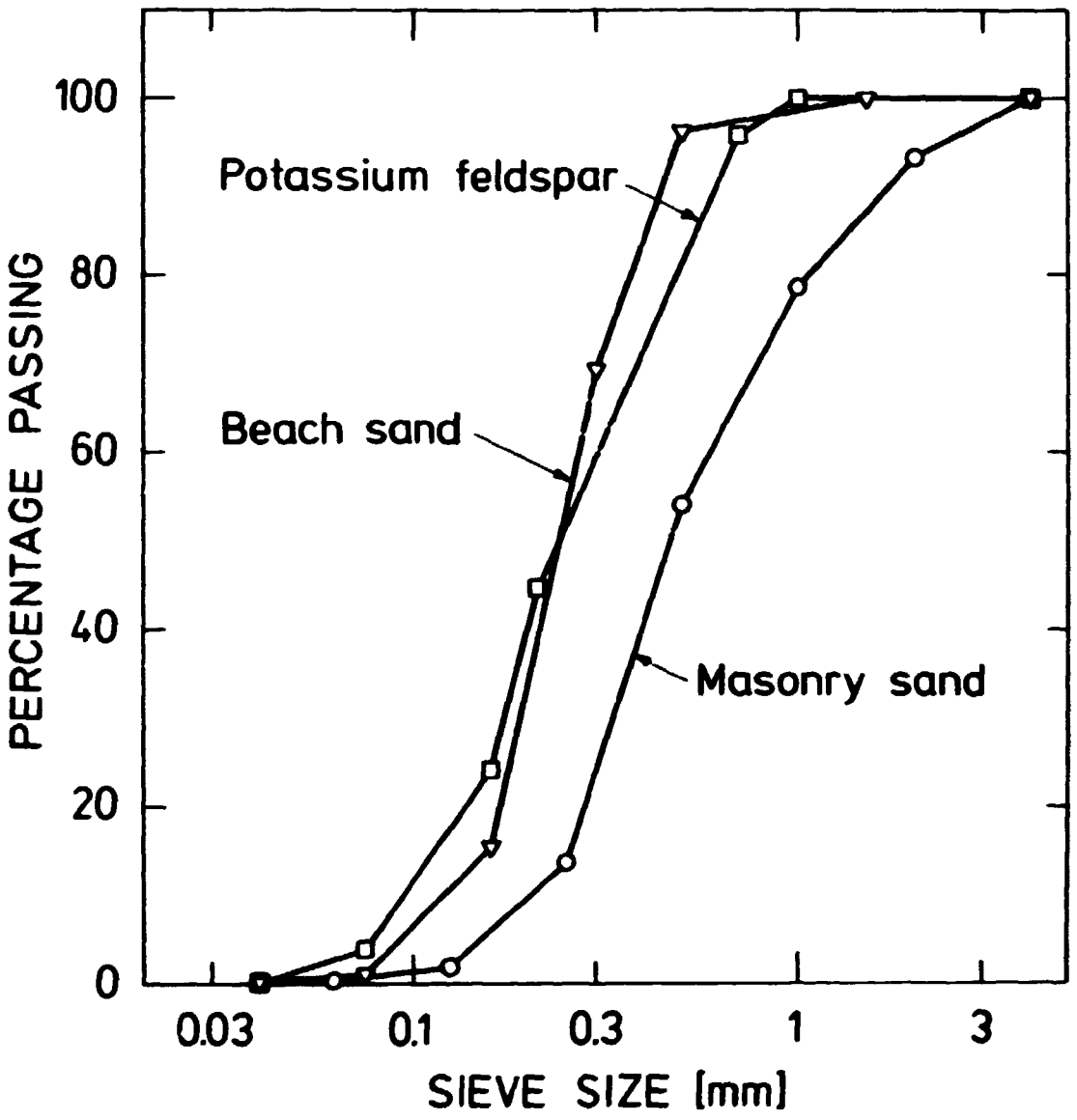


Fig. 39. Grading curves for aggregate particles used in the construction of calibration pads at Walker Field airport (masonry sand) and Risø National Laboratory (beach sand and potassium feldspar).

Fig. 40. Manufacture of calibration pad at the CSIRO Institute of Energy and Earth Resources in Sydney (North Ryde), Australia. Samples of the wet concrete mix are taken for the later preparation of powdered assay material.

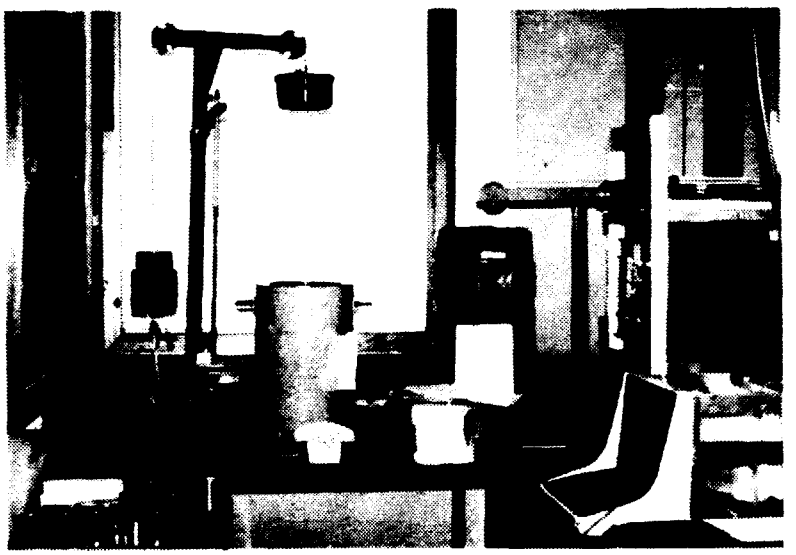

Fig. 41. Manually operated laboratory gamma-ray spectrometers at the CSIRO Institute of Energy and Earth Resources. Sample cans are seen in the left corner of the picture.

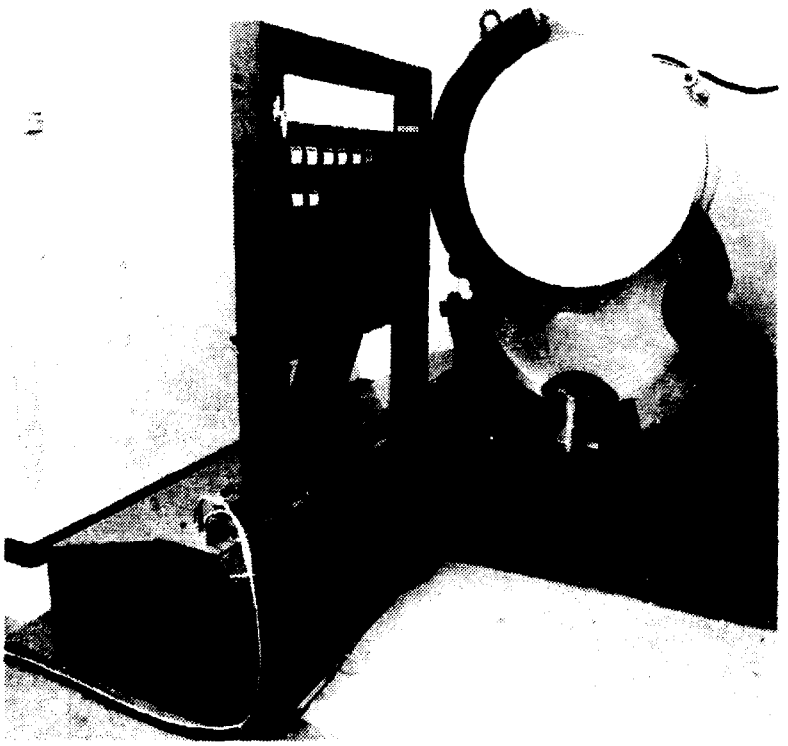

Fig. 42. Laboratory gamma-ray spectrometer with sample changer installed at Risø National Laboratory. The magazine with the sample cans automatically positions the next sample to be analysed in front of the sample changer wheel which can turn 90° forth or back. A robot arm with an electromagnetic head is used for exchanging a sample.

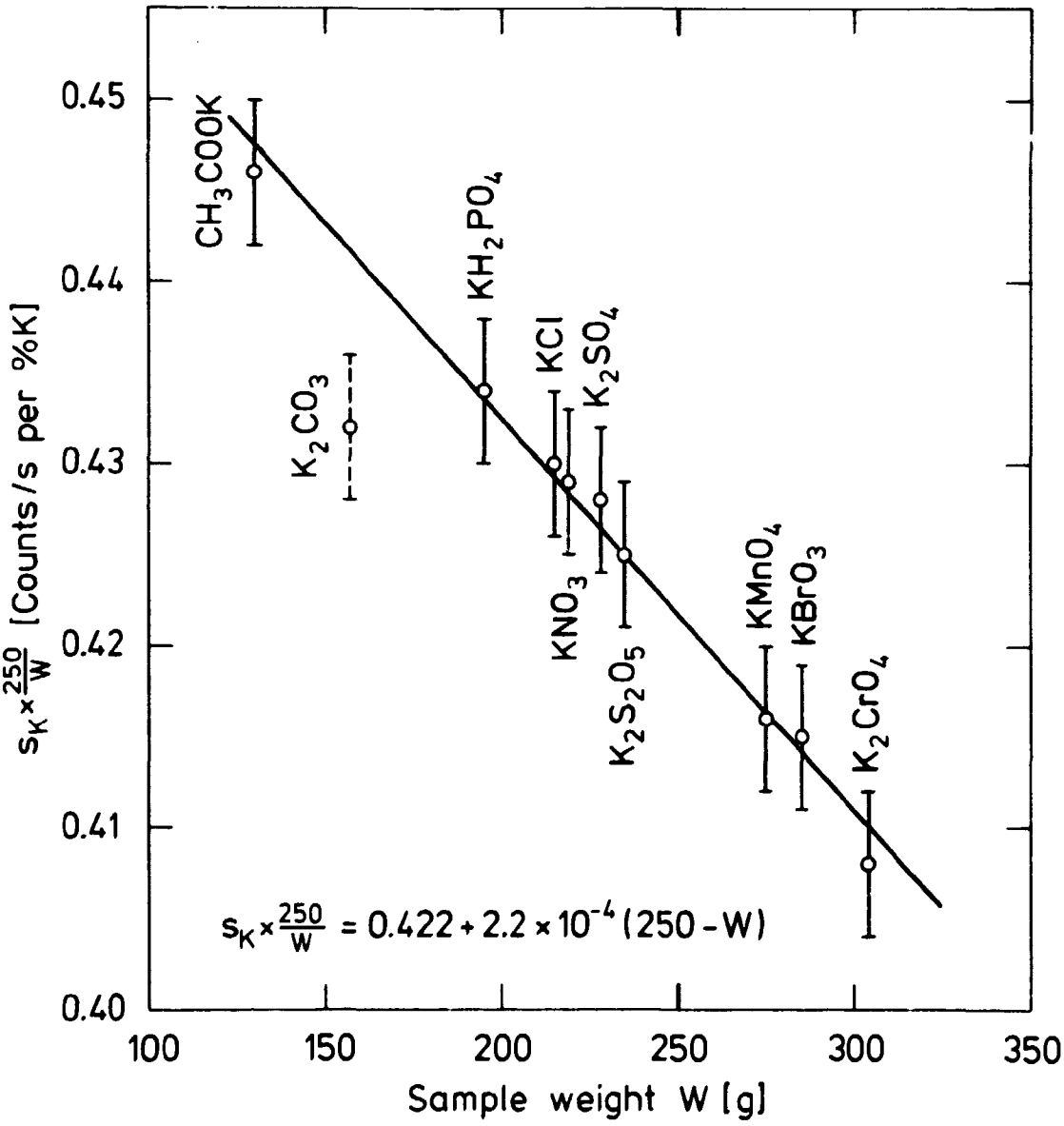


Fig. 43. Potassium calibration line for the laboratory spectrometer at Risø. For each potassium salt used a potassium window sensitivity has been calculated from the K concentration suggested by the chemical formula for the salt. The low sensitivity recorded with $K_2CO_3$ is ascribed to residual, chemically bound water.

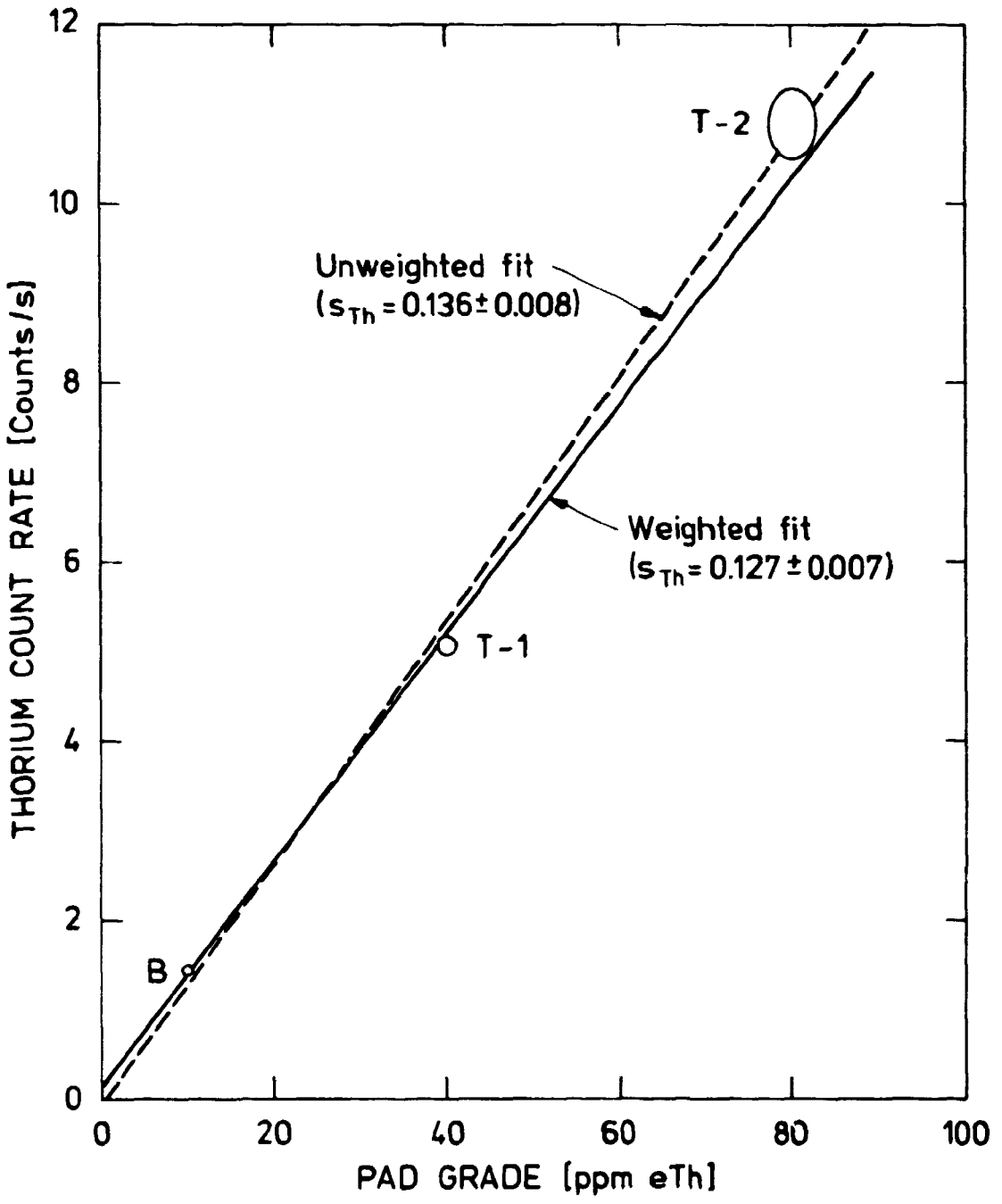


Fig. 44. Hypothetical thorium calibration lines for portable spectrometer calibrated on two T pads and one B pad. The most reliable linear fit is obtained by the use of weight factors which contain the variance associated with counting statistics and uncertainty on the pad grades.

Fig. 45. Monitoring of the radioelement concentrations in calibration pad at Lanseria airport, Republic of South Africa. The facility includes four pads recessed into a disused runway section.

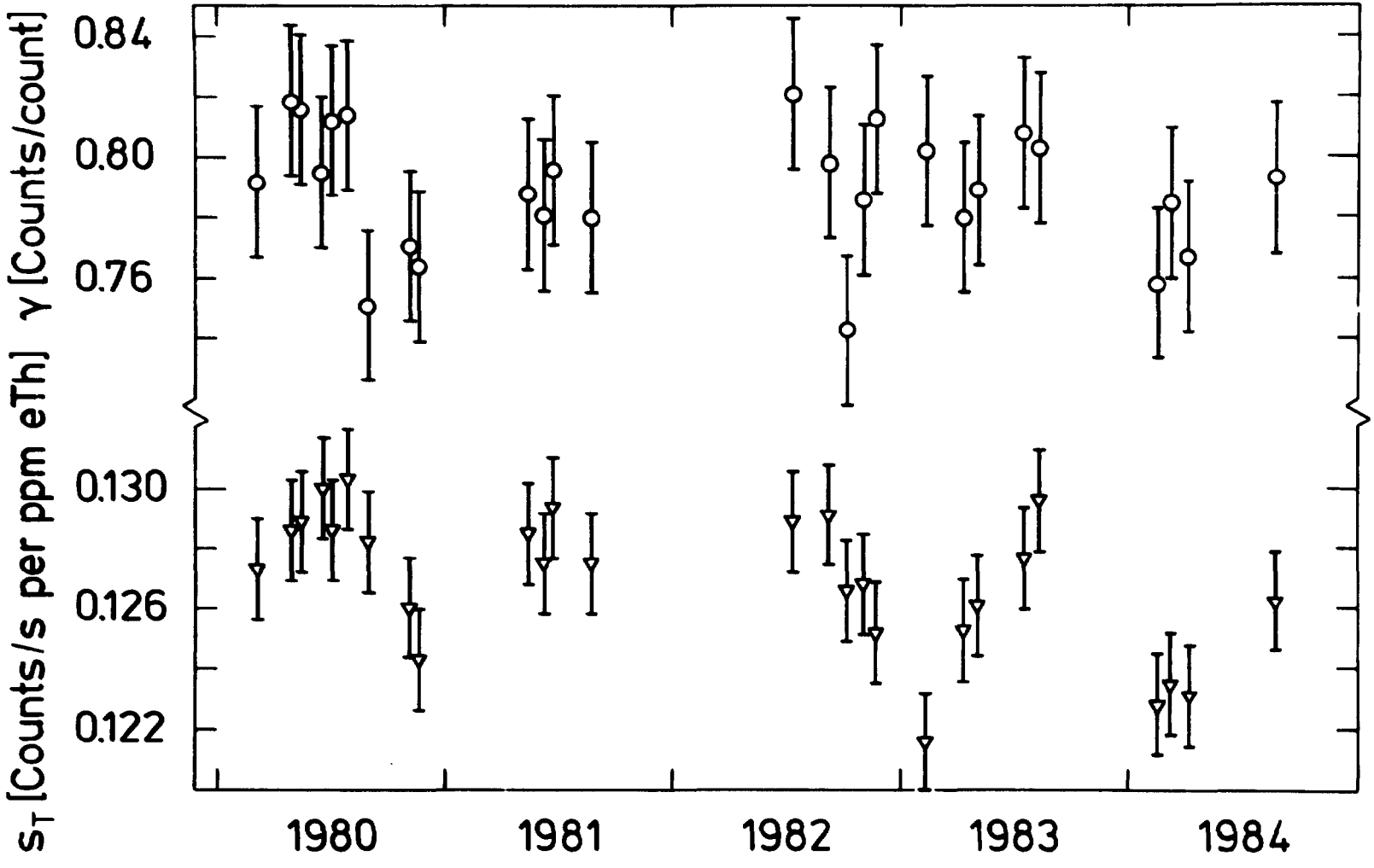


Fig. 46. Thorium window sensitivities ($s_T$) and "γ" stripping ratios recorded with the GR-410 monitoring spectrometer on the pads at Risø. The series of thorium sensitivities suggests a seasonal variation of ± 3% on the thorium calibration grades due to a varying amount of pad moisture.

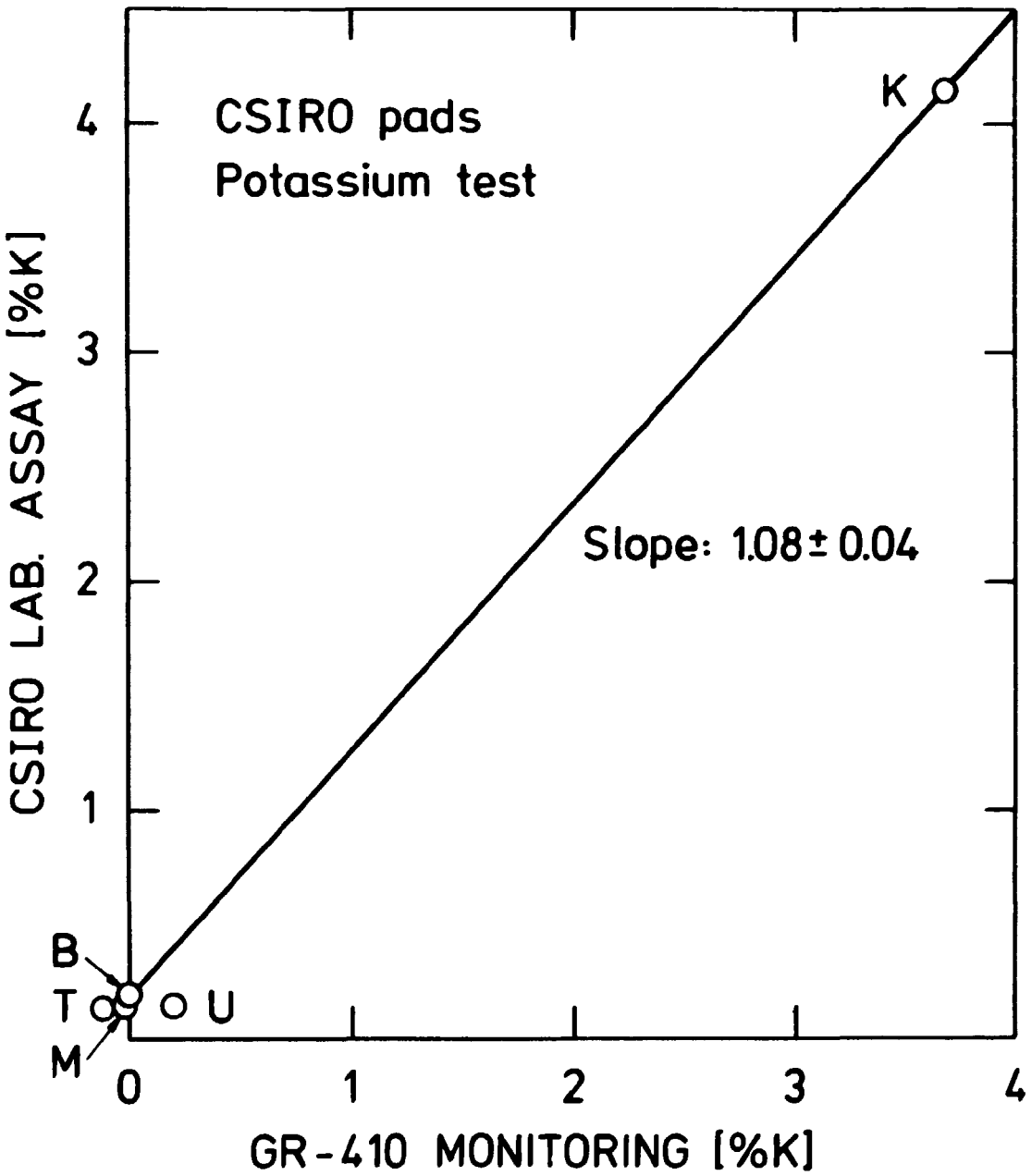


Fig. 47. Estimated potassium grades for the CSIRO calibration pads in Sydney, Australia. Ordinate values are "dry" laboratory grades. Abscissa values are monitored in-situ grades.

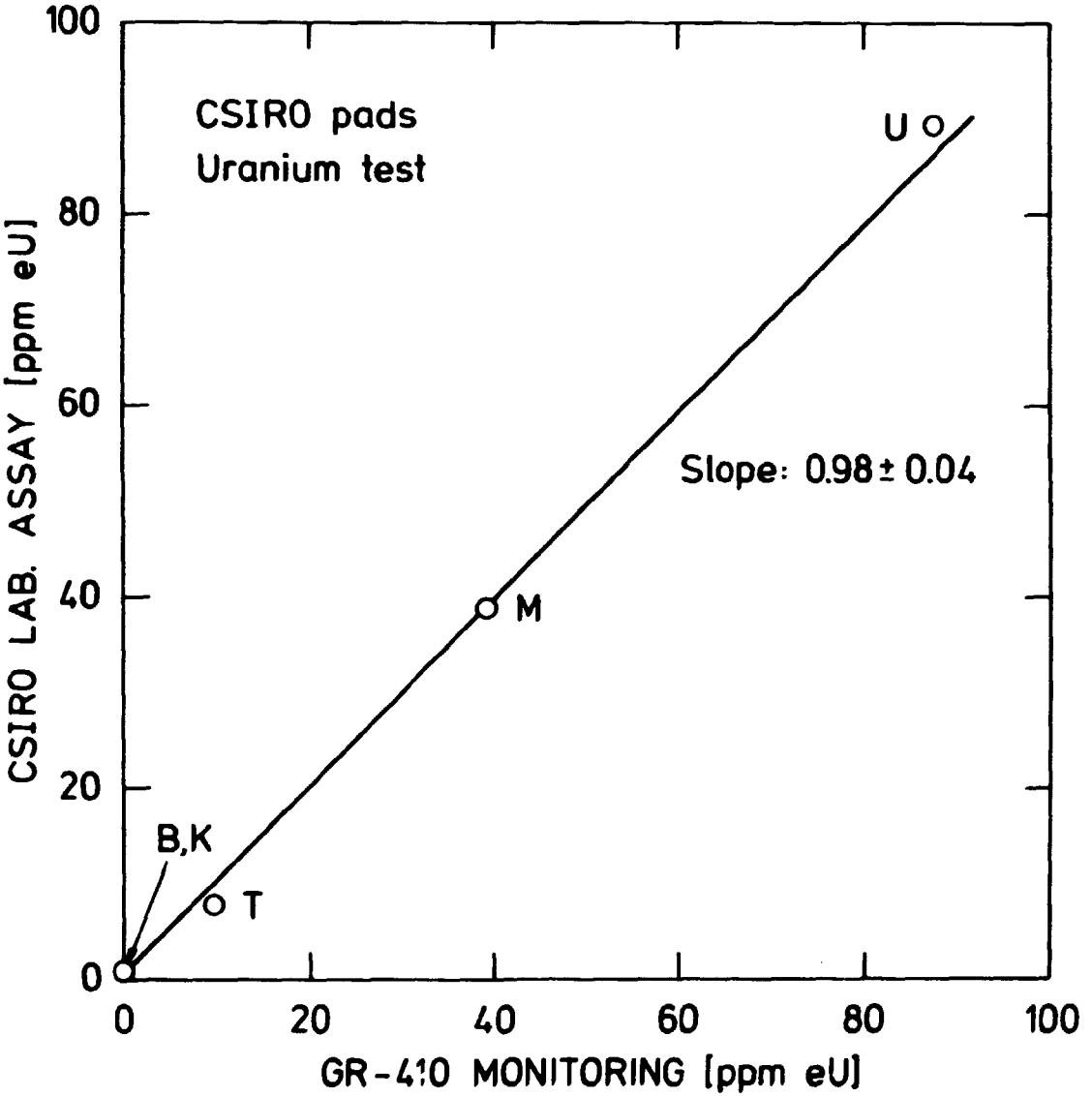


Fig. 48. Estimated uranium (radium) grades for the CSIRO calibration pads in Sydney, Australia. Ordinate values are "dry" laboratory grades. Abscissa values are monitored in-situ grades.

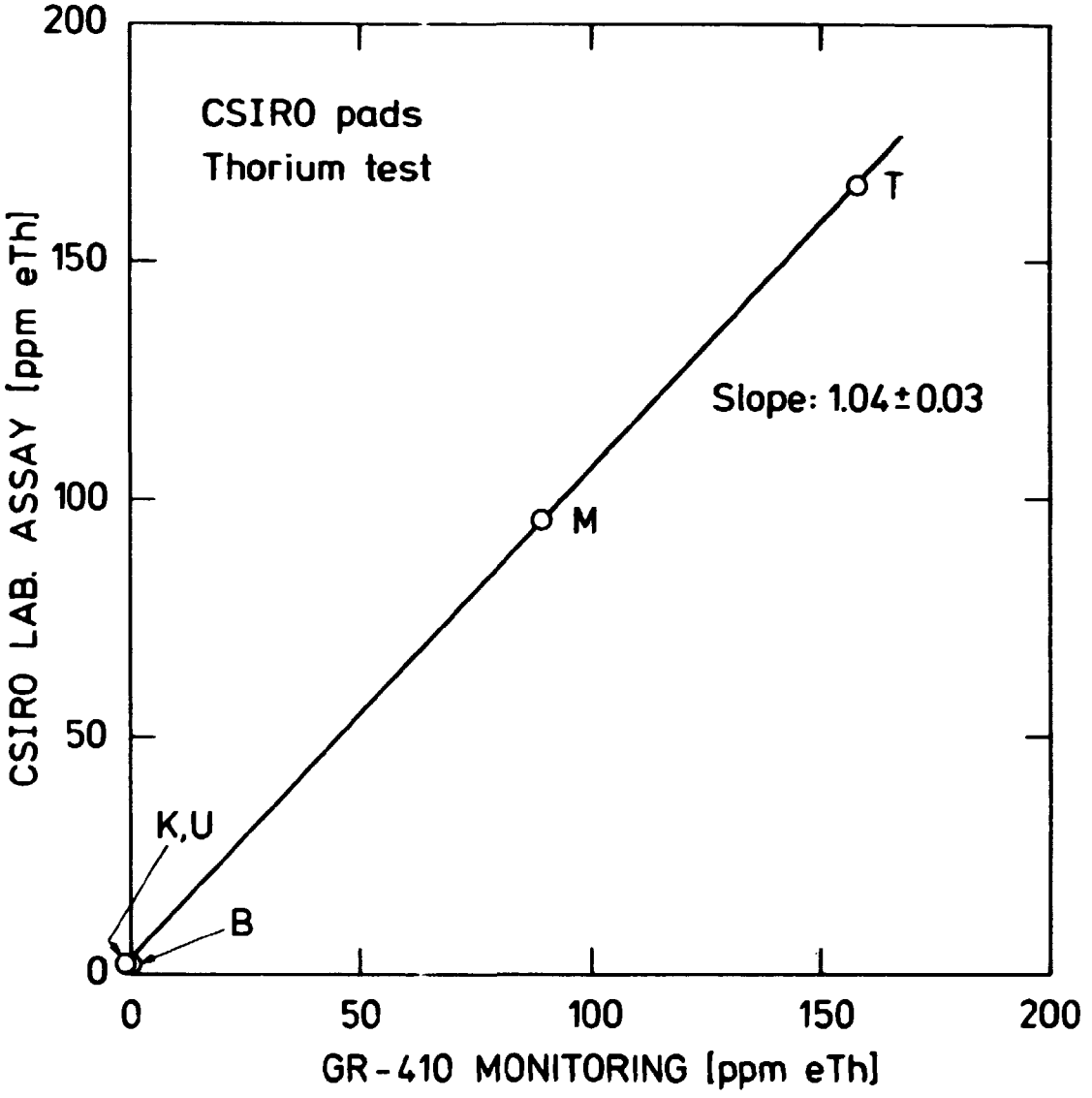


Fig. 49. Estimated thorium grades for the CSIRO calibration pads in Sydney, Australia. Ordinate values are "dry" laboratory grades. Abscissa values are monitored in-situ grades.

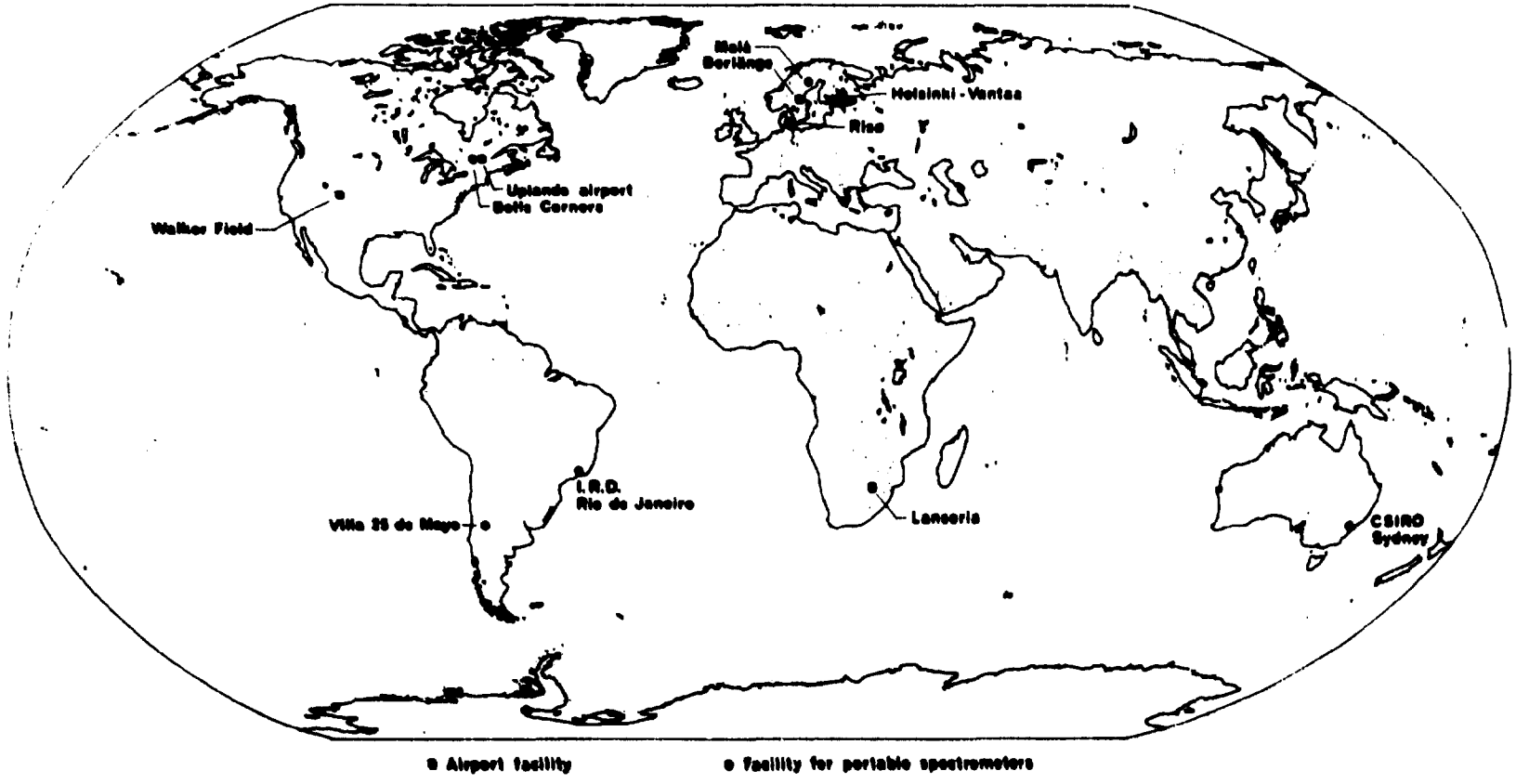


Fig. 50. Locations of the spectrometer calibration facilities included in the IAEA pads intercomparison experiment.